International
Progress Report

IPR-01-44

Äspö Hard Rock Laboratory

TRUE Block Scale project
Preliminary characterisation stage

Combined interference tests and tracer tests

Peter Andersson
Jan-Erik Ludvigson
Eva Wass

GEOSIGMA AB

October 1998

Svensk Kärnbränslehantering AB
Swedish Nuclear Fuel
and Waste Management Co
Box 5864
SE-102 40 Stockholm Sweden
Tel +46 8 459 84 00
Fax +46 8 661 57 19

Äspö Hard Rock
Laboratory

Report no.
IPR-01-44

No.
F56K

Author
Andersson, Ludvigson, Wass

Date

Checked by

Date

Approved
Christer Svemar

Date
02-08-23

Äspö Hard Rock Laboratory

TRUE Block Scale project
Preliminary characterisation stage

Combined interference tests and tracer tests

Peter Andersson
Jan-Erik Ludvigson
Eva Wass

GEOSIGMA AB

October 1998

Keywords: TRUE, block scale, interference test, tracer test, tracer dilution test

Abstract

One of the components of the TRUE Block Scale Preliminary Characterization Stage (PCS) is to conduct a combined interference and tracer test programme in the instrumented array within the Äspö HRL. The overall objectives of the combined interference and tracer tests are to test the present deterministic structural model (Hermanson, 1998) and to test the possibility to conduct combined interference/tracer tests with injection of tracer in internal points belonging to the internal network of discrete features. In total, 19 interference tests were performed, six of them with a duration of 1-2 days and the rest with a duration of 30-60 minutes. Flow measurements using the tracer dilution technique was performed simultaneously in 3-6 observation sections during the long-term interference tests. Tracer injections were made in three observation sections during one of the tests. The flow and pressure responses obtained during the tests gave valuable input for updating the deterministic structural model. The tracer test results was used to get estimates of transport parameters in one of the potential target structures within the block.

Sammanfattning

Detta arbete har utförts som en del av projektet TRUE Block Scale Preliminary Characterization Stage (PCS). Syftet är att utföra ett kombinerat interferens- och spårämnestestprogram i den instrumenterade uppställningen i Äspö HRL. Det övergripande syftet är att testa den aktuella strukturmodellen (Hermansson, 1998) och att undersöka möjligheten att utföra kombinerade interferens/spårämnestester med injektion av spårämnen i punkter tillhörande nätverket av diskreta strukturer. Totalt utfördes 19 interferenstester , sex av dem med en varaktighet av 1-2 dagar och resterande med en varaktighet av 30-60 minuter. Under de längre försöken utfördes samtidigt flödesmätningar med spårämnesteknik i 3-6 observationssektioner. I ett av testerna injicerades spårämnen i tre observationssektioner. Beräknade flödes- och tryckresponser gav värdefull data för uppdatering av den deterministiska strukturmodellen. Resultaten av spårförsöken användes för att bestämma transportparametrar i en strukturerna i blocket.

Executive Summary

An experiment aiming at increasing the understanding of flow and transport phenomena in a fracture network in the block scale (L=50 m), TRUE Block Scale Project, is underway at the Äspö HRL. The experiment is divided into four experimental stages (Winberg, 1997a). The second of these stages is the Preliminary Characterization Stage (PCS).

The objectives of the Preliminary Characterization Stage are to;

- characterize the block in broad terms using a limited number of boreholes
- identify and quantify major conductive structures (fracture zones), fractures sets and boundary conditions
- assess connectivity of fracture network using hydraulic cross-hole interference tests
- perform a preliminary assessment of transport parameters over longer distances using injection of tracers in conjunction with hydraulic cross-hole tests.

Based on collected data from these five boreholes and from the mapping of the tunnel the structural model of the block has been updated in sequence. The most recent deterministic structural model (October 97-model), reported by Hermanson (1998) does not include data from borehole KI0023B. However, the model has been successively updated using information from the drilling and characterization of borehole KI0023B.

The boreholes have been instrumented with multi-packer systems in accordance with the structural model valid at the time of their respective completion. The test sections pack off both identified boundary conditions (structures) and potential structures that may be used for the planned future tracer tests after the Detailed Characterization Stage.

One of the components of the Preliminary characterization stage is to conduct a combined interference and tracer test programme in the instrumented array. This report describes the results of this programme.

The overall objectives of the combined interference and tracer tests are;

1) to test the present deterministic structural model (Hermanson, 1998) (test of external deterministic discrete feature network), and specifically the relative role of subhorizontal and NE subvertical structures for establishing connectivity in the studied rock volume.

2) to test the possibility to conduct combined interference/tracer tests with injection of tracer in internal points belonging to the internal network of discrete features (test of the internal discrete feature network).

The planned tests were divided into three categories depending on the level of ambition of each test given by the roman numbers (I, II and III) which represents:

I) Long term pumping (> 5 days). Assessment of flow rate in selected sections, measurement of tracer breakthrough in pumped section,

II) Intermediate term pumping (< 5 days). Assessment of flow rate in selected sections.

III) Short time pumping (< 1 days). No tracer injection.

In total, 19 tests were performed, one long term, five intermediate term and 13 short time pumping tests.

The flow rates were determined by tracer dilution tests in three to six sections during each interference test (type I and II). The dilution tests were performed both under natural gradient and under stressed conditions (pumping during interference tests). Thus, it was possible to simultaneously measure both flow and pressure changes due to the pumping. The duration of each tracer dilution test was about 20-24 hours.

The long term interference test ESV-1c also involved tracer injections in three sections, two in the same structure (#20), KI0025F:R4 and KA2563A:R5, and one in the newly identified structure #13, in section KI0023B:P4 (test INW-1a, see Table 1-1). The tracer injections were performed as decaying pulse injections and sampling was performed in the water withdrawn from the source section, KI0023B:P6 (structure #9). The tracers used were three different fluorescent dyes namely, Uranine (KI0025F:R4), Rhodamine WT (KA25623A:R5) and Amino G Acid (KI0023B:P4).

The hydraulic responses have been evaluated in different steps in which part of the data has been sorted out for further (quantitative) evaluation. This procedure was necessary in order to restrict the quantitative evaluation to a manageable amount of data.

Firstly, time-drawdown- and time-recovery plots were prepared for sections showing a drawdown (or recovery) of more than s_p=0.2 m by the end of the tests. To account for the different flow rates used in the tests and to make the response plots comparable between tests, the final drawdown by stop of flowing (s_p) is normalized with respect to the flow rate (Q). The ratio s_p/Q is plotted on the Y-axis. On the X-axis, the ratio of the response time and the squared distance R in space between the (midpoint of the) source section and (the midpoint of) each observation section (t_R/R^2) is plotted. The latter ratio is inversely related to the hydraulic diffusivity of the rock, which parameter indicates the speed of propagation in the rock of the drawdown created in the flowing section.

From the response plots of s_p/Q versus t_R/R^2 for each test, sections with anomalously fast response times (high hydraulic diffusivities) and large (normalized) drawdowns can be identified. Such sections showing primary responses can be assumed to have a distinct hydraulic connection to the flowing section and may be intersected by fracture zones or other conductive structures in the rock. On the other hand, sections with delayed and weak responses may correspond to sections in the rock mass between such structures.

From the calculated values of s_p/Q (index 1) and t_R/R^2 (index 2) for each observation section during each test a common response matrix, showing the response patterns for all tests, was prepared by classifying the responses by means of the index 1 and -2.

The results from the qualitative analysis were compared with the structural (October 97) model and checked for consistency and possible need of revision.

The derivative of the drawdown (or recovery) was used as a diagnostic tool in the interpretation of the flow geometry and deduction of hydraulic boundaries. The derivative was generated by the SKB-code PUMPKONV and plotted together with the drawdown/recovery curves in logarithmic diagrams.

The quantitative interpretation was made using the code AquiferTest (Waterloo Hydrologic). As a standard interpretation model, the Hantush model for constant flow rate tests in a leaky (or non-leaky) aquifer with no aquitard storage was used.

Each interpreted intercept of different structures with the tested boreholes has been evaluated based on the response matrices. However, it should be noted that the evaluation is based purely on hydraulic responses. Thus, geological and geophysical indications have not been considered here. Only structures that have been tested, directly or indirectly, are discussed. The 19 hydraulic interference tests described in this report have produced a large data base for information and updating of the structural model presented in Hermanson (1998), later updated in Hermanson (in prep.).

The estimated transmissivity and storativity for structures #5, #6 and #7, tested by the global tests, are significantly higher ($2\text{-}6\cdot10^{-5}$) than those estimated for structure #20 (and possible sub-parallel structures) from the local tests ($7\text{-}15\cdot10^{-7}$). However, the hydraulic diffusivity of these structures seems to be in the same order of magnitude (or slightly higher for structure #20).

The tracer dilution tests showed that the “natural” flow varies quite a lot within the block scale volume. High flow rates were measured in two borehole sections KA2511A:S4 (structures #6 and #16) and KA2563A:R5 (structure #20), 1200 and 600 ml/h, respectively. The flow rates in the other measured sections were typically less than 10 ml/h, or even less than 1 ml/h. This large difference cannot be explained by differences in transmissivity alone. Also the hydraulic gradient must vary considerably within the block. The high flow rates may result from a closely located intercept with a structure having lower hydraulic head.

The tracer test performed by pumping in structure #9 and injecting in structures #13 and #20 resulted in tracer breakthrough from only one of the three injection points, KA2563A:R5 (structure #20), which also was the only section where the flow rate increased as a result of pumping. Thus, the flow path involved transport between two different structures. A tracer recovery of 44% along the 16 m long flow path (geometrical distance) indicates that mass losses occur along the flow path, possibly due to a combination of a weak sorption of the tracer and hydraulic head conditions (intersections with other structures having lower hydraulic head).

The transport parameters derived from the numerical modelling indicate that structure #20 has similar characteristics as the thoroughly investigated Feature A at the TRUE-1 site.

Contents

List of Figures

List of Tables

1 INTRODUCTION

1.1 Background

An experiment aiming at increasing the understanding of flow and transport phenomena in a fracture network in the block scale (L=50 m), TRUE Block Scale Project, is underway at the Äspö HRL. The experiment is divided into four experimental stages (Winberg, 1997a). The second of these stages is the Preliminary Characterization Stage (PCS).

The objectives of the Preliminary Characterization Stage are to;

- characterize the block in broad terms using a limited number of boreholes
- identify and quantify major conductive structures (fracture zones), fractures sets and boundary conditions
- assess connectivity of fracture network using hydraulic cross-hole interference tests
- perform a preliminary assessment of transport parameters over longer distances using injection of tracers in conjunction with hydraulic cross-hole tests.

At the end of the Preliminary Characterization Stage the following milestones should be met;

- Is the experimental volume suitable for further research?
- Can major tracer tests be performed given the information available?

During 1997, two boreholes, KI0025F and KI0023B, have been drilled, using the triple-tube method, from the I-tunnel at tunnel length L=3/510 m. These boreholes, 76 mm in diameter, are gently inclined (I=20 degrees) and complement the existing 56 mm boreholes, KA2511A, KA3510A and KA2563A, the latter drilled as a pilot borehole as part of the TRUE Block Scale Scoping Stage. The boreholes have been characterized using different geological, geophysical and hydrogeological methods.

Based on collected data from these five boreholes and from the mapping of the tunnel the structural model of the block has been updated in sequence. The most recent deterministic structural model (October 97-model), reported by Hermanson (1998) does not include data from borehole KI0023B. However, the model has been successively updated using information from the drilling and characterization of borehole KI0023B.

The boreholes have been instrumented with multi-packer systems in accordance with the structural model valid at the time of their respective completion. The test sections pack off both identified boundary conditions (structures) and potential structures that may be used for the planned future tracer tests after the Detailed Characterization Stage. During

the course of the characterization and structural modelling, the pressure responses obtained in the borehole array have been compiled in a response matrix (Winberg, 1997b). These responses and the inferred connectivity have been successively used to update the deterministic structural model. The disturbances induced by interception of structures in the borehole during drilling are however not very precise in a quantitative sense. The data is of valuable qualitative stature mainly because of the short duration of the disturbance and the associated limited radius of influence.

So far the work in the PCS has been directed towards establishing bounding structures, and potential collection and injection points in structures which bound an interior block, approximately 50x50x50 m large. These structures are referred to as the external network of discrete features. Plans are to study the interior block, and its internal network of discrete features, further during the Detailed Characterization Stage with the aim of establishing tracer test geometry including injection points for tracer in the internal block.

One of the components of the Preliminary characterization stage is to conduct a combined interference and tracer test programme in the instrumented array. This report describes the results of this programme.

1.2 Objectives and scope

The overall objectives of the combined interference and tracer tests are;

1) to test the present deterministic structural model (Hermanson, 1998) (test of external deterministic discrete feature network), and specifically the relative role of subhorizontal and NE subvertical structures for establishing connectivity in the studied rock volume.

2) to test the possibility to conduct combined interference/tracer tests with injection of tracer in internal points belonging to the internal network of discrete features (test of the internal discrete feature network).

The first aim can be regarded as a test of the present understanding of the deterministic structural model. The second aim is answering up to the milestone whether tests can be conducted in the block scale, inside the block delineated by the interpreted deterministic structures.

In the test proposal by Winberg et al. (1998) it is shown that, using the geometry of the available borehole array and the available pressure responses, alternative hypotheses can be formulated and tested regarding the structural model, and how the included structures connect. Further, how and where a test of the internal network of features can be tested.

The planned tests were divided into three categories depending on the level of ambition of each test given by the roman numbers (I, II and III) which represents:

I) Long term pumping (> 5 days). Assessment of flow rate in selected sections, measurement of tracer breakthrough in pumped section,

II) Intermediate term pumping (< 5 days). Assessment of flow rate in selected sections.

III) Short time pumping (< 1 days). No tracer injection.

The planned tests and their specific objectives were listed by Winberg et al. (1998), cf. Table 1-1. However, it should be noted that some of the positions of structures later have been reevaluated as result of additional data from the tests described in this report and drilling of new boreholes. The positions of the sinks and sections used for flow measurements using the tracer dilution technique are shown in Figure 1-1.

The list of tests was later modified to include a number of shorter tests (type III), cf. Table 1-2. The type III tests were not given any specific objective for each individual test. The overall objective for these tests were to test the structural model in a qualitative manner using a flow period of only 30 minutes for each test.

Table 1-1. Listing of performed interference tests (type I and II) in the TRUE Block Scale array (from Winberg et al. (1998)

Test	Objective	Performance
ESV-1:a-c (I and II)	Direct tests of defined subvertical vertical structure. Properties of Structure #20 and assessment of its connectivity to other structures.	Isolate structure at its three intercepts. Make sections circulating. Possible to perform test by flowing one or more sections including the structure.
ESV-2 (II)	Direct test of defined subvertical structure. Properties of Structure #6 and assessment of its connectivity to other structures	Isolate structure in new borehole KI0023B and in KA2563A. Preferential source section is the one in KI0023B.
ENW-1 (II or III)	Indirect test of external network and role of interpreted subhorizontal structures, particularly Structure #18 and #16	Isolate Structure #5 in KA3573A and flow the borehole.
ENW-2 (II)	Indirect test of external network and role of unaccounted Structure #7 at L=52.4 m in KA2511A	Isolate Structure #7 in KA2511A , replace 4/2 mm pressure line with a 8/6 mm hose and flow the section.
INW-1 a:b (I or II)	Indirect test of internal network. Performed in conjunction of one or two of Tests SV-1a/SV-1c above	Isolate unlabelled structure between 85-86 m in KI0023B and make section circulating. Inject tracer in section parallel to conducting in both or either of Tests SV-1 b-c.

Table 1-2. List of performed type III interference tests. Associated structures as interpreted by Hermanson (in prep) (September 1998 Structural model).

Test #	Source section	Structure #
1	KI0023B:P4	#13
2	KA2512A	#5
3	KA2598A	#1, #8
4	KA2563A:R1	#9, #10
5	KA2563A:R4	#13, #18
6	KA2511A:S4	#6, #16
7	KI0025F:R3	?
8	KI0025F:R5	#6, #7
9	KI0025F:R2	#19
10	KI0023B:P7	#6, #20
11	KI0023B:P5	#18
12	KI0023B:P2	#19
13	KA3573A:P1	#15

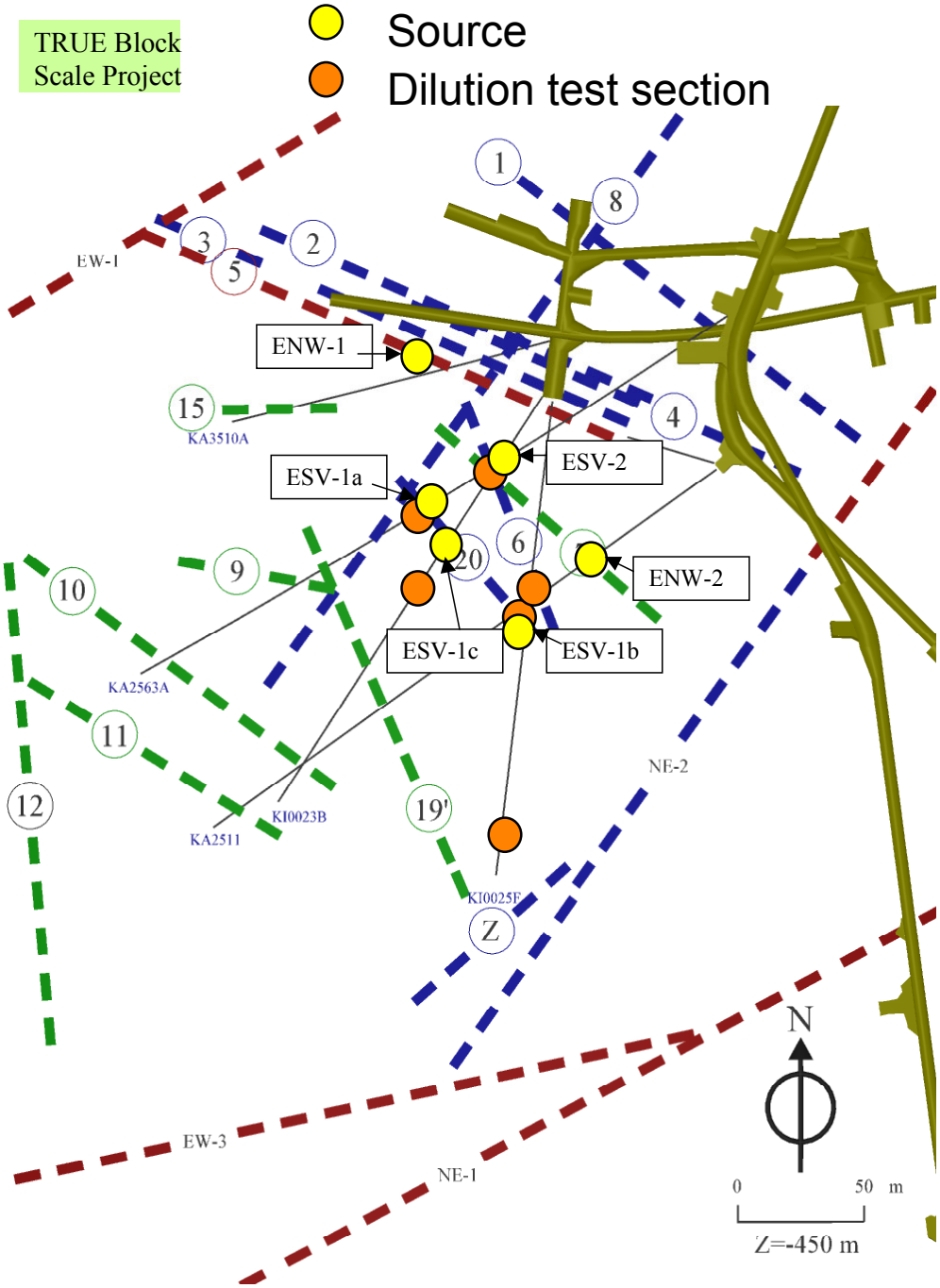

Figure 1-1. *Positions of sinks and dilution test sections during the TRUE Block Scale Interference Tests ENW-2, ENW-1, ESV-2 and ESV-1a-c. Overlapping markers represent the same section. The position of the structures are based on the October 1997 structural model (Hermanson, 1998).*

2 EXPERIMENTAL SETUP

2.1 Equipment and tracers used

Each of the four characterization boreholes (KA2511A, KA2563A, KI0023B and KI0025F) is instrumented with 6-9 inflatable packers such that 5-9 borehole sections are isolated. The packer positions are given in the pressure response matrices (Figures 4-1 and 4-2). Each borehole section is connected to a pressure transducer which is connected the Äspö HRL Hydro Monitoring System (HMS). Each of the sections planned to be used for tracer tests are equipped with three nylon hoses, two with an inner diameter of 4 mm and one with an inner diameter of 2 mm. The two 4 mm hoses are used for injection, sampling and circulation of fluids in the borehole section whereas the 2 mm hose is used for pressure monitoring. In borehole KA2511A some special arrangements were made to enable higher flow rates from the source sections by using hoses with 6 mm inner diameter.

Three additional boreholes (KA3510A, KA3573A and KA3600F) associated with the prototype repository were also supplied with pressure transducers connected to field data loggers. The two latter boreholes were also instrumented with double-packer systems, cf. Figure 4-1 for packer positions.

The borehole sections used as sources for the interference tests were connected to a flow regulation unit where flow could be both measured and controlled. The flow data were stored on a field data logger. In a second stage of the test programme (type III tests) the flow was measured manually with a graduated measuring glass and a stopwatch.

The tracer dilution tests were performed using three identical equipment set-ups for tracer tests, i.e. allowing three sections to be measured simultaneously. A schematic drawing of the tracer test equipment is shown in Figure 2-1. The basic idea is to have an internal circulation of the borehole volume. The circulation makes it possible to obtain a homogeneous tracer concentration in the borehole section and to sample the tracer concentration outside the borehole in order to monitor the injection (dilution) rate of the tracer with time.

Circulation was controlled by a pump with variable speed (A) and measured by a flow meter (B). Tracer injections were made with a plunger pump (C1) and sampling was made by continuously extracting a small volume of water from the system through a flow controller (constant leak) to a fractional sampler (D). The tracer test equipment has earlier been used in the TRUE-1 tracer tests, cf. Andersson (1996). The tracers used were Uranine (Sodium Fluorescein) from KEBO (purum quality), Amino G Acid from Aldrich (technical quality) and Rhodamine WT from Holiday Dyes Inc. (technical quality).

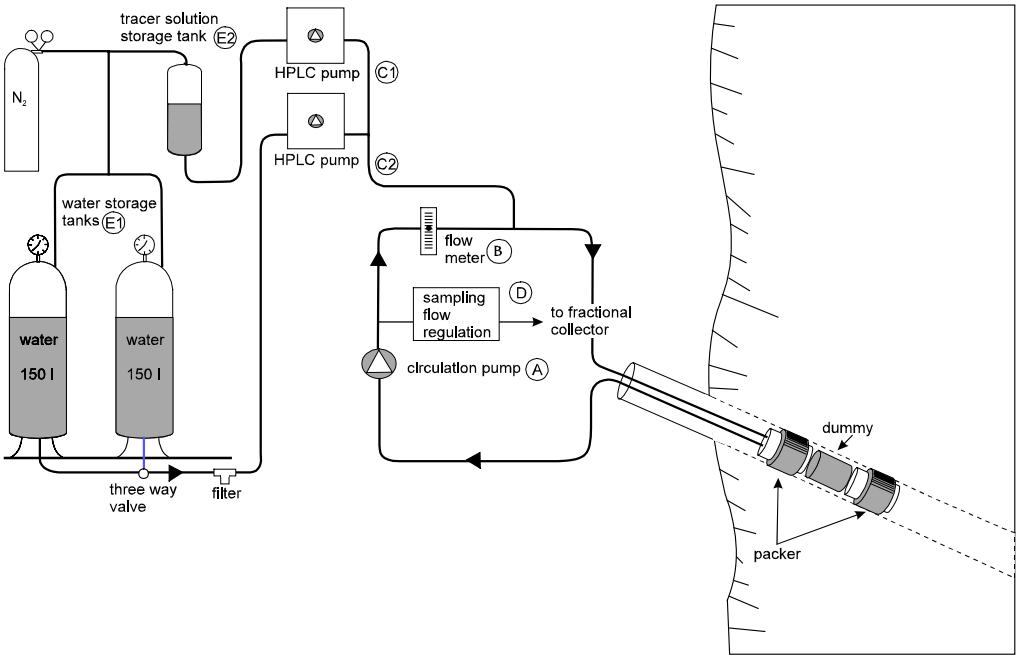

Figure 2-1. *Schematic drawing of the equipment used for tracer tests in the TRUE Project.*

2.2 Performance of interference tests

2.2.1 Measurements of flow rate from open borehole sections

Prior to the start of the interference tests flow rate measurements were made in all sections in boreholes KA2511A, KA2563A, KI0023B, KI0025F, KA3573A and KA3600F by opening of pressure, flow and circulation lines connected to the sections. Water samples were also collected to determine electrical conductivity of the water in each borehole section. This data was used to determine which flow rate to use for the interference tests and for calculation of hydraulic head. The data are presented in Chapter 4.2. Notable is that a partial collapse of the borehole instrumentation in KI0023B occurred a few days after the flow rate measurements. This resulted in a total blocking of sections P1 and P2 and a leakage from section P3 of about 12 ml/min.

2.2.2 Test sequence and duration of the interference tests

The three tests focused on the external network, ENW-1, ENW-2 and ESV-2 were performed in a one week cycle:

Day 1: Start of tracer dilution tests in three sections (Sec 1-3) (natural gradient)

Day 2: Stop of tracer dilution tests in first three sections (Sec 1-3), change of sections and start of tracer dilution tests in three other sections (Sec 4-6) (natural gradient)

Day 3: Start pumping in source section for the interference test

Day 4: Stop dilution test in Sec 4-6, change of sections and start of tracer dilution tests in Sec 1-3 (pump gradient).

Day 5: Stop of pumping in source section.

Day 6-7: Recovery phase for interference test.

The tests focused on structures #9 and #20, ESV-1a-c, were also performed in a similar manner but here only three sections were used for tracer dilution tests and the flow period was shortened to one day thus enabling a shorter duration of the test period. In the last of the type II tests, ESV-1c, the pumping period was prolonged to 19 days due to the tracer injection performed, cf. Chapter 2.2.4. A summary of the test periods and flow rates used during all 19 interference tests is given in Table 2-1.

Both constant flow (CF) and constant head (CH) tests were used partly due to restrictions set by the equipment (not able to regulate flow rates above 5 l/min) and partly for practical reasons. The type of test is also listed in Table 2-1.

The boreholes used for pumping and monitoring of pressure responses in the TRUE Block Scale Interference Tests are listed in Table 2-2 together with the system used for pressure monitoring (HMS system or field logger). In total, 42 sections were monitored of which 19 were used as source section, cf. Figure 2-2.

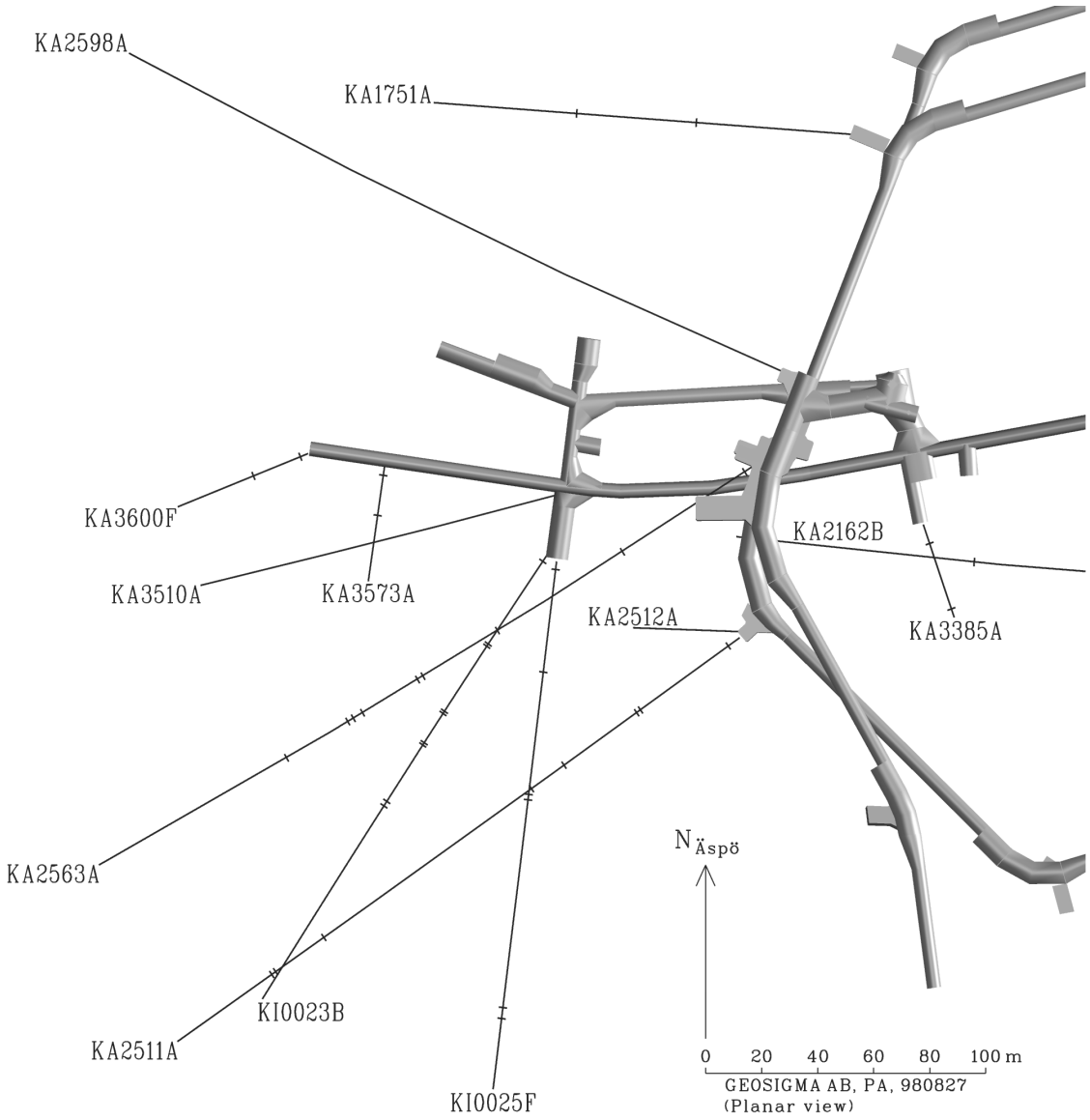

Figure 2-2. *Planar view of the TRUE Block Scale area including all boreholes used for pressure monitoring. The tics on the borehole projections represent packer positions, cf. Figure 4-1 for exact packer positions.*

The logging frequency of the HMS system was manually set before start of each pumping phase and recovery phase by the HMS operator. The logging frequency was set to enable transient evaluation of pressure data. This means a logging frequency of one scan every second during the first ten minutes, one-minute frequency up to two hours and ten-minute frequency up to two days. All pressure transducers were individually calibrated before start of the first interference test.

Boreholes KA1751A and KA2162B were both monitored through a hydraulic multiplexer which enables a maximum logging frequency of 5 and 10 minutes, respectively. The field loggers, used for KA3510A, KA3573A and KA3600F, were set to a predefined sequential measurement frequency ranging from two seconds to one hour.

Table 2-1. Summary of performed interference tests during TRUE Block Scale Preliminary Characterization Stage. (CH=Constant head, CQ=Constant flow). Packer positions are given in Figure 4-1.

Test #	Source section	Test type	Q* (l/min)	S_p ** (m)	Q/s_p (m^2/s)	Flow period (h)	Structure
ENW-2	KA2511A:S5	CQ	3.10	2.9	1.78E-05	48	#7
ENW-1	KA3573A:P2	CH	9.3	36.1	4.29E-06	48	#5
ESV-2	KI0023B:P8	CQ	4.14	7.86	8.78E-06	48	#7
ESV-1a	KA2563A:R5	CQ	1.55	18.9	1.37E-06	24	#20
ESV-1b	KI0025F:R4	CH	0.39	415	1.57E-08	24	#20
ESV-1c	KI0023B:P6	CQ	1.04	62	2.80E-07	384	#9
1	KI0023B:P4	CH	0.8	386	3.45E-08	0.5	#13
2	KA2512A:P1	CH	20	300	1.11E-06	1	#5
3	KA2598A:P1	CH	40	240	2.78E-06	3.5	#1, #8
4	KA2563A:R1	CH	0.23	309	1.24E-08	0.5	#9, #10
5	KA2563A:R4	CH	0.24	307	1.30E-08	0.5	#13, #18
6	KA2511A:S4	CH	3.4	35.8	1.58E-06	0.5	#6, #16
7	KI0025F:R3	CH	0.36	419	1.43E-08	0.5	?
8	KI0025F:R5	CH	0.63	410	2.56E-08	0.5	#6, #7
9	KI0025F:R2	CH	3.6	10.7	5.61E-06	0.5	#19
10	KI0023B:P7	CH	3.8	280	2.26E-07	0.5	#6, #20
11	KI0023B:P5	CH	0.43	414	1.73E-08	0.5	#18
12	KI0023B:P2	CH	1.9	236	1.34E-07	0.5	#19
13	KA3573A:P1	CH	1.2	216	9.26E-08	0.5	#15

* Flow at the end of pumping period
** Drawdown at the end of the pumping period

Table 2-2. Boreholes used for pressure monitoring in the TRUE Block Scale Interference Tests. Packer positions are given in Figure 4-1.

Borehole	# of sections	Monitoring
KA1751A	3	HMS
KA2162B	4	HMS
KA2511A	5	HMS
KA2512	1	Field logger *
KA2563A	7	HMS
KA3385A	2	HMS
KI0023B	9	HMS
KI0025F	6	HMS
KA3510A	1	Field logger
KA3573A	2	Field logger
KA3600F,	2	Field logger

***** Only monitored in two tests.

2.2.3 Tracer dilution tests

The flow rates were determined by tracer dilution tests in three to six sections during each interference test (type I and II). The dilution tests were performed both under natural gradient and under stressed conditions (pumping during interference tests). Thus, it was possible to simultaneously measure both flow and pressure changes due to the pumping. The duration of each tracer dilution test was about 20-24 hours.

In total, 13 borehole section were equipped to enable tracer dilution tests. However, due to a partial collapse of the borehole instrumentation in KI0023B, the three inner sections (P1-P3) could not be used. Sections P5, P7 and P9 in KI0023B were also excluded due to the long section lengths and large volume of these sections. Thus, seven sections were finally chosen for the tracer dilution tests, cf. Table 2-3. The results of the tracer dilution tests are presented in Chapter 3.

Table 2-3. Borehole sections used for tracer dilution tests. Packer positions are given in Figure 4-1.

Borehole/section	Length (m)	Structure(s)
KA2511A:S4	17	#6?, #16
KA2563A:R5	3	#20
KI0025F:R2	4	#19
KI0025F:R4	2	#20
KI0023B:P4	1.0	#13
KI0023B:P6	1.0	#9
KI0023B:P8	1.0	#7

2.2.4 Radially converging tracer test

Interference test ESV-1c also involved tracer injections in three sections, two in the same structure (#20), KI0025F:R4 and KA2563A:R5, and one in the newly identified structure #13, in section KI0023B:P4 (test INW-1a, see Table 1-1). The tracer injections were performed as decaying pulse injections and sampling was performed in the water withdrawn from the source section, KI0023B:P6 (structure #9). The tracers used were three different fluorescent dyes namely, Uranine (KI0025F:R4), Rhodamine WT (KA25623A:R5) and Amino G Acid (KI0023B:P4).

The samples taken during the tracer test were analyzed in direct conjunction with the tests for dye tracer content at the Äspö HRL office using a Turner TD-700 Laboratory Fluorometer. The results are presented in Chapter 4.5.

3 EVALUATION

3.1 Hydraulic interference tests

3.1.1 Qualitative interpretation

The hydraulic responses have been evaluated in different steps in which part of the data has been sorted out for further (quantitative) evaluation. This procedure was necessary in order to restrict the quantitative evaluation to a manageable amount of data.

Firstly, time-drawdown- and time-recovery plots were prepared for sections showing a drawdown (or recovery) of more than s_p=0.2 m by the end of the tests. This threshold value was selected with consideration of the amplitude of the tidal effects. These types of plots were used to estimate the response times (t_R) for each section. The response time is here defined as the time after start of flowing when a drawdown (or recovery) of 1 kPa (0.1 m) is observed in the logarithmic plots for the actual observation section.

To account for the different flow rates used in the tests and to make the response plots comparable between tests, the final drawdown by stop of flowing (s_p) is normalized with respect to the flow rate (Q). The ratio s_p/Q is plotted on the Y-axis. On the X-axis, the ratio of the response time and the squared distance R in space between the (midpoint of the) source section and (the midpoint of) each observation section (t_R/R^2) is plotted. The latter ratio is inversely related to the hydraulic diffusivity of the rock, which parameter indicates the speed of propagation in the rock of the drawdown created in the flowing section. The distances in space between source and observation points, R, are given in Appendix 2 for all tests.

From the response plots of s_p/Q versus t_R/R^2 for each test, sections with anomalous fast response times (high hydraulic diffusivity) and large (normalized) drawdowns can be identified. Such sections showing primary responses can be assumed to have a distinct hydraulic connection to the flowing section and may be intersected by fracture zones or other conductive structures in the rock. On the other hand, sections with delayed and weak responses may correspond to sections in the rock mass between such structures.

From the calculated values of s_p/Q (index 1) and t_R/R^2 (index 2) for each observation section during each test a common response matrix, showing the response patterns for all tests, was prepared by classifying the responses by means of the above index 1 and -2. For index 1 the following class limits and drawdown characteristics were used:

Index 1 (s_p/Q)

$s_p/Q > 1 \cdot 10^5$ s/m^2	Excellent
$3 \cdot 10^4 < s_p/Q \leq 1 \cdot 10^5$ s /m^2	High
$1 \cdot 10^4 < s_p/Q \leq 3 \cdot 10^4$ s /m^2	Medium
$s_p/Q \leq 1 \cdot 10^4$ s /m^2	Low

For index 2 the following class limits and response characteristics were used:

Index 2 (t_R/R^2)

$t_R/R^2 < 0.01$ s/m^2	Excellent (E)
$0.01 \leq t_R/R^2 < 0.1$ s/m^2	Good (G)
$0.1 \leq t_R/R^2 < 0.3$ s/m^2	Medium (M)
$t_R/R^2 \geq 0.3$ s/m^2	Bad (B)

The most significant responses during each test are also displayed graphically in the actual borehole array in two different projections.

The results from the qualitative analysis were compared with the structural (October 97) model and checked for consistency and eventual need of revision. It should be pointed out that the response diagrams of s_p/Q versus t_R/R^2 described above were only used as a diagnostic tool to identify the most significant responses during each test and to construct the response matrix. The diagrams should be used with some care since the true distances (along pathways) between the source and observation sections are uncertain which may affect the position of a certain section in the horizontal direction in the diagrams. However, in most cases, the shortest distance between the source and observation section, as used here, is considered as a sufficient and robust approximation for the above purpose.

Another potential source of error in the response diagrams may occur if (internal) hydraulic interaction exists between sections along an observation borehole. For example, such interaction could either be due to packer leakage (insufficient packer sealing) or rock leakage through interconnecting fractures around the packers. This fact may give a false impression that good hydraulic communication exists between such observation sections and the actual source section. However, any analysis method will suffer from this potential source of error.

3.1.2 Quantitative interpretation

The main purpose of the quantitative interpretation of the interference tests in this study is to estimate the hydraulic parameters and the hydraulic characteristics of the most significant responses during each test as identified from the qualitative interpretation. The transmissivity, storativity and hydraulic diffusivity, and in some cases also the leakage coefficient, are estimated from the tests. The estimated hydraulic parameters may represent the hydraulic properties of some of the fracture zones tested. In addition, the quantitative interpretation also provides some (soft) information on the flow geometry during the tests including effects of outer hydraulic boundaries.

The quantitative interpretation was made using the code AquiferTest (Waterloo Hydrologic). As a standard interpretation model, the Hantush model for constant flow rate tests in a leaky (or non-leaky) aquifer with no aquitard storage was used. This model was used because of its generality and its ability to analyse pure radial flow (Theis' type curve) as well as leaky (pseudo-spherical) flow. The type curve for r/L=0 in the Hantush' model (no leakage) corresponds to the classical Theis' type curve for radial flow. In the analysis of the constant head tests, a varying flow rate was applied. In addition, tests showing periods with (pseudo)radial flow were analyzed by Cooper-Jacob's method in semi-logarithmic graphs. The drawdown curves were analyzed as a function of the actual time since start of flowing whereas the recovery curves were analysed by plotting the recovery versus the equivalent time dt_e.

In addition, the derivative of the drawdown (or recovery) was used as a diagnostic tool in the interpretation of the flow geometry and deduction of hydraulic boundaries. The derivative was generated by the SKB-code PUMPKONV and plotted together with the drawdown/recovery curves in logarithmic diagrams.

To reduce the interpretation work, only the drawdown curves were used for analysis except for tests ENW-1 and ESV-1a in which the recovery curves were used due to disturbances of other activities in the tunnel during the drawdown phase, cf. Chapter 4-1. In cases of undisturbed tests the drawdown and recovery curves were quite similar.

3.2 Tracer dilution tests

Flow rates were calculated from the decay of tracer concentration versus time through dilution with natural unlabelled groundwater, c.f. Winberg (*ed*), (1996).

The dilution of tracer with time in the injection sections was determined by analyzing the samples withdrawn from the sections. The so-called "dilution curves" were plotted as the natural logarithm of concentration versus time. Theoretically, a straight line relationship exists between the natural logarithm of the relative tracer concentration (c/c_0) and time (t):

$$Q_{bh} = -V \cdot \Delta \ln (c/c_0) / \Delta t \qquad 3\text{-}1$$

where Q_{bh} (m^3/s) is the groundwater flow rate through the borehole section and V (m^3) is the volume of the borehole section. The flow, Q_{bh}, may be translated into Darcy velocity by taking into account the distortion of the flow caused by the borehole and the angle between borehole and flow direction, c.f. Rhén et al. (1991). The relation between the flow in the rock, the Darcy velocity, q_w (m/s), and the measured flow through the borehole with a dilution test, Q_{bh}, can be expressed as:

$$Q_{bh} = q_w \cdot L_{bh}^2 \left[r_d \cdot \alpha \cdot \sin\beta + \pi \cdot \cos\beta \left(\frac{a_{D1}}{2} + \frac{a_{D2}}{4} + \frac{a_{D3}}{6} \right) \right] \quad 3\text{-}2$$

where

$$r_d = \frac{2r_w}{L_{bh}} \quad 3\text{-}3$$

Assuming a 90° angle between borehole and flow direction the relationship between Q_{bh} and q_w may be estimated from

$$Q_{bh} = q_w \cdot L_{bh} \cdot 2r_w \cdot \alpha \quad 3\text{-}4$$

where L_{bh} is the length of the borehole section (m), r_w is the borehole radius (m) and α is the factor accounting for the distortion of flow caused by the borehole. The factor α was given the value 2 in the calculation, which is the theoretical value for a homogeneous porous media.

3.3 Tracer test

The evaluation of the tracer test has involved computer modelling using a simple one-dimensional advection-dispersion model (Van Genuchten & Alves, 1982). From the computer modelling, dispersivity and mean travel times were determined using an automated parameter estimation program, PAREST (Nordqvist, 1994). PAREST uses a non-linear least squares regression where regression statistics (correlation, standard errors and correlation between parameters) also is obtained.

The chosen one-dimensional model assumes a constant fluid velocity and negligible transverse dispersion, cf. Equation 3-5.

$$\partial C/\partial t = D(\partial^2 C/\partial x^2) - v \cdot \partial C/\partial x \quad 3\text{-}5$$

where: D = Dispersion coefficient
v = fluid velocity (m/s)
C = concentration of solute
x = distance from injection point (m)
t = time (s)

According to Ogata & Banks (1961) and Zuber (1974), the dispersion in a radially converging flow field can be calculated with good approximation by equations valid for one-dimensional flow. Although a linear flow model (constant velocity) is used for a converging flow field, it can be demonstrated that breakthrough curves and parameter estimates are similar for Peclet numbers of about 10 and higher.

Van Genuchten (1982) gives a solution for a step input with dispersion over the injection boundary. The solution of Equation 3-5, then is:

$$C/C_o = \tfrac{1}{2}\,\mathrm{erfc}\,[(x-v\cdot t)/Z] + (V/\pi)^{1/2}\exp\,[(x-v\cdot t)^2/(4D\cdot t)] - \tfrac{1}{2}\,[1+v\cdot x/D+V]\exp\,[v\cdot x/D]\,\mathrm{erfc}[(x+v\cdot t)/Z] \qquad 3\text{-}6$$

where: $Z = 2(D\cdot t)^2$
$V = v^2 t/D$

Variable injection scheme was simulated by superposition of the solution given in Equation 3-6.

The fit of the breakthrough curves using a three-parameter fit included velocity, v, dispersion coefficient, D, and the so called F-factor which corresponds to injected mass divided by fracture volume, M_{inj}/V_f. The result of the evaluation is presented in Chapter 4.5.

Based on the mean travel times, t_m, determined from the parameter estimation, the hydraulic fracture conductivity, K_{fr} (m/s), was calculated assuming radial flow and validity of Darcy's law (Gustafsson & Klockars, 1981);

$$K_{fr} = \ln (r/r_w)\,(r^2-r_w^2)/2\cdot t_m\cdot\Delta h \qquad 3\text{-}7$$

where: r = travel distance (m)
r_w= borehole radius (m)
t_m= mean travel time of tracer (s)
Δh= head difference (m)

The equivalent fracture aperture, b (m), was calculated from:

$$b = Q\cdot t_m/\pi\cdot(r^2-r_w^2) \qquad 3\text{-}8$$

where Q (m^3/s), is the mean pumping rate.

Flow porosity, θ_k, was calculated using:

$$\theta_k = K/K_{fr} \quad (3\text{-}9)$$

where K is the hydraulic conductivity of the packed-off section of the borehole determined from steady state evaluation of the interference test (Moye, 1967):

$$K = (Q/\Delta h \cdot L) \cdot ((1+\ln L/2r_w)/2\pi) \quad (3\text{-}10)$$

where L (m) is the length of the packed-off section. It should be noted that the term flow porosity may be misleading to use in a fractured heterogeneous rock as it is defined for a porous media. However, it is often used in fractured media as a scaling factor for transport, but then defined over a finite thickness which, in his case, is defined as the length of the packed-off borehole section (L = 1.0 m).

The values calculated using Equations 3-7 to 3-10 are presented together with parameters determined from the numerical modelling of the conservative tracer breakthrough in Table 4-5.

4 RESULTS AND INTERPRETATION

4.1 Log of events

The TRUE Block Scale Interference Tests were performed in two campaigns, between March 3rd and April 29th, 1998 (type I- and II-tests) and between May 18th to May 20th, 1998 (type III-tests). Several other activities were ongoing in the Äspö HRL during this period. Some of these activities have affected the pressures in the Block Scale area. There are especially two other activities interfering with some of the tests namely the LaScala Project (hydraulic single-hole tests in borehole KA2598A) and the Chemlab Project (removal and insertion of the Chemlab probe in borehole KA2512A). The events presented in Table 4-1 lists all activities that possibly have affected each test.

Table 4-1. Log of events for the TRUE Block Scale Interference Tests.

Date	Activity	Comment
980305-980306	Flow measurements from tubing of KA2511A, KA2563A, KI0023B, KI0025F, KA3573A and KA3600F	Pressure measurements partly disturbed by water sampling programme
980309	Start of dilution tests in KI0025F:R2 and KI0023B:P4	Test in KA2563A:R5 stopped due to leakage in equipment
980310	Start of dilution tests in KI0025F:R4, KI0023B:P8 and KA2511A:S4	Partial collapse of equipment in KI0023B discovered (sections P1-P3 affected)
980311	Start of interference test ENW-2, pumping in KA2511A:S5	Disturbance in drawdown phase from opening of KA2598A
980312	Start of dilution tests in KI0025F:R2, KI0023B:P4 and KA2563A:R5	
980313	Stop pumping, test ENW-2	Disturbance in recovery phase from opening of KA2598A
980316	Start of dilution tests in KI0025F:R2, KI0023B:P4 and KA2511A:S4	
980317	Start of dilution tests in KI0025F:R4, KI0023B:P6 and KA2563A:R5	
980318	Start of interference test ENW-1, pumping in KA3573A:P2	Disturbance in drawdown phase from opening of KA2512A
980319	Start of dilution tests in KI0025F:R2, KI0023B:P4 and KA2511A:S4	
980320	Stop pumping, test ENW-1	
980323	Start of dilution tests in KI0025F:R4, KI0023B:P6 and KA2563A:R5	
980324	Start of dilution tests in KI0025F:R2, KI0023B:P4 and KA2511A:S4	Disturbance from opening of KA2598A used as type III interference test

Date	Activity	Comment
980325	Start of interference test ESV-2, pumping in KI0023B:P8	
980326	Start of dilution tests in KI0025F:R4, KI0023B:P6 and KA2563A:R5	Disturbance from opening of KA2598A
980327	Stop pumping, test ESV-2	
980330	Start of dilution tests in KI0025F:R4, KI0023B:P6 and KA2511A:S4	
980331	Start of interference test ESV-1a, pumping in KA2563A:R5	Disturbance in drawdown phase from opening of KA2598A
980401	Stop pumping, test ESV-1a	Disturbance in recovery phase from opening of KA2598A
980402	Start of dilution tests in KI0023B:P4, KI0023B:P6 and KA2563A:R5	
980403	Start of interference test ESV-1b, pumping in KI0025F:R4	
980404	Stop pumping, test ESV-1b	
980406	Opening of borehole KA2512A	Used as type III interference test
980407	Start of dilution tests in KI0025F:R4, KI0023B:P4 and KA2563A:R5	Disturbance from opening of KA2598A
980408	Start interference test ESV-1c, pumping in KI0023B:P6	
980415	Tracer injections in KI0023B:P4, KI0025F:R4 and KA2563A:R5	
980415-980424	Tracer sampling in water from KI0023B:P6	
980424	Stop pumping, test ESV-1c	
980427	Interference test (type III) in KI0023B:P4	
980518	Interference tests (type III) in KA2563A:R1, KA2563A:R4 and KA2511A:S4	
980519	Interference tests (type III) in KI0025F:R3, KI0025F:R5, KI0025F:R2 and KI0023B:P7	
980520	Interference tests (type III) in KI0023B:P5, KI0023B:P2 and KA3573A:P1	

4.2 Initial conditions

Before starting the actual test sequence some initial measurements were made to determine the initial conditions regarding hydraulic head, flow rates and electrical conductivity of pumped water from the borehole sections in the TRUE Block Scale area, cf. Table 4-2.

Table 4-2. Results of flow and electrical conductivity measurements from open borehole sections in the TRUE Block Scale area.

Borehole	sec	Flow (ml/min)	No. of tubes	Tube dim (mm)	El. Cond. (mS/m)	Hydraulic head (masl)	Structure #
KA2511A	S1	<10	1	8/6	No sample	Tight	18
KA2511A	S2	250	1	4/2	1020	-27.44	10
KA2511A	S3	350	1	4/2	976	-30.68	17,19,20
KA2511A	S4	3360	2	6/4	1160	-31.47	6,16
KA2511A	S5	4800	1	8/6	1120	-35.41	7
KA2563A	R1	230	1	4/2	1220	-26.46	9,10
KA2563A	R2	<10	1	4/2	No sample	Tight	19
KA2563A	R3	<10	1	4/2	No sample	Tight	?
KA2563A	R4	310	1	4/2	1340	-28.90	13,18
KA2563A	R5	1840	2	6/4	1440	-28.00	20
KA2563A	R6	1350	1	6/4	1280	-32.20	6,7
KA2563A	R7	2160	1	6/4	1030	-39.19	4,5,17
KI0023B	P1	(2460)	1	6/4	1260	-21.66	10
KI0023B	P2	(2020)	2	6/4	1440	-26.98	19
KI0023B	P3	(42)	2	6/4	1180	Leaking	?
KI0023B	P4	840	2	6/4	1720	-30.31	13
KI0023B	P5	420	2	6/4	1570	-28.27	18
KI0023B	P6	2840	2	6/4	1570	-28.65	9
KI0023B	P7	3440	2	6/4	1560	-29.90	6,20
KI0023B	P8	6300	2	6/4	1420	-35.72	7
KI0023B	P9	6400	2	6/4	1560	-47.74	5
KI0025F	R1	300	1	4/2	1660	-24.78	Z
KI0025F	R2	3530	2	6/4	1740	-25.07	19
KI0025F	R3	290	1	4/2	1660	-26.71	?
KI0025F	R4	720	2	6/4	1720	-28.07	20
KI0025F	R5	600	1	4/2	1580	-35.40	6,7
KI0025F	R6	280	1	4/2	1640	-38.08	5
KA3573A	P1	10000	3	6/4	1090	-	15
KA3573A	P2	28125	3	6/4	1140	-	5
KA3600F	P1	730	1	4/2	1250	-	15?
KA3600F	P2	1280	1	4/2	1120	-	5,7

The flow rates presented in Table 4-2 are in most cases not reflecting the hydraulic conductivity of the borehole sections due to the restrictions given by the tubing dimension (inner diameter), length, and number of tubes available for flow. However, these flow rates served as a good design basis for the interference tests. The values within brackets for borehole KFI0023B represent values determined prior to the collapse of the equipment, cf. Chapter 2.2.1.

The hydraulic head values, determined from the Äspö Hydro Monitoring System (HMS), show a generally sinking trend towards the tunnel. The only exceptions are the two sections associated with structure #13, KA2563A:R4 and KI0023B:P4, which seem to have lower head than surrounding sections. The gradients within different structures are discussed in Chapter 4.4.

4.3 Hydraulic interference tests

4.3.1 Response matrix and qualitative interpretation

The hydraulic responses were plotted in response diagrams for each test and summarised in a response matrix according to the procedures described in Chapter 3.1. The response matrix was divided into two separate sheets to get a better readability where the first sheet (Figure 4-1) shows all type I and II-tests and the three longest type III-tests (tests #1-3) while the second sheet (Figure 4-2) shows the 10 short-term type III-tests (tests #4-13).

The most significant responses during each interference test, identified from the response matrixes and the response diagrams described in Chapter 3.1, are presented and discussed below. An example of a response diagram showing the most significant responses is shown in Figure 4-3 for test ENW-2. The most significant responses are found towards the upper left corner of the diagram, i.e. sections with high values of s_p/Q (large specific drawdown) and low values of t_R/R^2 (high hydraulic diffusivity), in this case KI0023B:P8, KI0025F:R5, KA3600F:P1-P2, KA3573A:P1-P2, KA2563A:R6 and KA3510A:P1. The most significant responses identified during each test can be found in Table 4-3a-b and in Figures 4-8 to 4-13. The data point labels in the figures are a shortened version of the borehole section labels where the first letters are omitted and the last number refers to the section number. The response diagrams for all 19 tests are presented in Appendix 1.

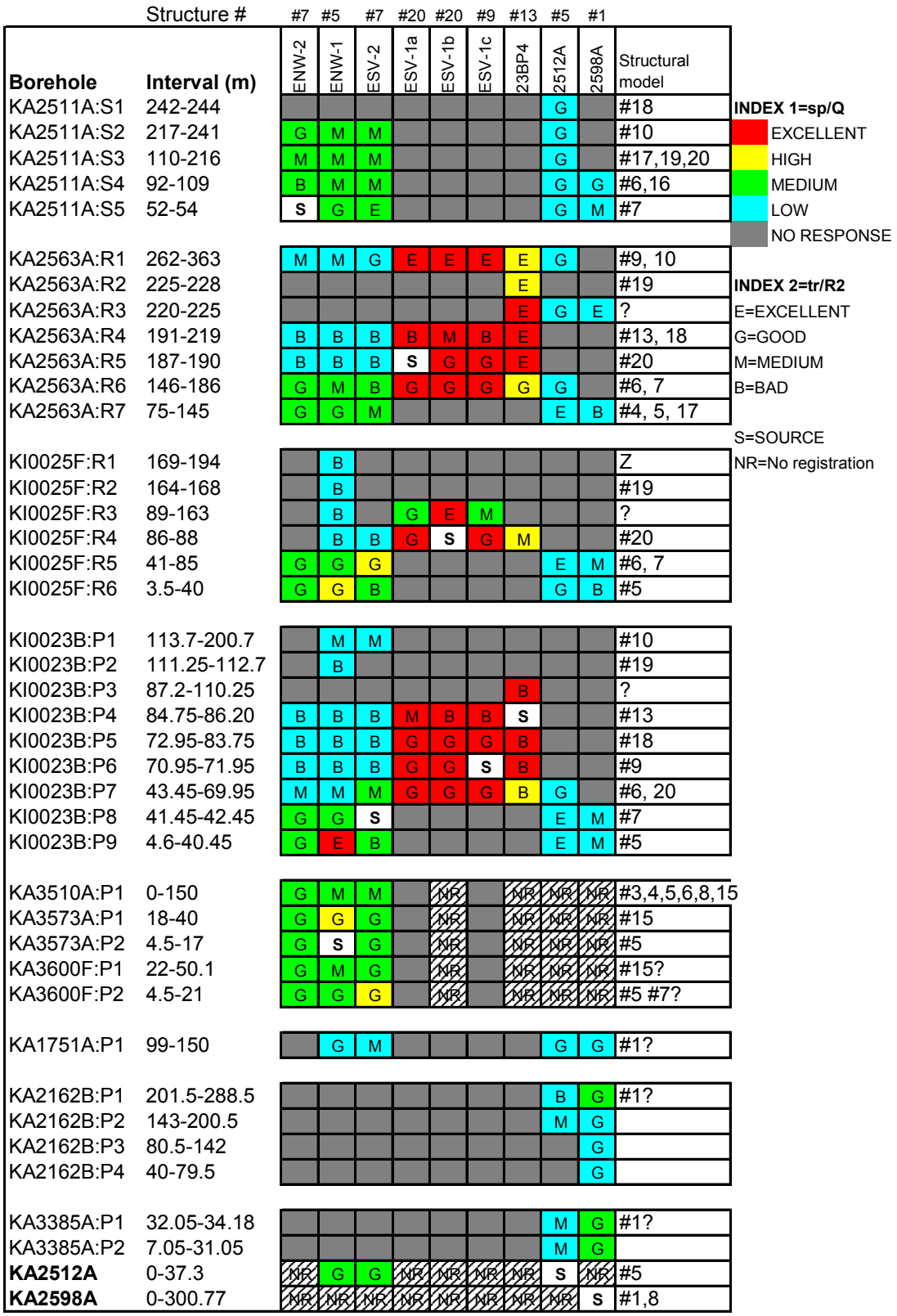

Figure 4-1. *Response matrix for TRUE Block Scale Interference Tests ENW-1-2, ESV-2, ESV-1a-c (type I and II) and # 1-3 (type III).*

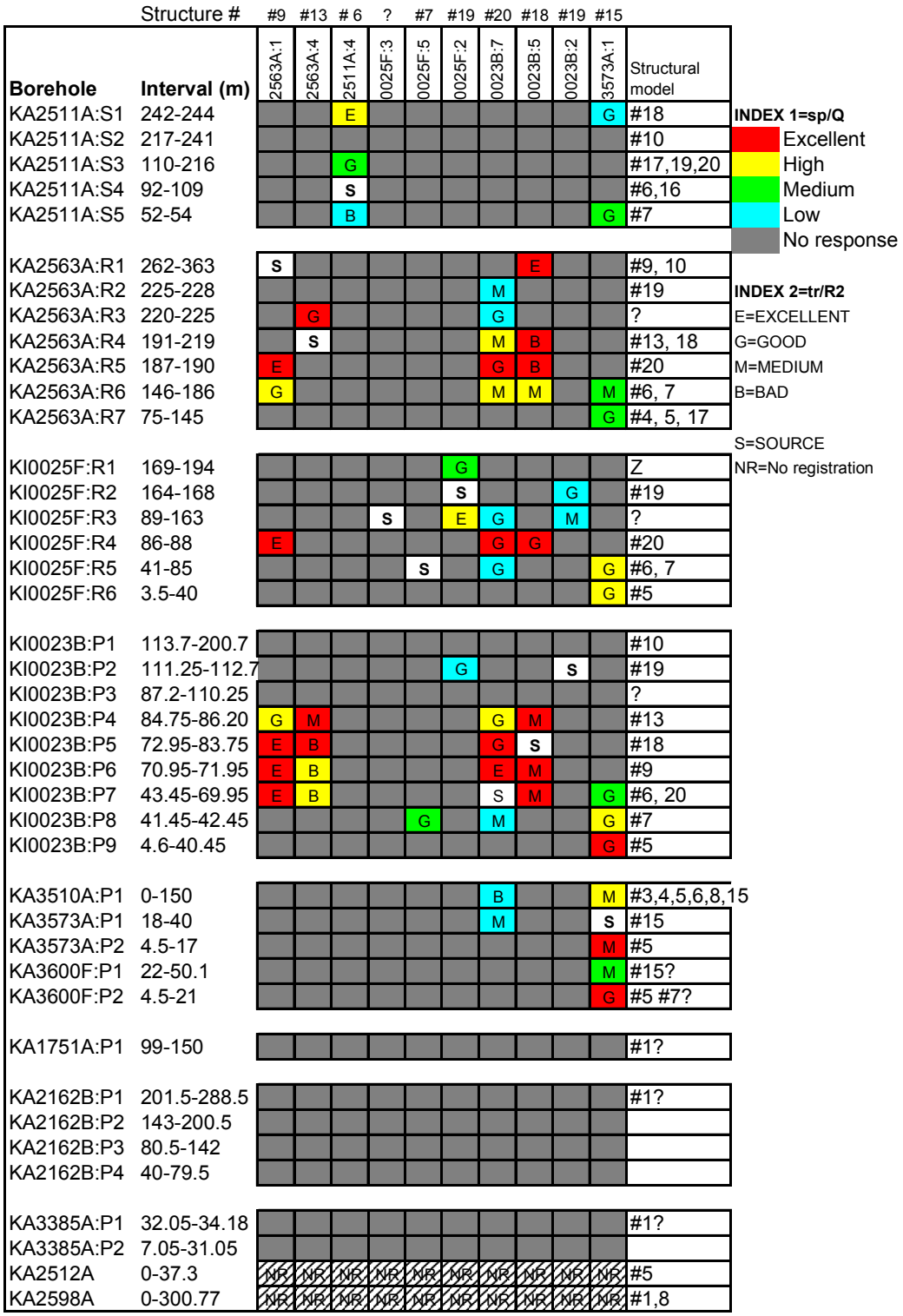

Figure 4-2. *Response matrix for TRUE Block Scale Interference Tests # 4-13 (type III).*

An example of the graphical representations of the most significant responses is shown in Figures 4-4a and 4-4b for tests ENW-2 and ESV-1b. Figure 4-4a shows a horizontal projection from above and Figure 4-4b a perpendicular vertical projection seen from east to west. The figures show the propagation of the disturbance created at the source in preferential directions. Three-dimensional vectors are drawn from the source section to the most significant responses in the receiver boreholes. The vectors intersect the receiver sections at conductive intervals as identified from e.g. flow logging or other investigations in the boreholes. The implications of the qualitative analysis on the structural (October 97) model is discussed below and summarised in Chapter 5.2.

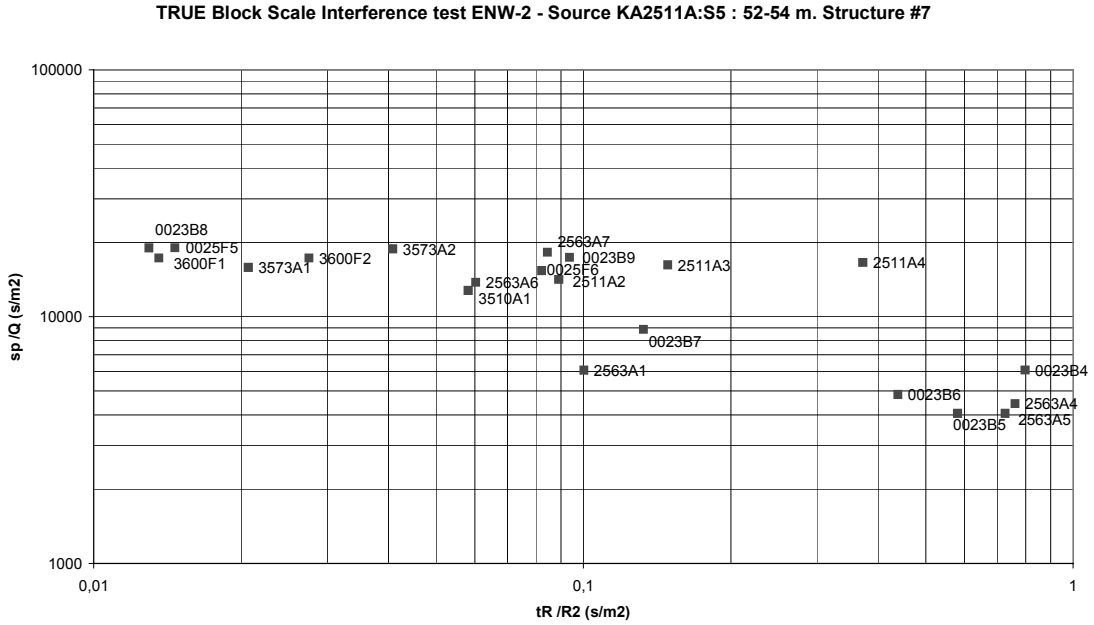

Figure 4-3. *Identification of the most significant responses in the observation boreholes during test ENW-2.*

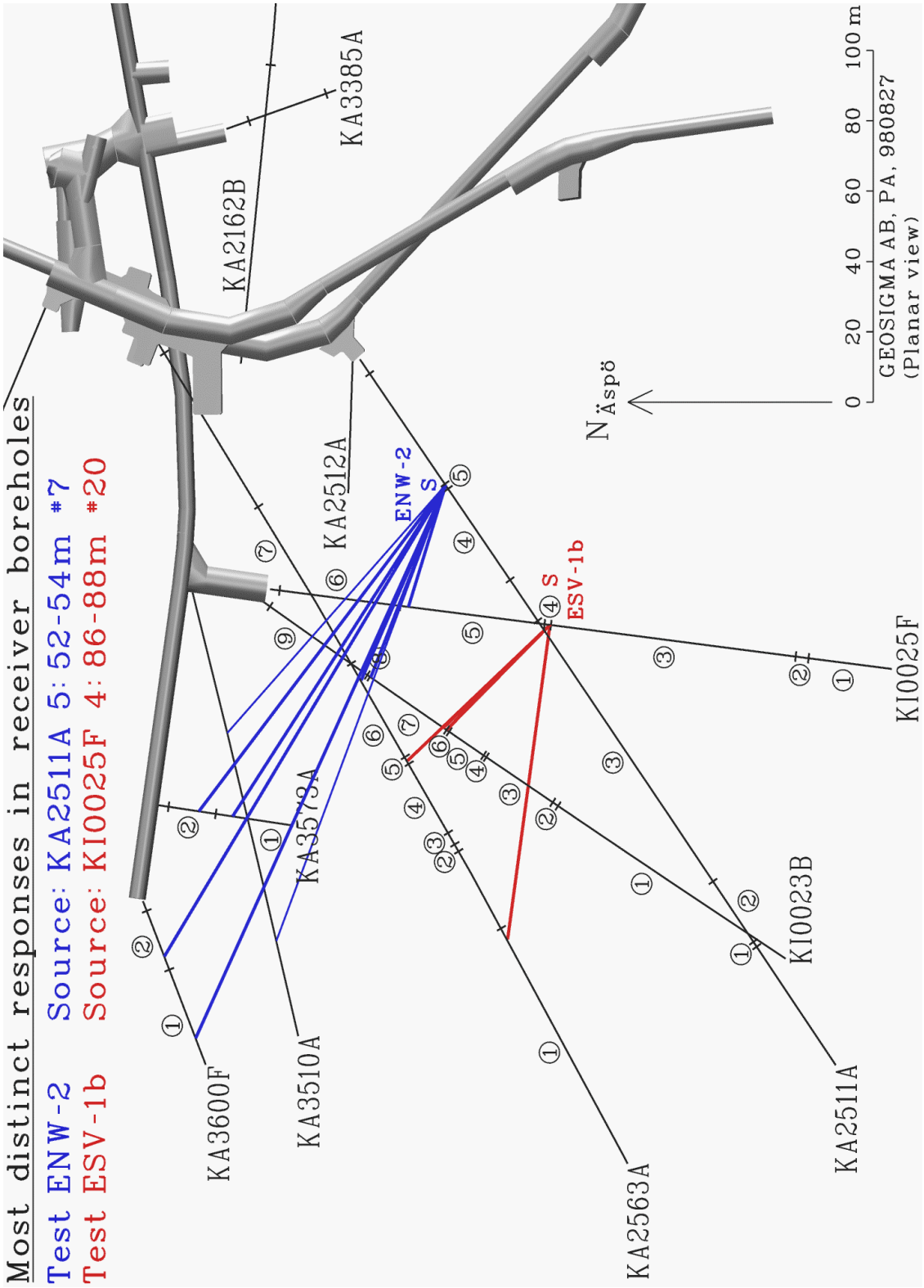

Figure 4-4a. *Graphical representation of the most significant responses in the observation boreholes during tests ENW-2 (blue) and ESV-1b (red). Horizontal projection from above. The numbers along the boreholes denote the observation sections in the boreholes.*

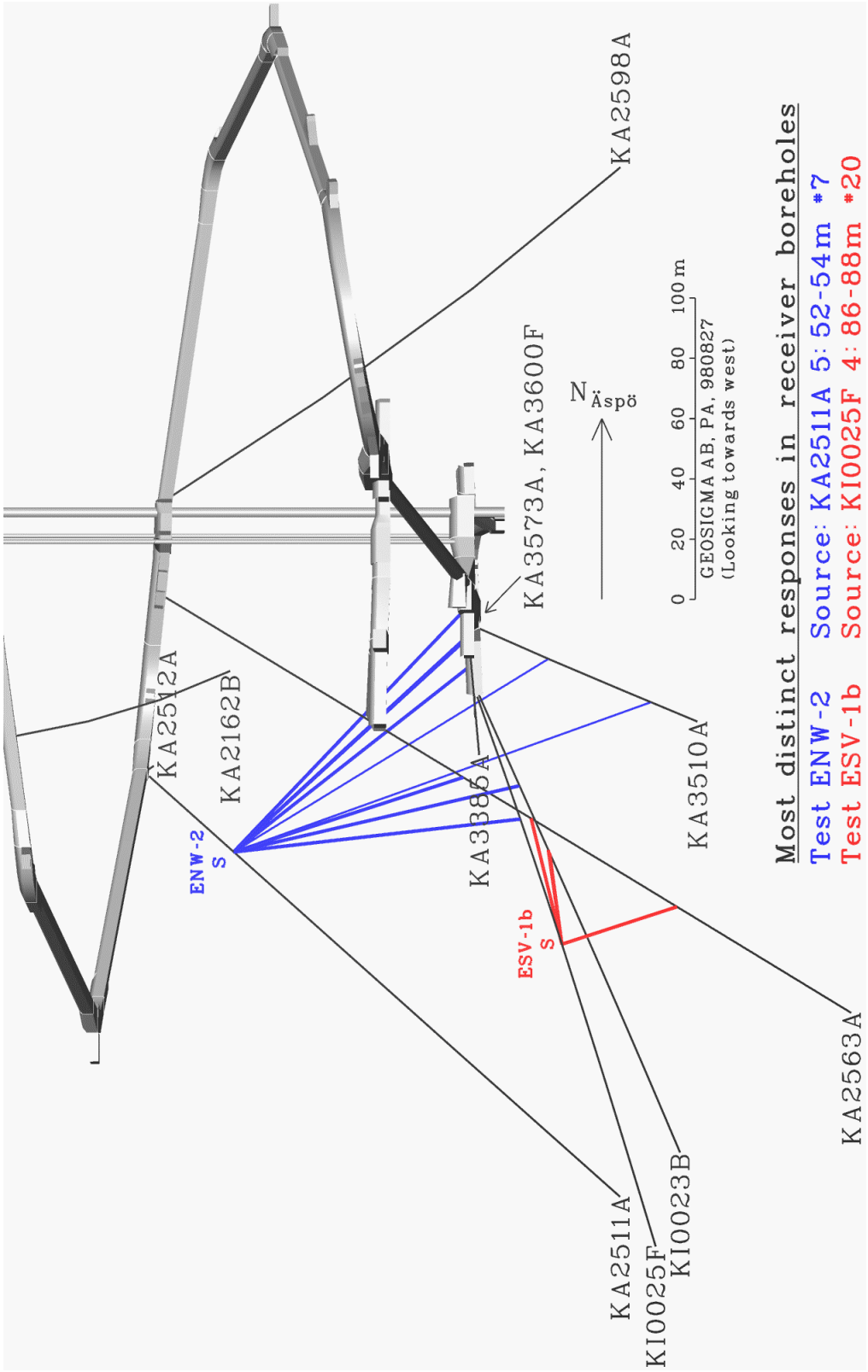

Figure 4-4b. *Graphical representation of the most significant responses in the observation boreholes during tests ENW-2 (blue) and ESV-1b (red). Perpendicular vertical projection looking from east to west. The numbers along the boreholes denote the observation sections in the boreholes.*

Test ENW-2 (structure #7)

The test shows a global response pattern with good responses in all sections intersecting structures #5, #6, and #7, cf. Figure 4-1. Secondary responses are also noted in structures #9 and #20. Both sections interpreted to intersect structure #7 according to Hermanson (1998), KI0025F:R5 and KA2563A:R6, respond well. The highest and fastest response was noted in section KI0023B:P8 which was interpreted to contain structure #6 in the October-97 model. Based on the hydraulic responses it is most likely that structure #7 intersects this section. This is also consistent with the updated September-98 model (Hermanson, in prep.). The good response in section KA3600F:P1 may indicate that this section is intersected by structure #7. In this case, the orientation of the structure needs to be slightly modified. However, according to this interpretation the structure should also intersect KA3510A, which also responds well hydraulically, but no such intercept was found (Hermanson, 1998). The good responses in KA3573A can be explained by good hydraulic communication with structures #5 and #15.

Test ENW-1 (structure #5)

This test shows a similar response pattern as test ENW-2 indicating that structures #5 and #7 are well connected hydraulically, cf. Figure 4-1. The sections intersected by structure #5 according to Hermanson (1998), KA2563A:R7, KA3510A:P1 and KI0025F:R6 respond well. An extremely high and fast response was noted in section KI0023B:P9, which is consistent with the orientation of structure #5. A very fast response was also noted in borehole KA2512 indicating that this borehole is intersected by structure #5, possibly in the flowing section at the end of the borehole (at 37 m borehole length). The good response in KA3600F:P2 supports the extension of structure #5 to the west. Notable is also the good response in KA1751A:P1 located 250 m from the source section. This response may be transmitted through structure EW-1 or through structure #8. A very fast response was also measured in the surface borehole section HAS04:P1 which is located about 300 m above the source section. This shows that structure #5 may be extended over several hundred meters also in the vertical direction.

Test ESV-2 (structure #7)

This test was originally designed to test structure #6. However, the updating of the structural model indicated that the source section KI0023B:P8 is intersected by structure #7 instead. The test has an almost identical response pattern as test ENW-2, cf. Figure 4-1. The four fastest and highest responses (KA3600F:P2, KI0025F:R5, KA2511A:S5 and KA3573A:P1) are all found in sections intersected by structure #7 while sections that are interpreted to be intersected by structure #6 (KA2563A:R6, KA2511A:S4) have delayed responses. Thus, the conclusion would be that the updated model (Hermanson, in prep.) is correct. Also in this test section KA1751A:P1 responds well which may be explained in the same way as in test ENW-1.

Test ESV-1a-c (structure #20, #9)

These three tests show very similar response patterns with excellent responses in the sections interpreted to be intercepted by structure #20, KA2563A:R5, KI0023B:P7 and KI0025F:R4. However, very good responses are also noted in several sections adjacent to these in each borehole, in particular sections P6 and P7 in KI0023B and KA2563A:R6. One explanation for this may be that there are several parallel or subparallel structures to #20. An excellent response is also noted in section KA2563A:R1, interpreted to be intersected by structure #9, in all three tests. This suggests that structure #9 exists and has a good hydraulic communication with structure #20. It should also be noted that test ESV-1c (KI0023B:P6) originally was designed to test structure #20. However, due to a slight change of packer positions compared to the original plan, structure #20 intercepts section P7 instead while section P6 contains structure #9.

Test #1, KI0023B:P4 (structure #13)

This test was performed in a structure not included in the October 97 model but later identified as a new structure (#13) having an orientation of 318/89 (strike/dip), i.e. parallel to #20 (Hermanson, in prep.). The test gives very good responses in sections R1-R6 in borehole KA2563A, cf. Figure 4-1. The far best response is monitored in section KA2563A:R4 which corresponds well with the interpreted intercept of structure #13, c.f. test #5. The response is also good in adjacent sections in borehole KI0023B. The overall response pattern is very similar to tests ESV-1a-c suggesting that the structure is hydraulically well connected to structure #20 and structure #9. The lack of responses in KA2511A and in KI0025F (other than section R4) indicates that the structure has a limited extension.

Test #2, KA2512:P1 (structure #5)

During the performance of the interference test programme it was noticed that the opening of borehole KA2512A caused large pressure disturbances in parts of the block. Thus, this test was not performed as a proper interference test but more a way to study these pressure disturbances qualitatively. The response matrix (Figure 4-1) shows the best responses in structures #5 and #7 which strengthens the assumption that the borehole penetrates structure #5. This is also observed in tests ENW-1 and ESV-2. There are also responses in boreholes KA2162A and KA3385A which indicates that structure #5 and #1 are hydraulically connected which also is consistent with the current structural model.

Test #3, KA2598A:P1 (structure #1, #8)

Borehole KA2598A was used for hydraulic tests in different scales (LaScala Project) and these tests were performed during the same time period as the interference tests. It was noticed that when KA2598A was opened to the atmosphere for change of the equipment, pressure responses were monitored in the Block Scale area. The response matrix (Figure 4-1) shows three good responses in KA2162B:P1, KA3385A:P1 and P2 and KA1751A:P1 indicating that structure #1 is well connected to KA2598A possibly through sub-parallel structures intersecting KA2598A between 10-20 meters borehole length. Analyses of earlier disturbances from opening of KA2598A also shows very good pressure responses in the outer part (0-75 m) of KA2563A where structure #1 intersects the borehole. This section was not measured during the interference tests (blind section). Another observation from the response matrix is that structures #5 and #7 respond. This could be explained by the existence of structure #8. This is also strengthened by the response in borehole section KA2563A:R3. One possibility is that structure #8 has hydraulic characteristics similar to structure NE-2, i.e. having higher hydraulic transmissivity in the shallower parts than in the lower parts of the laboratory.

Test #4, KA2563A:R1 (structure #9, #10)

This test shows very good responses in all sections intersected by structure #20. Good responses are also registered in KI0023B:P4, P5 and P6. This response pattern suggests that structure #9 exists and is well connected to structure #20. The response pattern is very similar to the test in structure #20. The multiple responses in KI0023B may indicate that several well interconnected minor structures exist in between structures #20 and #19.

Test #5, KA2563A:R4 (structure #13, #18)

The test in this section gives good responses in KI0023B:P4-P7 which indicates that this structure is hydraulically well connected to structure #20. However, the hypothesis that structure #18 is the hydraulic connector is questionable due to the fact that section KA2563A:R5 does not respond although the distance to the source is short. A more likely explanation is that the hydraulic responses are transmitted through a parallel or sub-parallel structure to #20. This is also indicated by the detailed flow logging (Gentzschein, 1997) where the major flow in this section was found in the section 205-210 m (Q=0.66 l/min) corresponding to the new identifed structure #13 (Hermanson, in prep.).

Test #6, KA2511A:S4 (structure #6, 16)

This section has been interpreted to be intersected by structures #6 and #16. However, the test only gives responses in the source borehole (sections S1, S3 and S5). The strong response in section S1 may be a "squeezing effect" caused by the influence of the pressure release in section S4 on the tubing from section S1 passing through. Such influence may occur in sections with low transmissivity (which is the case for section S1). The lack of responses in structure #6 indicates that the current interpretation of this structure is questionable, c.f. the discussion under test ESV-2.

Test #7, KI0025F:R3 (structure #?)

This test gives no hydraulic responses at all. However, the flow rate and resulting pressure drop was relatively small in the source section (0.2 l/min and 340 kPa, respectively) which partly may explain the lack of responses. This section did respond in tests ESV-1a-c and is likely to be intersected by some minor structures sub-parallel to #20.

Test #8, KI0025F:R5 (structure #7)

Only section KI0023B:P8 responds to this test possibly due to the limited radius of influence of the test. The responding section is interpreted to be intersected by structure structure #7, cf. the discussion of test ESV-2 above.

Test #9, KI0025F:R2 (structure #19)

This test in structure #19 confirms the existence and extension of the structure. The response in KI0025F:R1 suggests that structure #19 is well connected to structure Z. The lack of responses in other sections indicates that structure #19 has a limited hydraulic connectivity to the rest of the block. The lack of responses in section KA2563A:R2 and in borehole KA2511A indicates that structure #19 has a lower transmissivity, or does not exist, at a higher level in the laboratory.

Test #10, KI0023B:P7 (structure #6, #20)

The response pattern in this test is quite complicated to interpret. It is clear that structure #20 responds extremely well but also sections interpreted to be intersected by structure #6. A possible explanation is that this section is intersected by both these structures. The flow from this section was relatively high (3.6 l/min) Based on the detailed flow log (Gentzschein, 1998) and the current packer positioning it is likely that most of the water comes from the section 66-69.95 m, i.e. structure #20. The flow log also showed a minor inflow of 0.6 l/min between 46-51 m that could be in connection with structure #6 at 44 m borehole length.

Test #11, KI0023B:P5 (structure #18)

The test gives very good responses in structure #20, but the far best response is found in section KA2563A:R1 (structure #9). This indicates that structure #9 is well connected the source section. The lack of responses in KI0025F, other than structure #20, indicates that structure #9 ends after intersecting structure #20 somewhere in between boreholes KI0023B and KI0025F. This interpretation is consistent with the current interpretation of the orientation of structure #9 (Hermanson, 1998). The source section is interpreted to be intersected by the subhorizontal structure #18. It is difficult to judge from this test whether this structure transmits the response to structures #9 and #20. The source section is rather low transmissive (see Table 4-2) and it might also be a minor fracture sub-parallel to these structures.

Test #12, KI0023B:P2 (structure #19)

Only two sections respond to this test, KI0025F:R2 and R3 which is consistent with the test in KI0025F:R2 (test #9). Thus, the conclusions presented for test #9 are the same as for this test, cf., test #9.

Test #13, KA3573A:P1 (structure #15)

This test gives a response pattern similar to tests ENW-2 and ESV-2 except that structure #20 does not respond probably due to the larger distance from the source section. Thus, the test indicates that structure #15 is well connected to structures #5 and #7 which is logical given the short distance to these structures and the orientation of the structures. However, the most surprising result of this test was that the flow rate from the section had decreased significantly since the measurement done prior to the start of the interference tests, cf. Table 4-2. The reason for this is currently not known.

4.3.2 Quantitative evaluation

Time-drawdown responses

The time drawdown (or recovery) responses are quite different for the tests. The dominating flow geometry for the most significant responses is shown in Table 4-3a-b. For test ENW-2 most responses generally conform rather well to the Theis' type curve for radial flow. In some sections a slight leakage (support) flow is observed by the end of the test. No significant effects of outer no-flow boundaries are observed during the test. Tidal effects distort the data at late times.

During short test times the data curves deviate in some cases from the classical Theis' type curve (more linear than radial type of flow). This may be regarded as a scale (or skin) effect in the way that at early times the responses may be more dominated by local hydraulic conditions near the actual observation section (e.g. fracturing) whereas at longer times the responses will be more averaged, representing a larger volume of rock approaching an equivalent fractured porous medium. An example of a typical observation section drawdown response during test ENW-2 is shown in Figure 4-5 (section KI0023B:P8). On the data curve, the time is plotted in seconds on the horizontal scale and the drawdown in meters on the vertical scale. The suffix ".dra" to the sections in the plots denotes drawdown data and ".drd" drawdown derivative data. When recovery data are used for analysis the corresponding suffices are ".rec" and ".red". All evaluation plots are presented in a separate Appendix voulme (Andersson et al., in prep)

During test ENW-1 different types of main responses are observed. Several observation sections show effects of apparent no-flow (barrier) outer hydraulic boundaries by the end of the test as indicated by an increase of the drawdown (or recovery) derivative. This effect may possibly be interpreted as a limited lateral extent of the tested structure (#5) or alternatively, the presence of local flow restrictions (heterogeneity) along the structure. On the other hand, some sections show effects of recharge hydraulic boundaries, probably corresponding to leakage (support) flow by the end of the tests. Other sections show (pseudo)-radial flow with no effects of outer boundaries during the tests.

In test ESV-2 the responses generally show effects of apparent no-flow (barrier) hydraulic boundaries by the end of the test, indicated by an increase in the derivative. This fact may be interpreted as the presence of local flow restrictions along the structure in relation to the hydraulic conditions near the source section. Tidal effects are also distorting the late-time data in this test. An example of a typical observation section drawdown response during test ESV-2 is shown in Figure 4-6 (section KA3600F:P2).

The responses during test ESV-1a show predominantly radial flow with a slight leakance by the end of the test. The responses during tests ESV-1b and –1c are similar. No effects of negative hydraulic boundaries are observed. This may indicate that the dominating structure tested (#20) receives lateral support flow (leakage) from adjacent structures, e.g. #9 or structures sub-parallel to #20. Rather few observation sections outside the source borehole show a significant response during these tests. An example of a typical observation section drawdown response during test ESV-1c is shown in Figure 4-7 (section KI0025F:R4). Tidal effects distort the late time data.

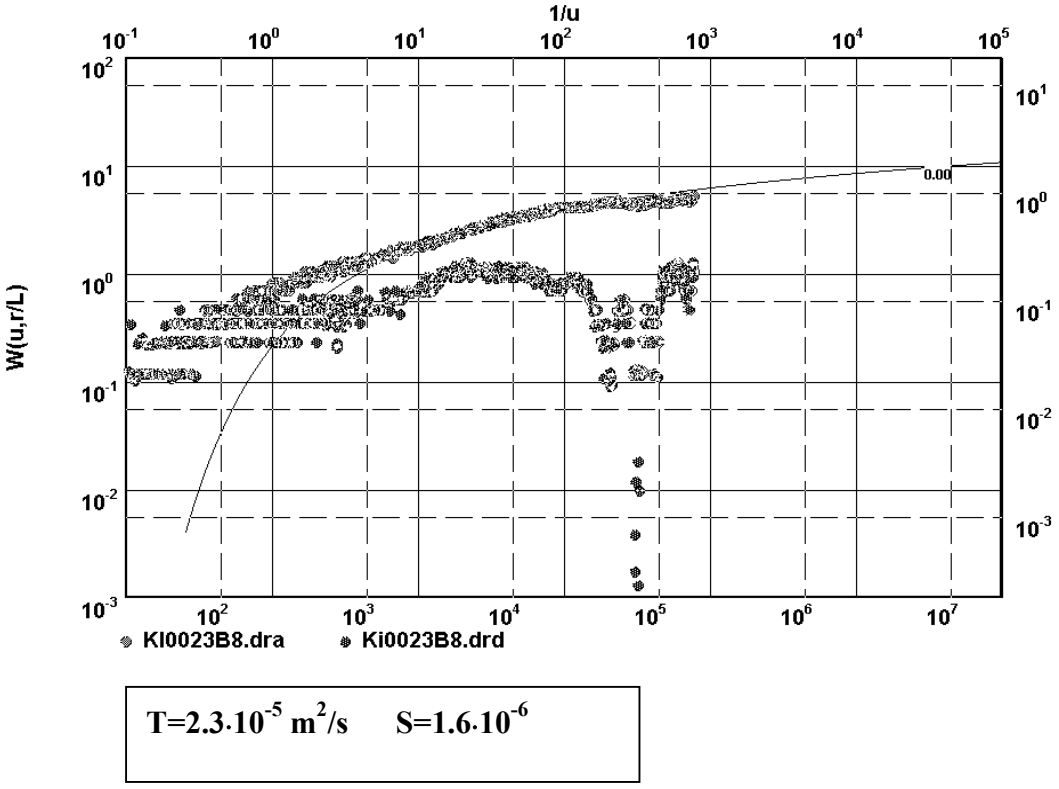

Figure 4-5. *Example of response in observation section KI0023B:P8 during interference test ENW-2.*

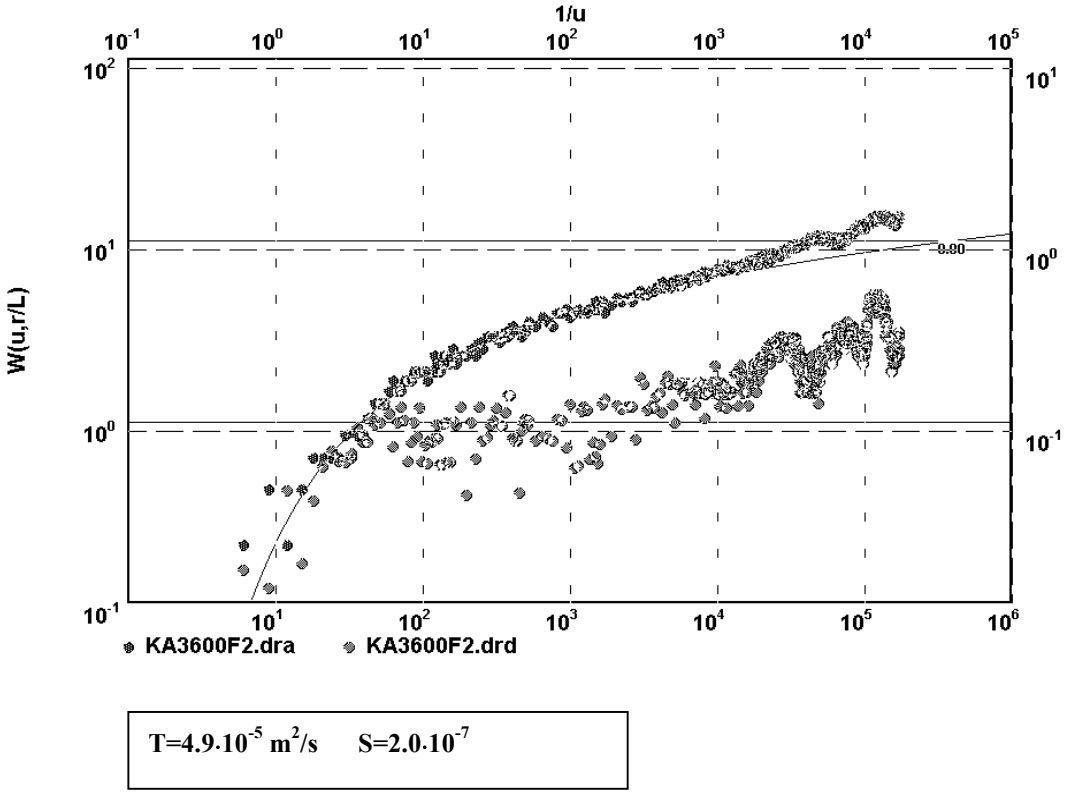

Figure 4-6. *Example of response in observation section KA3600F:P2 during interference test ESV-2.*

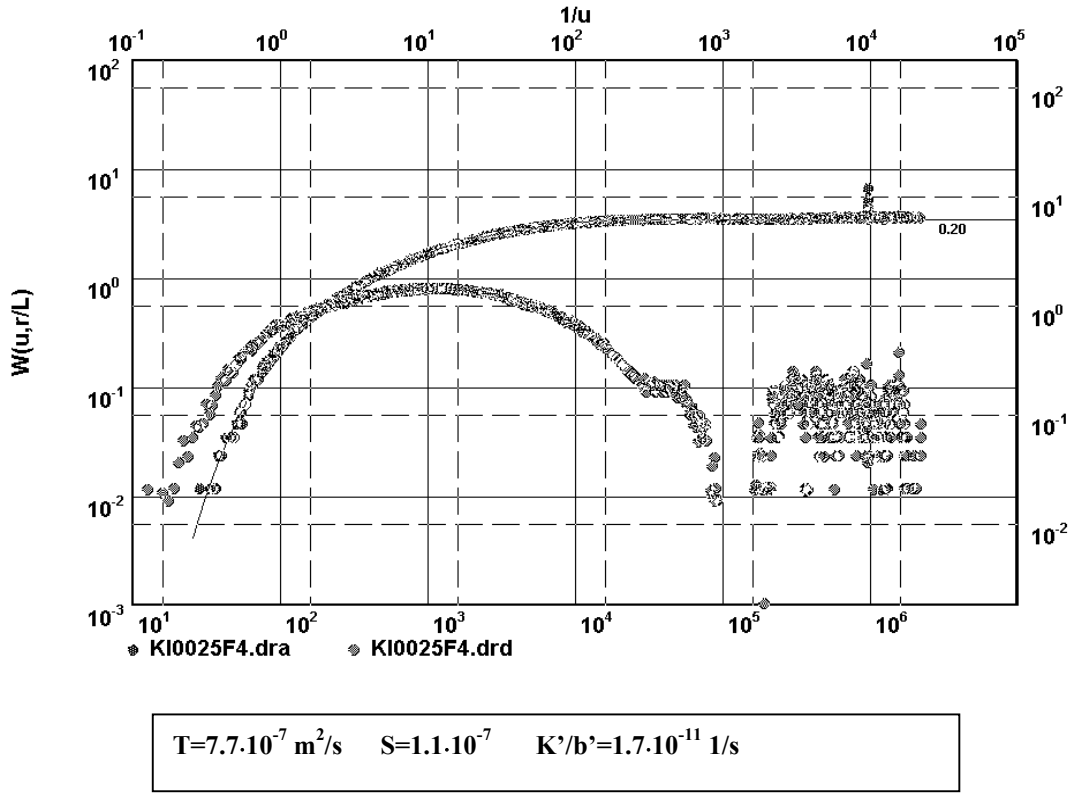

Figure 4-7. *Example of response in observation section KI0025F:R4 during interference test ESV-1c*

Estimated hydraulic properties for the tests

The estimated transmissivity and storativity of the most significant responses (as identified from the qualitative interpretation) are shown for the global tests ENW-2, ENW-1 and ESV-2 in Table 4-3a and fo the local tests ESV-1a-c in Table 4-3b and also in Figures 4-8 to 4-13, respectively in cross plots. The hydraulic parameters have generally been estimated from the parts of the data curves showing an (approximately) pseudo-radial flow before any outer boundary effects significantly have influenced the data. In most cases, only short periods with pseudo-radial flow, manifested by a nearly horizontal derivative curve, were observed during the tests. Therefore, the estimated hydraulic parameters should be regarded as approximate, representing an equivalent fractured porous medium on the scale of the tests. In particular, the results for observation sections within the source borehole should be regarded as uncertain due to potential hydraulic connections along the source borehole during the tests (non-radial flow). The results for such sections are within parenthesis in Tables 4-3a-b.

For tests ENW-1, ENW-2 and ESV-2 the estimated hydraulic properties are similar. The transmissivity generally ranges from c. 2-5·10^{-5} m^2/s while the storativity ranges from c. 7·10^{-8} to 9·10^{-6}. The estimated hydraulic diffusivity (T/S) for these tests generally ranges from c. 5-50 m^2/s.

For tests ESV-1a-c the estimated hydraulic properties are significantly lower compared to those from the global tests. The transmissivity is clustered around 1·10^{-6} m^2/s while the storativity generally ranges from c. 4·10^{-9} to 5·10^{-7}. Section KA2563A:R1 has a lower storativity in all tests. The estimated hydraulic diffusivity (T/S) for test ESV-1b is generally c. 10-20 m^2/s while tests ESV-1a and ESV-1c show lower diffusivity, ranging from c. 1-10 m^2/s except section KA2563A:R1 which has a higher diffusivity. The estimated diffusivity for this section during test ESV-1a is uncertain since it is located in the source borehole.

For tests ESV-1a-c the estimated leakage coefficient K'/b' was generally in the range from c. 5·10^{-12} to 5·10^{-11} 1/s.

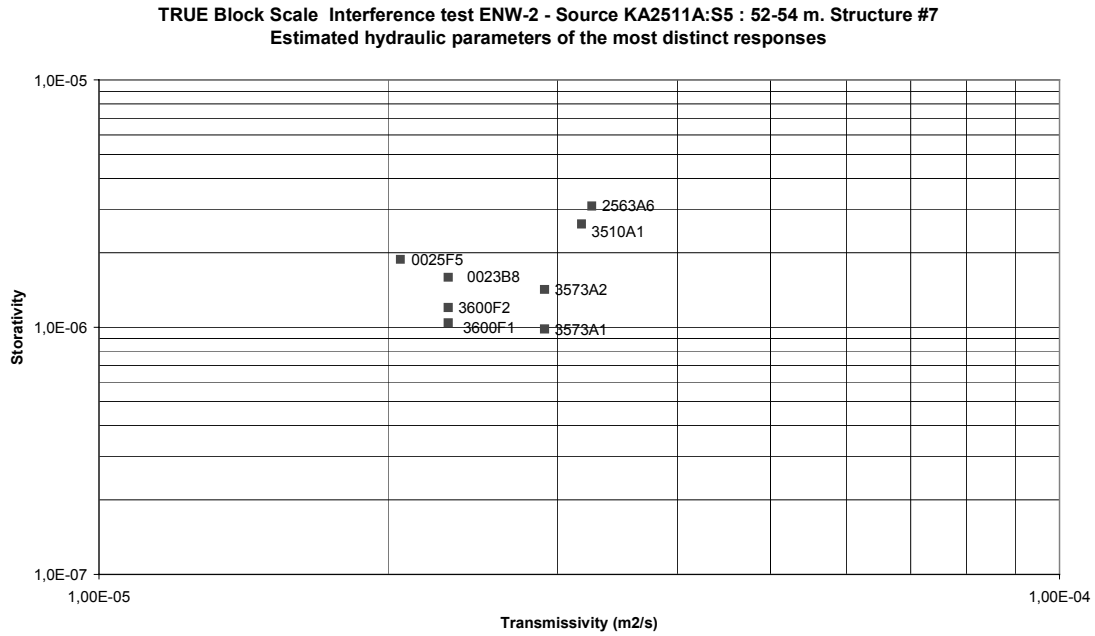

Figure 4-8. *Estimated transmissivity and storativity of most significant responses during interference test ENW-2.*

Table 4-3a. Summary of estimated hydraulic parameters for the most significant response sections during the global interference tests. Rad=Radial, NFB=No-flow hydraulic boundary.

Borehole section	Interval (m)	T (m^2/s)	S	T/S (m^2/s)	K'/b' (s^{-1})	Dom. Flow geometry
Test ENW-2	**Source: KA2511A:S5**			**Structure #7**		
KA2563A:R6	146-186	$3.3\cdot10^{-5}$	$3.1\cdot10^{-6}$	10.6	-	Rad
KI0025F:R5	41-85	$2.1\cdot10^{-5}$	$1.9\cdot10^{-6}$	11.0	-	Rad
KI0023B:P8	41.45-42.45	$2.3\cdot10^{-5}$	$1.6\cdot10^{-6}$	14.5	-	Rad
KA3510A:P1	0-150	$3.2\cdot10^{-5}$	$2.6\cdot10^{-6}$	12.2	-	Rad
KA3573A:P1	18-40	$2.9\cdot10^{-5}$	$9.8\cdot10^{-7}$	29.6	-	Rad
KA3573A:P2	4.5-17	$2.9\cdot10^{-5}$	$1.4\cdot10^{-6}$	20.5	-	Rad
KA3600F:P1	22-50.1	$2.3\cdot10^{-5}$	$1.0\cdot10^{-6}$	22.2	-	Rad
KA3600F:P2	4.5-21	$2.3\cdot10^{-5}$	$1.2\cdot10^{-6}$	20.0	-	Rad
Test ENW-1	**Source: KA3573A:P2**			**Structure #5**		
KA2511A:S5	52-54	$2.9\cdot10^{-5}$	$3.2\cdot10^{-6}$	8.9	-	Rad → NFB
KA2563A:R7	75-145	$2.8\cdot10^{-5}$	$4.9\cdot10^{-6}$	5.7	-	Rad → NFB
KI0025F:R5	41-85	$3.1\cdot10^{-5}$	$3.2\cdot10^{-6}$	9.6	-	Rad → NFB
KI0025F:R6	3.5-40	$1.9\cdot10^{-5}$	$6.8\cdot10^{-8}$	279		Rad
KI0023B:P8	41.45-42.45	$3.0\cdot10^{-5}$	$7.8\cdot10^{-6}$	3.8	-	Radi → NFB
KI0023B:P9	4.5-40.45	$2.6\cdot10^{-6}$	$1.2\cdot10^{-7}$	22.0	$3.9\cdot10^{-11}$	Leaky
KA3573A:P1	18-40	$(5.7\cdot10^{-6})$	$(3.4\cdot10^{-6})$	(1.7)	$(8.1\cdot10^{-10})$	Leaky
KA3600F:P2	4.5-21	$2.3\cdot10^{-5}$	$4.6\cdot10^{-6}$	5.0	-	Rad
KA1751A:P1	99-150	$2.8\cdot10^{-5}$	$9.2\cdot10^{-6}$	3.1	-	Rad
KA2512A	0-37.3	$1.9\cdot10^{-5}$	$3.1\cdot10^{-6}$	6.2	-	Rad

Borehole section	Interval (m)	T (m^2/s)	S	T/S (m^2/s)	K'/b' (s^{-1})	Dom. Flow geometry
Test ESV-2	**Source: KI0023B:P8**			**Structure #7**		
KA2511A:S5	52-54	$3.5\cdot10^{-5}$	$1.5\cdot10^{-6}$	22.6	-	Rad.→ NFB
KI0025F:R5	41-85	$4.3\cdot10^{-5}$	-	-	-	Rad. → NFB
KA3573A:P1	18-40	$4.9\cdot10^{-5}$	$1.0\cdot10^{-6}$	47.9	-	Rad. → NFB
KA3573A:P2	4.5-17	$3.5\cdot10^{-5}$	$4.0\cdot10^{-6}$	8.7	-	Rad. → NFB
KA3600F:P1	22-50.1	$3.9\cdot10^{-5}$	$2.2\cdot10^{-6}$	17.6	-	Rad. → NFB
KA3600F:P2	4.5-21	$4.9\cdot10^{-5}$	$2.0\cdot10^{-7}$	247	-	Rad. → NFB
KA2512A	0-37.3	$3.1\cdot10^{-5}$	$1.7\cdot10^{-6}$	17.8	-	Rad. → NFB

Table 4-3b. Summary of estimated hydraulic parameters of the most significant response sections during the local interference tests.

Borehole section	Interval (m)	T (m^2/s)	S	T/S (m^2/s)	K'/b' (s^{-1})	Dom. Flow geometry
Test ESV-1a	**Source: KA2563A:R5**			**Structure #20**		
KA2563A:R1	262-363	($1.0\cdot10^{-6}$)	($4.9\cdot10^{-10}$)	(2040)	($6.0\cdot10^{-14}$)	Rad→Leaky
KI0025F:R4	86-88	$9.6\cdot10^{-7}$	$5.7\cdot10^{-8}$	16.8	$5.6\cdot10^{-12}$	Rad→Leaky
KI0023B:P5	72.4-84	$7.4\cdot10^{-7}$	$5.1\cdot10^{-7}$	1.4	$4.5\cdot10^{-12}$	Rad→Leaky
KI0023B:P6	70.4-71.4	$8.3\cdot10^{-7}$	$2.6\cdot10^{-7}$	3.1	$5.6\cdot10^{-11}$	Rad→Leaky
KI0023B:P7	43.45-69.4	$9.5\cdot10^{-7}$	$2.9\cdot10^{-7}$	3.2	$3.4\cdot10^{-11}$	Rad→Leaky
Test ESV-1b	**Source: KI0025F:R4**			**Structure #20**		
KA2563A:R1	262-363	$1.0\cdot10^{-6}$	$1.2\cdot10^{-8}$	86.4	$2.1\cdot10^{-12}$	Rad→Leaky
KA2563A:R5	187-190	$8.1\cdot10^{-7}$	$5.0\cdot10^{-8}$	16.4	$9.9\cdot10^{-12}$	Rad→Leaky
KI0025F:R3	89-163	$8.1\cdot10^{-7}$	$6.0\cdot10^{-8}$	13.5	$2.1\cdot10^{-11}$	Rad→Leaky
KI0023B:P6	70.4-71.4	$7.3\cdot10^{-7}$	$8.2\cdot10^{-8}$	8.8	$1.6\cdot10^{-11}$	Rad→Leaky
KI0023B:P7	43.45-69.4	$9.1\cdot10^{-7}$	$7.3\cdot10^{-8}$	12.6	$1.6\cdot10^{-11}$	Rad→Leaky

Borehole section	Interval (m)	T (m^2/s)	S	T/S (m^2/s)	K'/b' (s^{-1})	Dom. Flow geometry
Test ESV-1c	**Source: KI0023B:P6**			**Structure #9**		
KA2563A:R1	262-363	$1.2\cdot10^{-6}$	$4.2\cdot10^{-9}$	294	$5.3\cdot10^{-13}$	Rad→Leaky
KA2563A:R5	187-190	$8.7\cdot10^{-7}$	$1.9\cdot10^{-7}$	4.5	$3.4\cdot10^{-11}$	Rad→Leaky
KI0025F:R4	86-88	$7.7\cdot10^{-7}$	$1.1\cdot10^{-7}$	7.0	$1.7\cdot10^{-11}$	Rad→Leaky
KI0023B:P5	72.4-84	$7.7\cdot10^{-7}$	$4.1\cdot10^{-7}$	1.9	$3.6\cdot10^{-11}$	Rad→Leaky
KI0023B:P7	43.45-69.4	$1.2\cdot10^{-6}$	$2.1\cdot10^{-7}$	5.9	$1.5\cdot10^{-11}$	Rad→Leaky

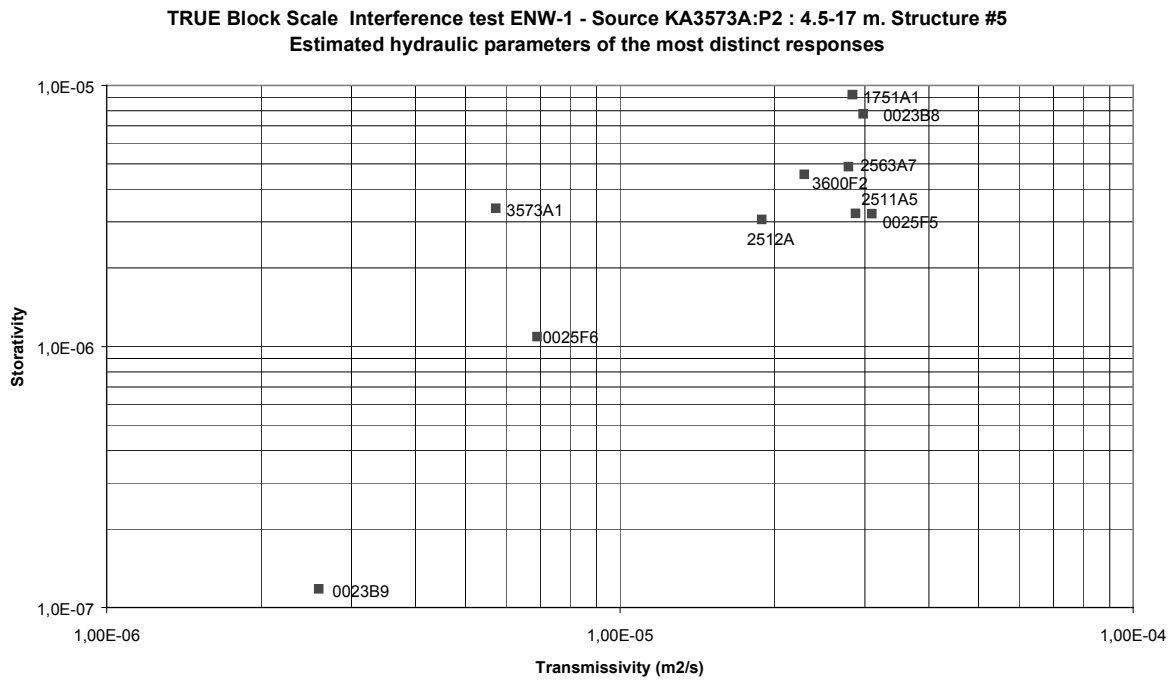

Figure 4-9. *Estimated transmissivity and storativity of most significant responses during interference test ENW-1.*

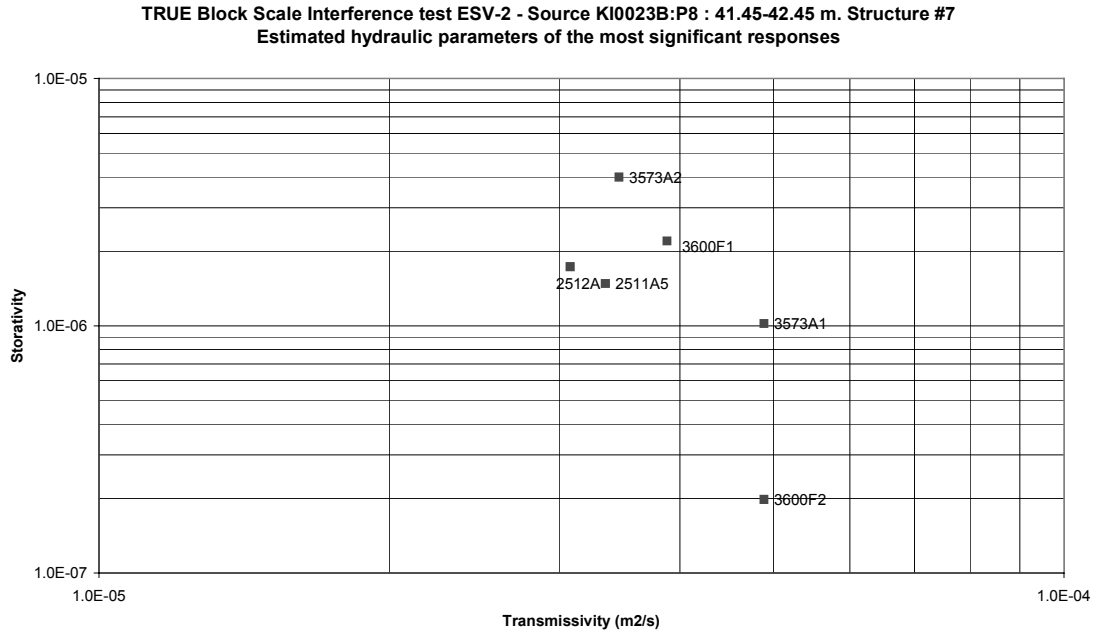

Figure 4-10. *Estimated transmissivity and storativity of most significant responses during interference test ESV-2.*

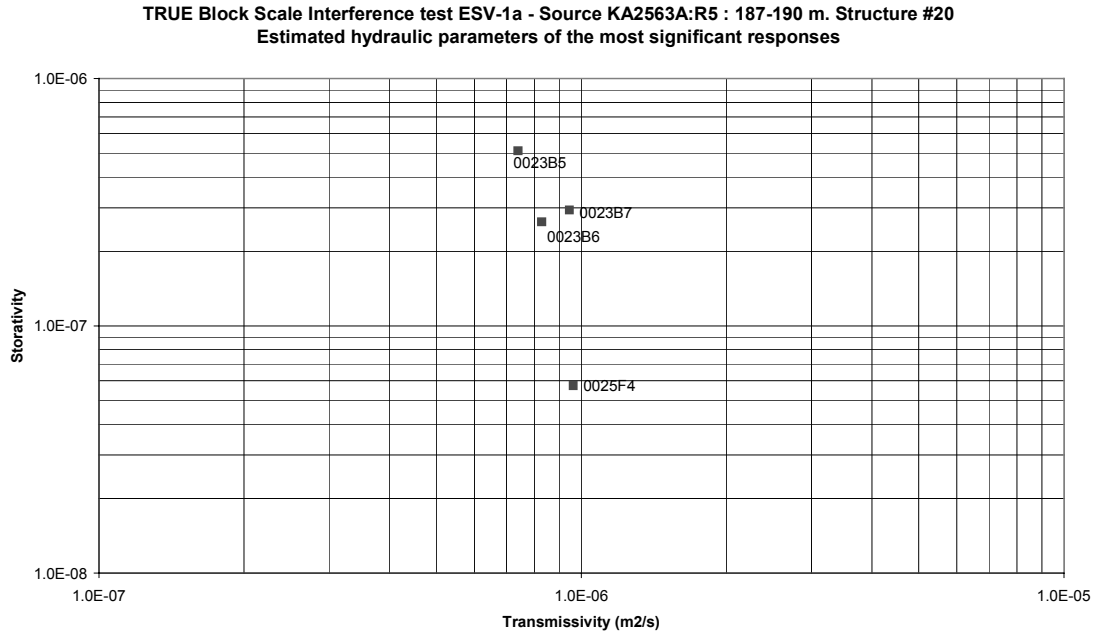

Figure 4-11. *Estimated transmissivity and storativity of most significant responses during interference test ESV-1a.*

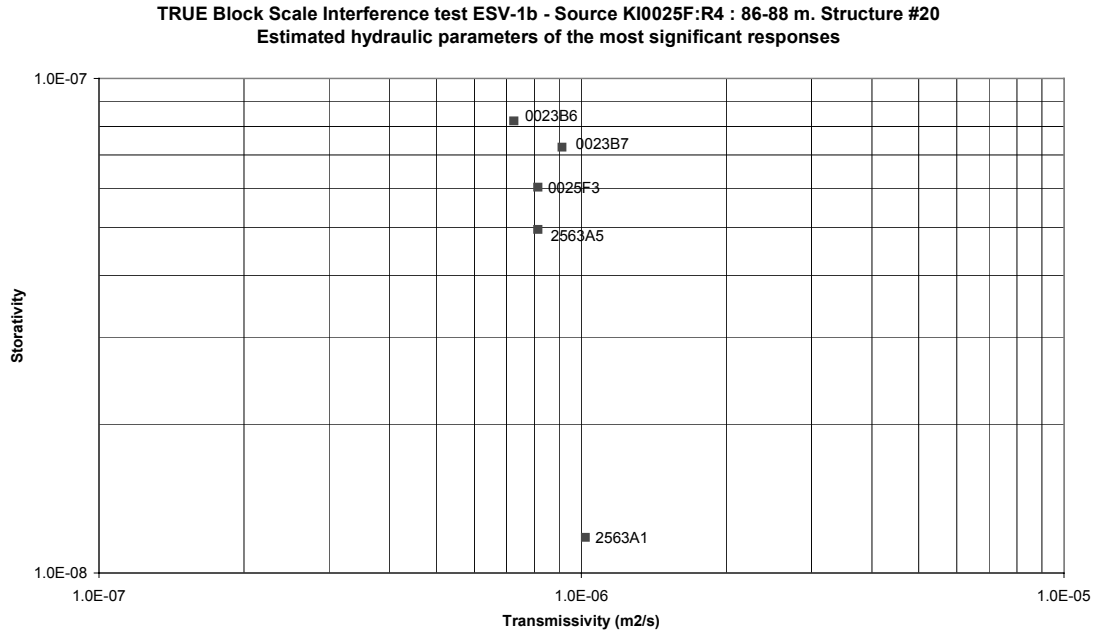

Figure 4-12. *Estimated transmissivity and storativity of most significant responses during interference test ESV-1b.*

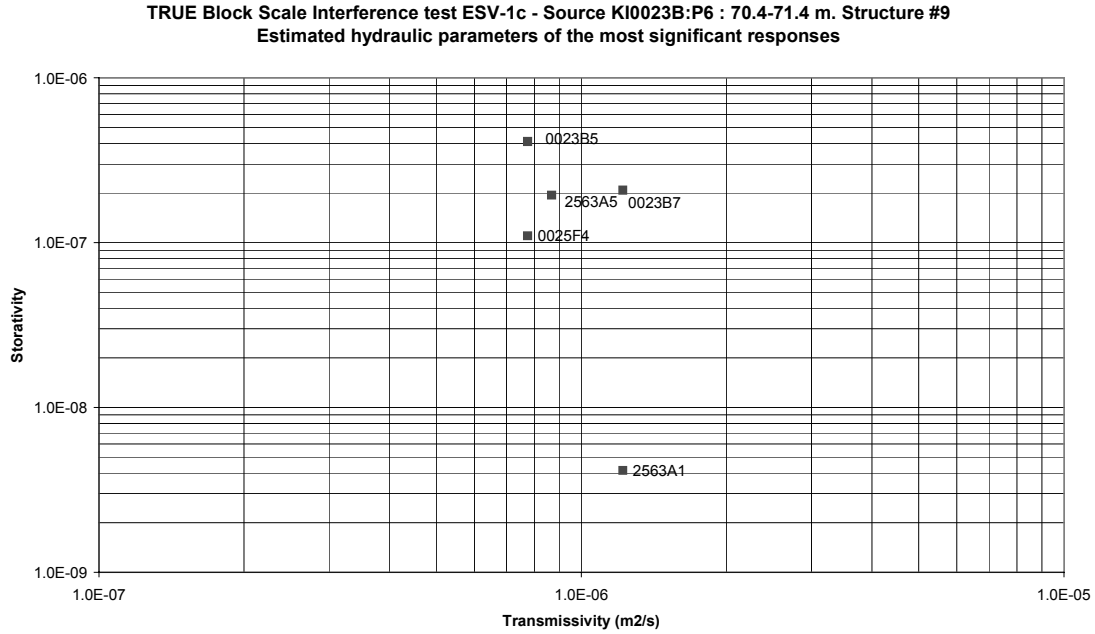

Figure 4-13. *Estimated transmissivity and storativity of the most significant responses during interference test ESV-1c.*

4.4 Flow measurements using tracer dilution technique

In total 51 measurements of flow rates using tracer dilution technique were performed during the interference tests both under natural gradient and under pump gradient. The results, presented in Table 4-4, shows that only two sections respond significantly to the

Table 4-4. Results of flow measurements (using tracer dilution tests) performed during TRUE Block Scale Interference Tests.

Test #	Pumped Structure	Measured Borehole	Structure	Q (natural) (ml/h)	Q (pump) (ml/h)
ENW-2	#7	KA2511A:S4	#6, 16	1100	1100
ENW-1	#5			1100	950
ESV-2	#7			1150	1100
ESV-1a	#20			1200	1050
ENW-2	#7	KA2563A:R5	#20		550
ENW-1	#5			540	560
ESV-2	#7			560	610
ESV-1b	#20			540	715
ESV-1c	#9			590	1420
ENW-2	#7	KI0023B:P8	#6,7	<1	<1
ENW-1	#5	KI0023B:P6	#9	<1	<1
ESV-2	#7			3	
ESV-1a	#20			2	7
ESV-1b	#20			4	6
ENW-2	#7	KI0023B:P4	#13	<1	<1
ENW-1	#5			<1	<1
ESV-2	#7			<1	<1
ESV-1b	#20			1	4
ESV-1c	#9			<1	<1
ENW-2	#7	KI0025F:R2	#19	6	2
ENW-1	#5			16	6
ESV-2	#7			18	18
ENW-2	#7	KI0025F:R4	#20	7	5
ENW-1	#5			5	5
ESV-2	#7			4	
ESV-1a	#20			2	2
ESV-1c	#9			2	2

pumping namely sections KA2563A:R5 and KI0023B:P6, intersected by structures #20 and #9, respectively. A response is also indicated in section KI0023B:P4 (test ESV-1b) but this response is judged as highly uncertain due to a very scattered data set.

The measurements also show large variations in flow rate between different sections. This may partly be explained by differences in transmissivity where sections KA2511A:S4, KA2563A:R5, KI0023B:P8 and KI0025F:R2 have a transmissivity in the range 10^{-5} - 10^{-6} m^2/s while the remaining three have transmissivity in the range 10^{-6} - 10^{-7} m^2/s (approximate numbers based on double-packer flow logging). However, it is also clear that the natural gradient vary considerably within the block as illustrated by the high flow rates in KA2511A:S4 and KA2563A:R5 compared to KI0023B:P8 and KI0025F:R2.

The hydraulic gradient was also calculated from the dilution rates using the assumptions described in Chapter 3.2, cf. Table 4-5. The calculated values also reflect the variation in hydraulic gradient ranging from 1.6 m/m to 0.0004 m/m, i.e. four orders of magnitude. The numbers indicate high gradients in structures #6 and #20 (two measurements), significantly lower in structures #9, #13 and #19 and extremely low in structure #7. These gradients were also qualitatively checked against measured natural head values but the comparison is difficult to make given the very few observation points in each structure and the fact that more than one structure often intersects a section.

Table 4-5. Darcy velocities, q_w , and hydraulic gradients, *I*, calculated from tracer dilution tests during TRUE Block Scale Interference Tests.

Borehole section	Darcy velocity (m/s)	Gradient (m/m)	Structure
KA2511A:S4	$1.6 \cdot 10^{-7}$	1.6	#6, 16
KA2563A:R5	$4.6 \cdot 10^{-7}$	1.2	#20
KI0023B:P4	$1.3 \cdot 10^{-9}$	0.07	#13
KI0023B:P6	$3.7 \cdot 10^{-9}$	0.04	#9
KI0023B:P8	$1.8 \cdot 10^{-9}$	0.0004	#7
KI0025F:R2	$4.6 \cdot 10^{-9}$	0.01	#19
KI0025F:R4	$3.7 \cdot 10^{-9}$	1.2	#20

Figures 4-14 and 4-15 shows examples of tracer dilution curves for KA2563A and KI0023B:P6 during interference tests ESV-1c and 1a, respectively. Both curves show a clear and distinct increase of the slope of the curves indicating an increased flow rate at the time for pump start. A complete set of tracer dilution curves including best regression estimate are given in Appendix 3.

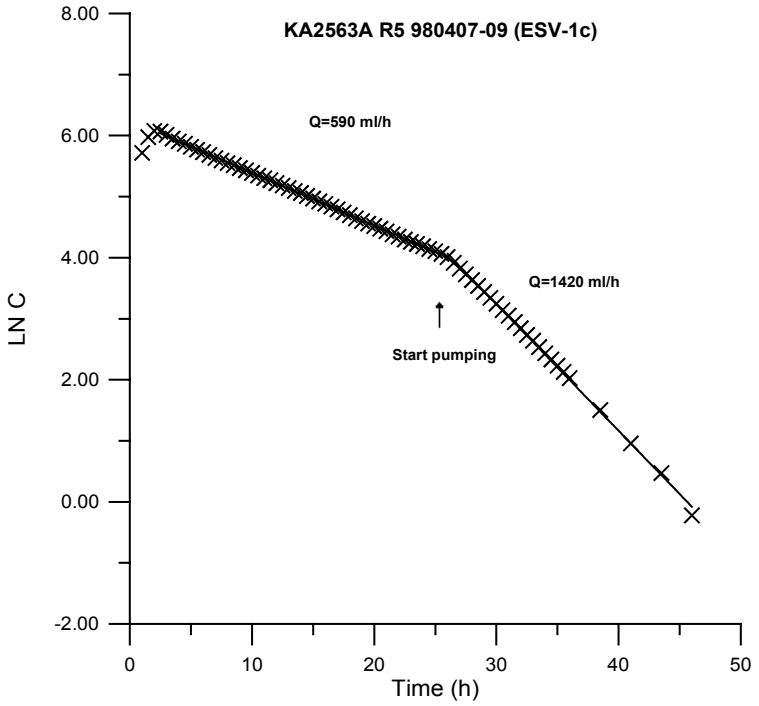

Figure 4-14. *Tracer dilution curve (Logarithm of the tracer concentration versus time) in borehole section KA2563A:R5 before and after pump start for interference test ESV-1c (pumping in KI0023B:P6).*

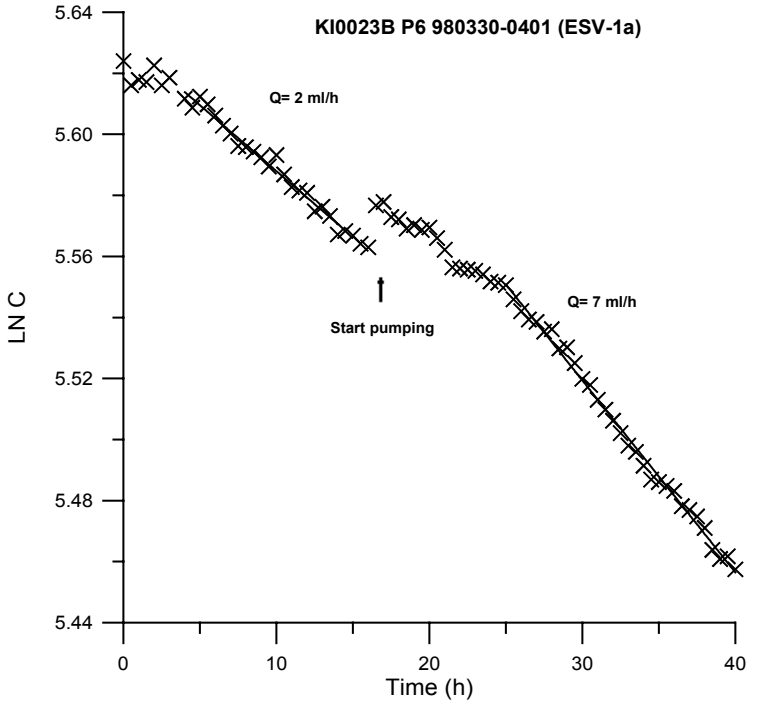

Figure 4-15. *Tracer dilution curve (Logarithm of the tracer concentration versus time) in borehole section KI0023B:P6 before and after pump start for interference test ESV-1a (pumping in KA2563A:R5).*

4.5 Tracer test

4.5.1 Tracer injections

The tracer test performed during ESV-1c, pumping in KI0023B:P6 (structure #9), involved injections in three borehole sections, two in structure #20 (KA2563A:R5 and KI0025F:R4) and one in section KI0023B:P4 (structure #13). The injection functions, presented as the logarithm of the tracer concentration versus time, are shown in Figures 4-16 to 4-18.

The injection flow rates were calculated from the dilution of tracer versus time as described in Chapter 2.2.3. The values obtained for sections KI0023B:P4 and KI0025F:R4 were very low, lower than the measurement limit of 1 ml/h and even lower than to those obtained from the dilution test performed immediately prior to the tracer injections, cf. Table 4-4. One reason for this is that the tracer injections were measured over a much longer time period giving better regression statistics and thus, more accurate values than the dilution tests. Another explanation may be that the pumping direction is reversed compared to the natural flow direction. The flow in KA2563A:R5, 1480 ml/min was almost the same as obtained in the dilution test (Table 4-4).

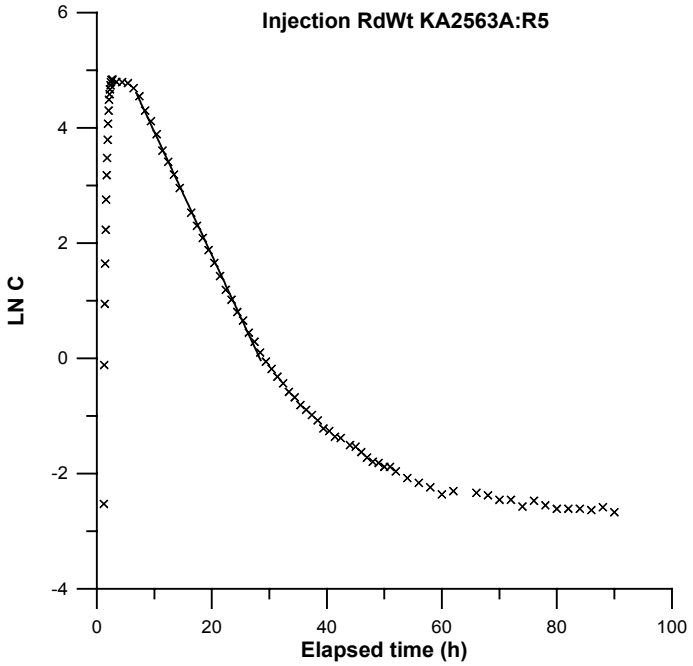

Figure 4-16. *Tracer concentration (ln C) versus time for injection of Rhodamine WT in borehole section KA2563A:R5 during interference test ESV-1c. The straight line represents the best linear regression fit.*

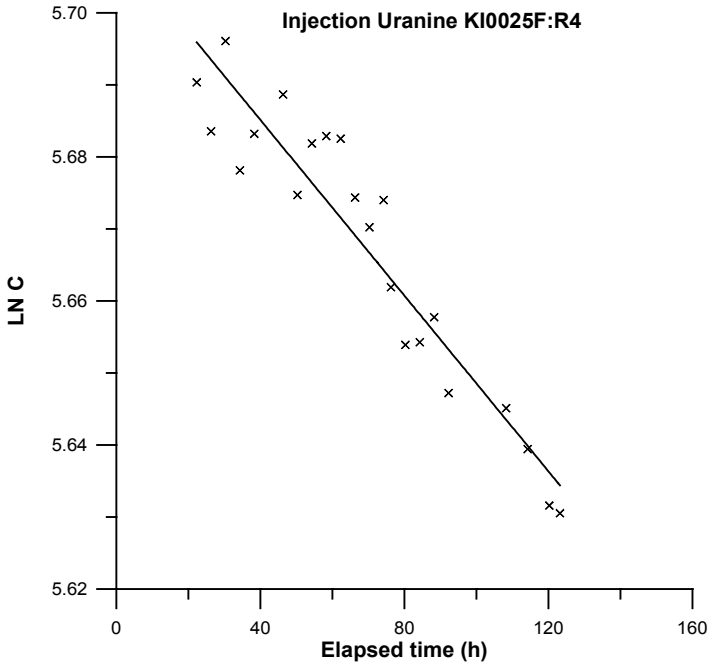

Figure 4-17. *Tracer concentration (ln C) versus time for injection of Uranine in borehole section KI0025F:R4 during interference test ESV-1c. The straight line represents the best linear regression fit.*

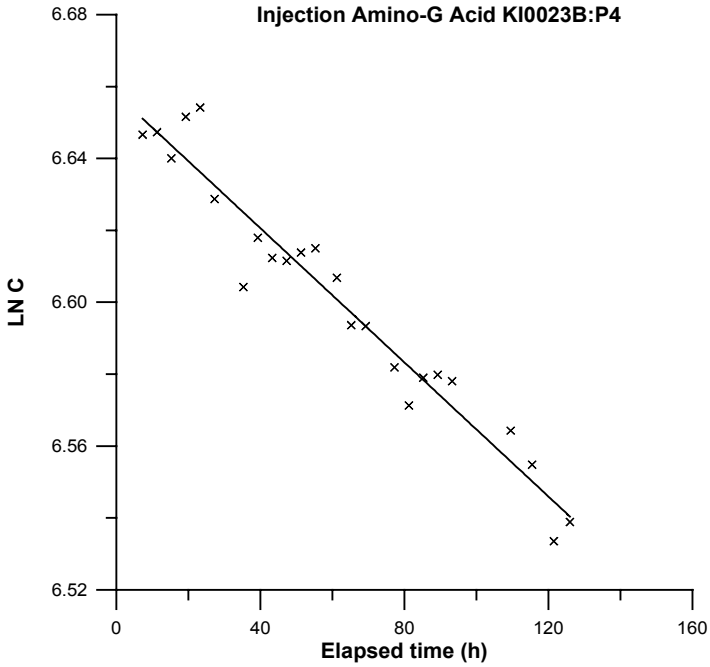

Figure 4-18. *Tracer concentration (ln C) versus time for injection of Amino G Acid in borehole section KI0023B:P4 during interference test ESV-1c. The straight line represents the best linear regression fit.*

4.5.2 Tracer breakthrough

Tracer breakthrough could only be detected from the injection of Rhodamine WT in KA2563A:R5. The breakthrough curve (Figure 4-19) shows one distinct peak after 30 hours of elapsed time. There are no visible signs of transport in multiple pathways although this may be hidden in the tailing of the curve.

The one-dimensional advection–dispersion model described in Section 3.3, could not fit the tail of the breakthrough curve very well. This may be explained by the presence of multiple pathways, but also by other phenomena, e.g. diffusion or sorption. Earlier field tracer tests in crystalline rock (e.g. Gustafsson and Klockars, 1981, Andersson et al., 1993) have shown that Rhodamine WT is weakly and reversibly sorbed on granite. However, this weak sorption was considered to be of small importance considering the objectives of the test.

The transport parameters derived from the numerical modelling and the analytical expressions described in Section 3.3 (Table 4-6) are very similar to those obtained for Feature A in the TRUE-1 tracer tests (Andersson et al., 1998).

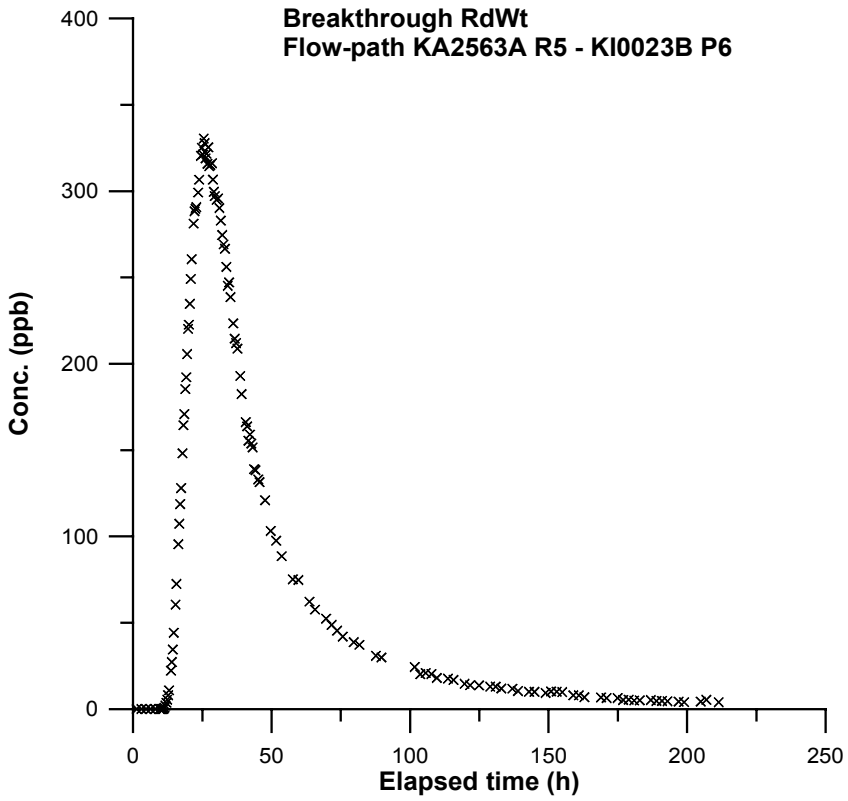

Figure 4-19. *Tracer breakthrough in KI0023B:P6 from injection of Rhodamine WT in borehole section KA2563A:R5 during interference test ESV-1c.*

Table 4-6. Summary of hydraulic and transport parameters for flow path KA2563A:R5 – KI0023B:P6.

Parameter	Value	Source
Travel distance, L (m)	15.9 m	Geometry
Mean head difference, Δh (m)	54 m	HMS
Mean velocity, v (m/s)	$1.9 \cdot 10^{-4}$ m/s	PAREST
Mean travel time, t_m (h)	23.5 h	PAREST
First arrival, t_a (h)	10.8 h	Breakthrough curve
Dispersivity, D/v (m)	1.6 m	PAREST
Peclet number, Pe	10	
Fracture conductivity, K_{fr} (m/s)	$1.7 \cdot 10^{-4}$ m/s	Eq. 3-7
Equivalent fracture aperture, b (m)	$1.9 \cdot 10^{-3}$ m	Eq. 3-8
Flow porosity	$2.3 \cdot 10^{-3}$	Eq. 3-9
Mass recovery , R (%)	44 %	Breakthrough curve

5 DISCUSSION AND CONCLUSIONS

5.1 Structural model

Each interpreted intercept of different structures with the tested boreholes has been evaluated based on the response matrices described in Chapter 4. However, it should be noted that the evaluation is based purely on hydraulic responses. Thus, geological and geophysical indications have not been considered here. Only structures that have been tested, directly or indirectly, are discussed below. A summary of all structures, including a judgement whether they have been verified or not by the hydraulic interference tests and a judgement of their hydraulic significance for the central parts of the investigated block, is presented in Table 5-1. The nineteen hydraulic interference tests described in this report (cf. Tables 1-1 and 1-2) have produced a large data base for information and updating of the structural model (Figure 1-1) presented in Hermanson (1998), later updated in Hermanson (in prep.) (Figure 5-1).

Structure #1

This structure was only indirectly tested as it only intersects a blind section in KA2563A at 12 m borehole length. The response pattern in test #3 (KA2598A) confirms the existence of a structure having similar orientation as structure #1. However, the cross-hole responses from tests in KA2598A occur when the section 5-35 m is opened suggesting that the responses were transmitted through a sub-parallel structure to #1 currently not included in the model.

Structure #5

The existence and orientation of this structure has earlier been confirmed (Hermanson, 1998). The direct test in this structure, test ENW-1, confirms the orientation and extension to the west with the intercepts in borehole sections KA3573A:P2 and KA3600F:P2. Further, the good response in KA2512A indicates that structure #5 intersects the bottom part of this borehole. Another important observation is that the surface borehole HAS04 responds fast indicating that the structure may be extended at least 300 m upwards. The global response pattern obtained from test ENW-1 may be explained by the intercepts with structures #6 and #7 being relatively close to the source section (KA3573A:P2).

Structure #6

This structure has a non-unique geological character according to Hermanson (1998). The interference tests performed in this structure (ESV-2, #6, #10) do not confirm the existence and orientation of the structure. Instead, the source section for test ESV-2, KI0023B:P8 seems to be associated with structure #7. This is also consistent with the updated structural model (Hermanson, in prep.). Test #6 (KA2511A:S4) did not give any responses other than in the source borehole indicating a limited extent of that structure. Thus, based on the results from the interference tests it is difficult to judge how this structure is hydraulically connected. Most of the response pattern observed may be explained by the existence of structures #5 and #7. If structure #6 exists with the extension indicated by Hermanson (1998) it must be highly heterogeneous or even discontinuous.

Structure #7

The tests performed in this structure (ENW-2, ESV-2 and #8) confirm the orientation and extent of the structure. The good hydraulic communication between structure #5 and #7 is clearly seen in test ENW-2, cf. the discussion about structure #5.

Structure #8

This structure has been identified at several locations in the tunnel but only associated with minor water seepage. However, based on the results of test #3 (KA2598A:P1) it is possible that a hydraulic connection exists in the NE-direction. However, the role of structure #8 as a hydraulic conductor seems to be limited, at least in the central and lower parts of the TRUE Block Scale volume.

Structure #9

This structure was only identified in one section (KA2563A:R1) in the October-97 model and is therefore considered to have a limited extent. The results of interference tests #4 (KA2563A:R1) and #11 (KI0023B:P5) clearly indicate that the structure exists and may be extended towards the intercept with structure #20. The mutual responses observed in KI0023B:P4-P7 may result from several interacting parallel or sub-parallel structures, i.e. structures #9, #13 and #20.

Structure #10

Only one test was performed in this structure (#4, KA2563A:R1) but due to the equipment failure in KI0023B:P1, no measurements could be made in this section. Thus, nothing further could be resolved about the hydraulic significance of structure #10.

Structure #13

This structure was not identified in the October 97-model. However, after the drilling of KI0023B this parallel structure to #20 was identified. Interference tests #1 (KI0023B:P4) and #5 (KA2563A:R4) confirm the existence and orientation of the structure. The tests also indicate that the structure is hydraulically well connected to structures #9 and #20.

Structure #15

This structure was only interpreted to intersect borehole KA3510A according to Hermanson (1998). However, the updated model (Hermanson, in prep.) suggests that structure #15 also intersects borehole section KA3573A:P1. The test in this section (#13) gives very good responses in several sections associated with structures #5, #6, and #7. This is consistent with the current interpretation of structure #15 intersecting these structures rather close to the source. No packers were installed in borehole KA3510A, which also intersects structures #4, #5 and possibly also #7. It was therefore not possible to identify any hydraulic responses in this borehole resulting from this structure.

Structure #16

This gently dipping structure, interpreted in boreholes KA2563A (56 m) and KA2511A (105 m), has been suggested as a possible hydraulic conductor between structures #5 and #6 and/or #7 (Hermanson, 1998). The interference tests only involved one borehole section intersected by structure #16 (KA2511A:S4). Test #6, performed in this section, only resulted in responses in the source borehole. Thus, there are no indications that structure #16 has any hydraulic significance in the investigated block. It is more likely that the connectivity between structures #5, #6 and #7 are resulting from the fact that they naturally intersect each other.

Structure #17

This is also a gently dipping structure, interpreted in boreholes KA2563A (109 m) and KA2511A (132 m), which has been identified as a possible conductor of pressure responses between structure #5 and #6 and/or #7. The results of the interference tests involving sections KA2563A:R7 and KA2511A:S4 do not support this conclusion, cf. the discussion under structure #16 above.

Structure #18

This is the third gently dipping structure that has been put forward as a possible hydraulic connector, in this case between structures #19 and #20. The structure was interpreted to intercept borehole section KA2511A:S1 where a relatively high inflow was expected. However, the flow measurements performed prior to the interference tests showed that this section was completely "dry". The structure is also interpreted to

intersect section KA2563A:R4. The interference test performed in this section (test #5) gave no response in the adjacent section (R5), intersected by structure #20. Thus, there are no indications that structure #18 is hydraulically significant.

Structure #19

The two tests performed in this structure (#9 and #12) confirm the existence, extension and orientation of the structure. The tests also indicate that the structure is well connected to structure Z and that it has a lower transmissivity at higher levels in the laboratory.

Structure #20

This structure is well defined in three borehole sections (KA2563A:R5, KI0023B:P7 and KI0025F:R4). The interference tests performed in these three sections (ESV-1 a,b and #10) showed very similar response patterns with responses in several adjacent sections interpreted to be intersected by structures #9 and #13. Thus, these three structures are well interconnected. No responses were found in structure #5, #6 and #7 except for borehole section KA2563A:R6 where a significant response was obtained.. One possibility is that structure #8 is the hydraulic connector

Table 5-1. Summary of the structures investigated by the TRUE Block Scale Interference Tests and their hydraulic significance for flow within the TRUE block. (NT=Not Tested)

Structure #	Test(s) #	Existence confirmed	Hydraulic significance (T=Transmissivity)
1	3	Yes	High T but not important for TRUE block
2	NT	-	-
3	NT	-	-
4	NT	-	-
5	ENW-1, 2	Yes	High T in all directions, well defined boundary
6	6, 8, 10	?	Heterogeneous, partly high T, may connect #20 to #7
7	ENW-2, ESV-2, 8	Yes	High T, good connectivity to #5 and #15, identified in many boreholes
8	3	Yes	Low T, limited importance for connectivity of the investigated block

Structure #	Test(s) #	Existence confirmed	Hydraulic significance (T=Transmissivity)
9	ESV-1c, 4	Yes	Moderate T, good interaction with #13 and #20, heterogeneous or limited extent, potential target structure
10	4	?	Probably not important for the central part of the block
11	NT	-	-
12	NT	-	-
13	1,5	Yes	Moderate T, good interaction with #9 and #20, heterogeneous, potential target structure
15	13	?	High to moderate T, good interaction with #5, #6 and #7, possibly not connected to #20
16	6	?	No hydraulic significance
17	NT	-	-
18	5,11	?	Probably no hydraulic significance
19	9,12	Yes	Heterogeneous, potential boundary to the south
20	ESV-1a,b,10	Yes	Heterogeneous, partly high connectivity within the structure, potential target structure
Z	NT	-	-

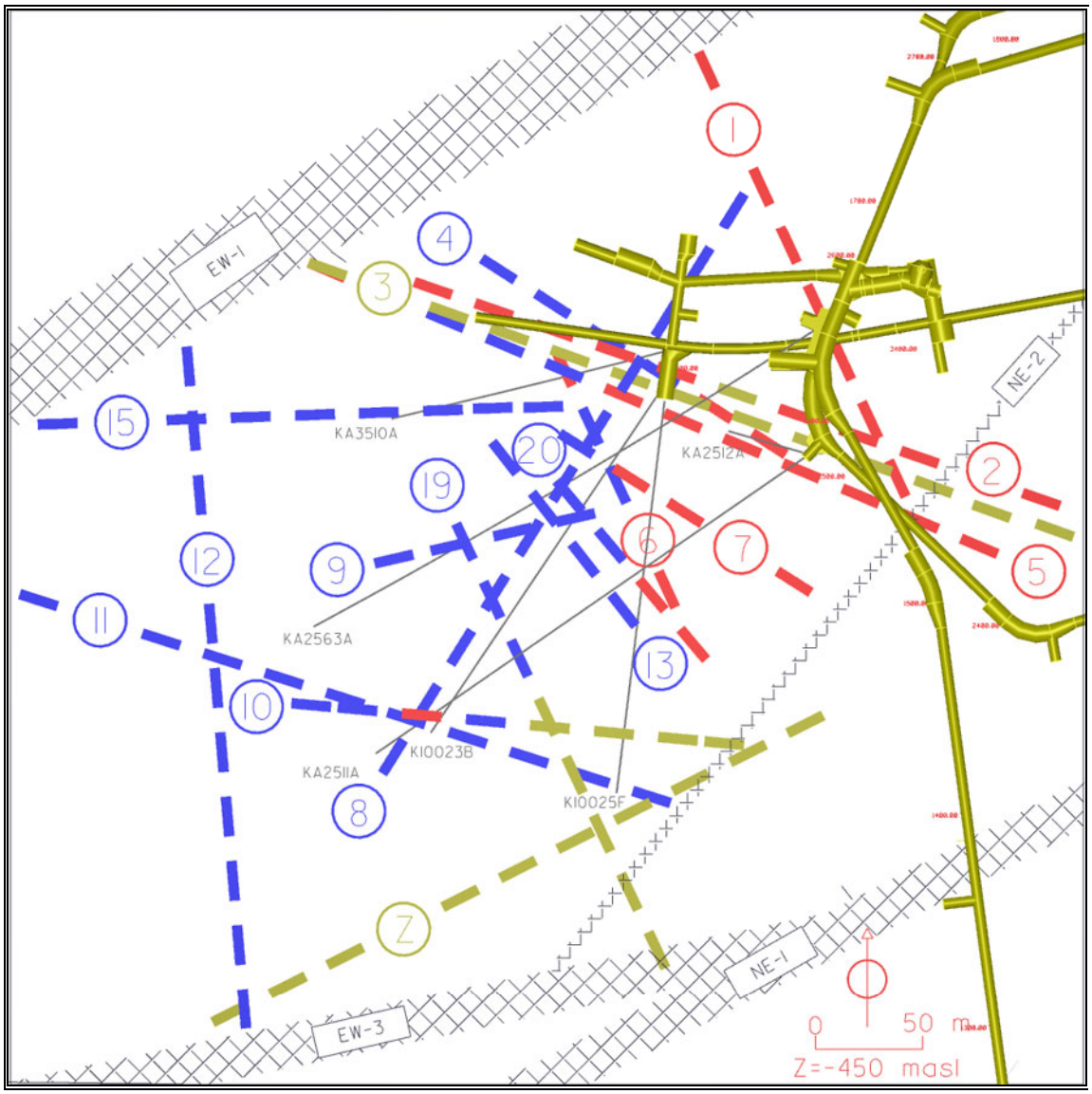

Figure 5-1. *September 1998 updated structural model. The identified structures are coloured according to the geological signature, where fracture is represented by red, fault by blue, swarm by green and zone by yellow. Hatched grey areas represent site scale zones from Rhén et al. (1997), cf. Hermanson (in prep.).*

5.2 Hydraulic parameters

In Table 5-2 the estimated ranges of hydraulic parameters for the structures tested during the interference tests are summarized. The estimated transmissivity and storativity for structures #5 and #7, tested by the global tests, are significantly higher than those estimated for structures #20 and #9 (and possible sub-parallel structures) from the local tests. However, the hydraulic diffusivity of these structures seems to be in the same order of magnitude (or slightly higher for structure #20).

Table 5-2 shows that the transmissivity estimated by e.g. Cooper-Jacob's method from the global and local tests, respectively, are quite uniform while the estimated ranges of storativities are larger. This is well in agreement with the results of numerical simulations of interference tests in heterogeneous media by Meier et al. (1988). Thus, the hydraulic diffusivity, rather than the transmissivity, better reflects the connectivity pattern in heterogeneous rock.

Table 5-2. Summary of estimated, general ranges of hydraulic parameters of the structures tested during the interference tests. NFB=(Apparent) No-flow hydraulic boundary.

Test	Struc-ture	T-range (m^2/s)	S-range	T/S-range (m^2/s)	K'/b'-range (s^{-1})	Dominating flow geometry
ENW-2	7	$2\text{-}4\cdot10^{-5}$	$1\text{-}3\cdot10^{-6}$	10-30	No leakage	Radial flow
ENW-1	5	$2\text{-}4\cdot10^{-5}$	$0.07\text{-}9\cdot10^{-6}$	1-10 (279)	$5\text{-}15\cdot10^{-11}$ -	Radial, Leaky Radial→NFB.
ESV-2	7	$3\text{-}5\cdot10^{-5}$	$0.2\text{-}4\cdot10^{-6}$	1-50 (250)	No leakage	Radial → NFB
ESV-1a	20	$7\text{-}10\cdot10^{-7}$	$5\text{-}50\cdot10^{-8}$	1-20	$5\text{-}50\cdot10^{-12}$	Radial → Leaky
ESV-1b	20	$7\text{-}10\cdot10^{-7}$	$1\text{-}8\cdot10^{-8}$	10-100	$2\text{-}20\cdot10^{-12}$	Radial → Leaky
ESV-1c	9	$7\text{-}12\cdot10^{-7}$	$0.04\text{-}4\cdot10^{-7}$	1-10 (300)	$0.5\text{-}40\cdot10^{-12}$	Radial → Leaky

5.3 Flow and transport parameters

The tracer dilution tests showed that the "natural" flow varies quite a lot within the block scale volume. Extremely high flow rates were measured in two borehole sections KA2511A:S4 (structures #6 and #16) and KA2563A:R5 (structure #20), 1200 and 600 ml/h, respectively. The flow rates in the other measured sections were typically less than 10 ml/h, or even less than 1 ml/h. This large difference cannot be explained by differences in transmissivity alone (cf. Chapter 4.4). Also the hydraulic gradient must vary considerably within the block. Estimates of the hydraulic gradient based on the measured flow rates indicate high gradients in structures #20 and #6 (1-2 m/m) while structures #9, #13 and #19 have low gradients (0.01-0.1 m/m), or even extremely low in structure #7 (0.0004 m/m). The high flow rates may result from a closely located intercept with a structure having lower hydraulic head. The extremely low gradient in structure #7 is somewhat surprising considering the short distance to the tunnel (about 40 m).

The tracer test performed by pumping in structure #9 resulted in tracer breakthrough from only one of the three injection points, KA2563A:R5 (structure #20), which also was the only section where the flow rate increased as a result of pumping. The two other injections in KI0023B:P4 (structure #13) and KI0025F:R4 (structure #20) did not result in any measurable tracer breakthrough within the time frames of the test (about 18 days). Thus, it has been shown that it is possible to perform tracer tests between different structures within the investigated block.

A tracer recovery of 44% along the 16 m long flow path indicates that mass losses occur along the flow path, possibly due to a combination of a weak sorption of the tracer (Rhodamine WT) and hydraulic head conditions (intersections with other structures having lower hydraulic head).

The transport parameters derived from the numerical modelling indicate that structure #20 has similar characteristics as the thoroughly investigated Feature A at the TRUE-1 site.

REFERENCES

Andersson, P., Nordqvist, R., Persson, T., Eriksson, C-O., Gustafsson, E., Ittner, T., 1993. Dipole tracer experiment in a low-angle fracture zone at Finnsjön – results and interpretation. The Fracture Zone Project – Phase 3. SKB Technical Report TR 93-26.

Andersson, P., 1996. TRUE 1st stage tracer test programme. Experimental data and preliminary evaluation of the TRUE-1 radially converging tracer test (RC-1). Äspö Hard Rock Laboratory Progress Report HRL-96-24.

Andersson, P., Johansson, H., Nordqvist, R., Skarnemark, G., Skålberg, M., Wass, E., 1998. TRUE 1st stage tracer test programme. Tracer tests with sorbing tracers, STT-1. Experimental description and preliminary evaluation. Äspö Hard Rock Laboratory International Progress Report IPR-99-36.

Andersson, P., Ludvigsson, J-E., Wass, E., in prep. TRUE Block Scale Project. Preliminary Characterization Stage. Combined Interference Tests and Tracer Tests. Appendix volume. Evaluation plots and data sheets for interference test interpretation. Äspö Hard Rock Laboratory International Progress Report IPR-01-47.

Gentzschein, B., 1997. TRUE Block Scale Project. Detailed flow logging of core borehole KA2563A. SKB Internal Report.

Gentzschein, B., 1998. TRUE Block Scale Project. Detailed flow logging in core borehole KI0023B using a double packer system. SKB Internal Report.

Gustafsson, E., Klockars, C-E., 1981. Studies of groundwater transport in fractured crystalline rock under controlled conditions using non-radioactive tracers. Swedish Nuclear Fuel and Waste Management Company. SKBF/KBS Technical Report TR 81-07

Hermanson, J., 1998. TRUE Block Scale Project. October 1997 structural model; Update using characterisation data from KA2511A and KI0025F. Äspö Hard Rock Laboratory International Progress Report IPR-01-45.

Hermanson, J., in prep. TRUE Block Scale Project. Preliminary Characterisation Stage. September 1998 Structural model; Update using characterisation data from KI0023B. Äspö Hard Rock Laboratory International Progress Report IPR-01-42.

Meier P.M., Carrera J. and Sánchez-Vila, 1998. An evaluation of Jacob's method for the interpretation of pumping tests in heterogeneous formations. Water Res. Res, Vol. 34, No 5, pp. 1011-1025, May 1998.

Moye, D.G., 1967. Diamond drilling for foundation exploration. Civil Eng. Trans., Inst. Eng. Australia (Apr. 1967), 95-100.

Nordqvist, R., 1994. Documentation of some analytical flow and transport models implemented for use with PAREST - Users manual. GEOSIGMA GRAP 94 006, Uppsala.

Ogata, A., Banks, R., 1961. A solution to the differential equation of longitudinal dispersion in porous media. U.S. Geol. Surv. Prof. Paper 411-A, Washington.

Rhén, I., Gustafson, G., Stanfors, R., Wikberg, P., 1997. Geoscientific evaluation 1997/5. Models based on site characterisation 1986-1995.
SKB Technical Report TR 97-06.

Rhén, I., Forsmark, T., Gustafson, G., 1991. Transformation of dilution rates in borehole sections to groundwater flow in the bedrock. Technical Note 30. In: Liedholm, M. (ed), 1991: SKB-Äspö Hard Rock Laboratory, Conceptual Modeling of Äspö, Technical Notes 18-32. General Geological, Hydrogeological and Hydrochemical information. Swedish Nuclear Fuel and Waste Management Company. Äspö Hard Rock Laboratory Progress Report PR 25-90-16 b.

Van Genuchten, M., Th., 1982. One-dimensional analytical transport modeling, in Proceedings: Symposium on unsaturated flow and transport modeling. Rep. PNL-SA-10325, Pacific Northwest Lab., Richland, Washington

Van Genuchten M. Th., and Alves, W. J., 1982. Analytical solutions of the one-dimensional convective-dispersive solute transport equation. U.S. Dep. Agric. Tech. Bull. 1661.

Waterloo Hydrogeologic Inc. Aquifer Test version 2.0.

Winberg A (ed), 1996. First TRUE Stage - Tracer Retention Understanding Experiments. Descriptive structural-hydraulic models on block and detailed scales of the TRUE-1 site. Swedish Nuclear Fuel and Waste Management Company. Äspö Hard Rock Laboratory International Cooperation Report ICR 96-04.

Winberg, A., 1997a. Tracer Retention Understanding Experiments (TRUE). Test plan for the TRUE Block Scale Experiment. Äspö Hard Rock Laboratory International Cooperation Report ICR 97-02.

Winberg, A., 1997b. Pressure responses due to drilling of KI0025F. SKB Internal Report.

Winberg, A., Follin, S., Hermanson, J., Andersson, P., 1998. TRUE Block Scale Project. Proposal for interference tests in the preliminary characterization stage borehole array. SKB Internal Report.

Zuber, A., 1974. Theoretical possibilities of the two-well pulse method. Isotope Techniques in Groundwater Hydrology 1974, Proc. Symp., Vienna 1974, IAEA, Vienna

APPENDIX 1: Diagnostic response plots.

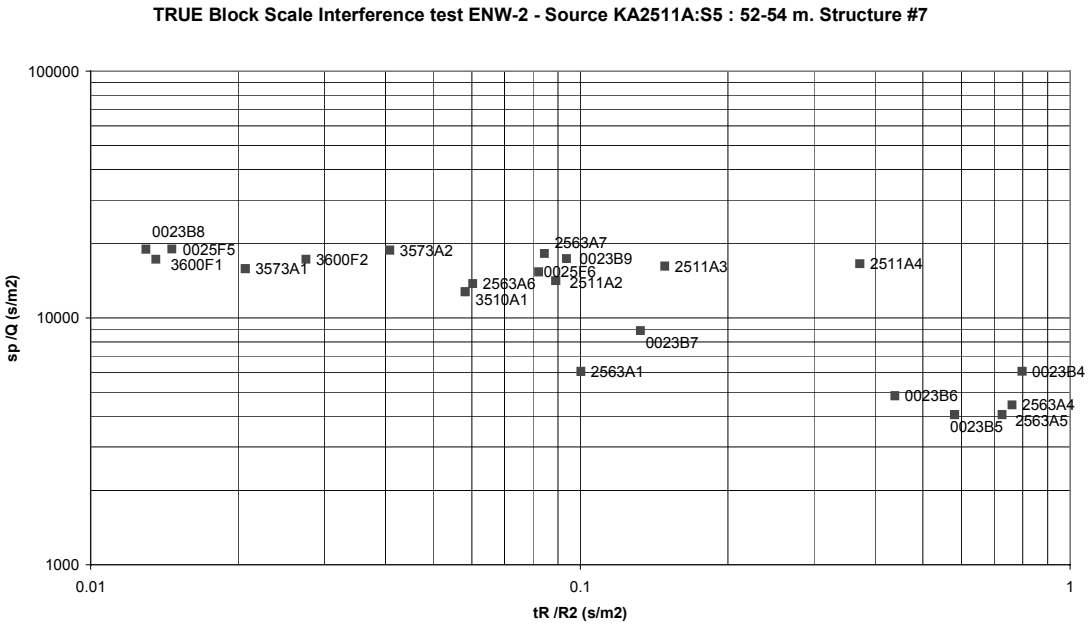

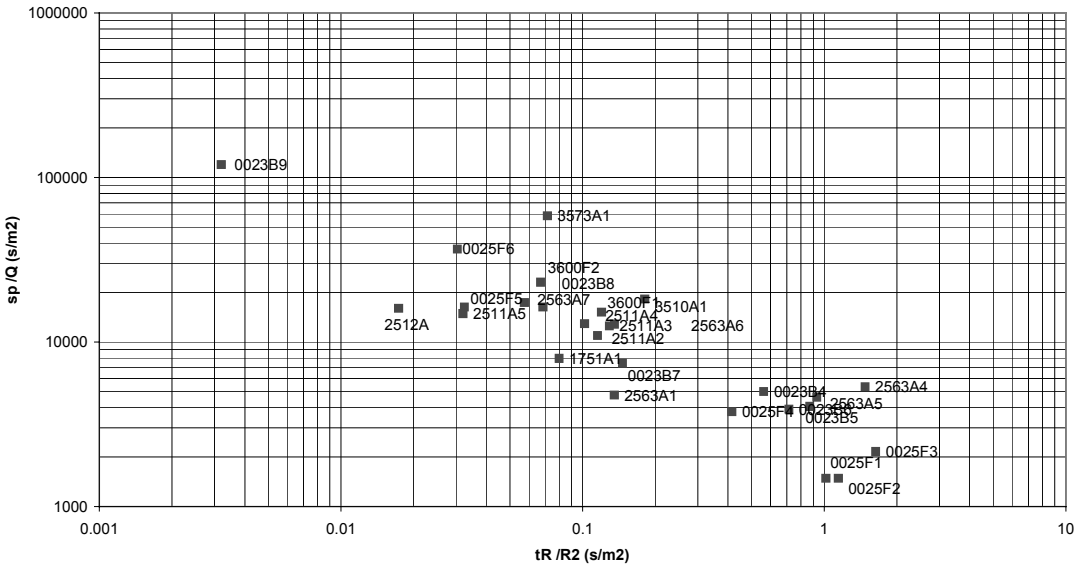

TRUE Block Scale Interference test ESV-2 - Source KI0023B:P8 : 41.45-42.45 m. Structure #7

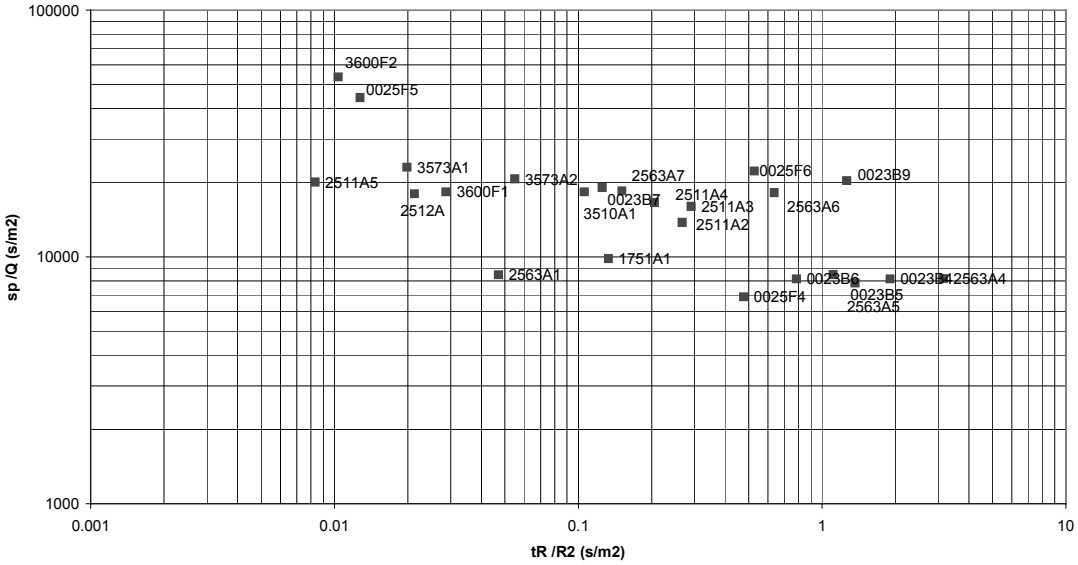

TRUE Block Scale Interference test ESV-1a - Source KA2563A:R5 : 187-190 m. Structure #20

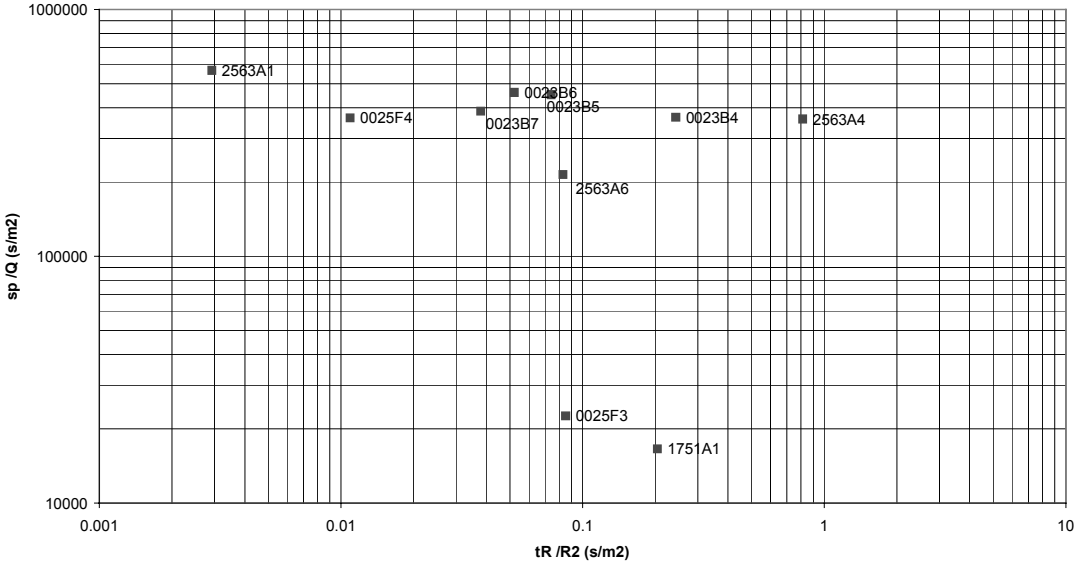

TRUE Block Scale Interference test ESV-1b - Source KI0025F:R4 : 86-88 m. Structure #20

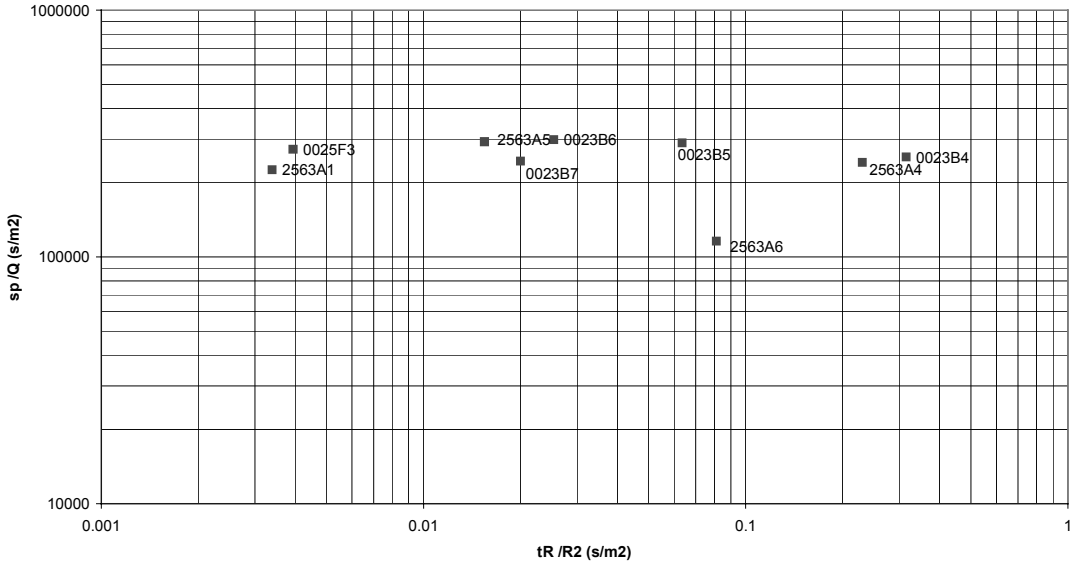

TRUE Block Scale Interference test ESV-1c - Source KI0023B:P6 : 70.95-71.95 m. Structure #9

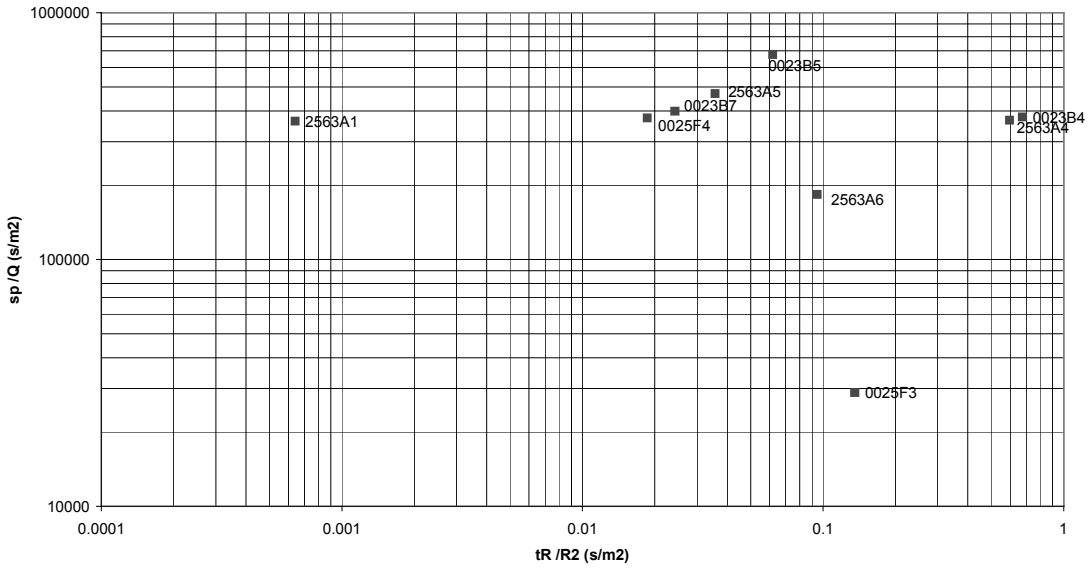

TRUE Block Scale Interference test #1 - Source KI0023B:P4 : 84.75-86.2 m. Structure #13

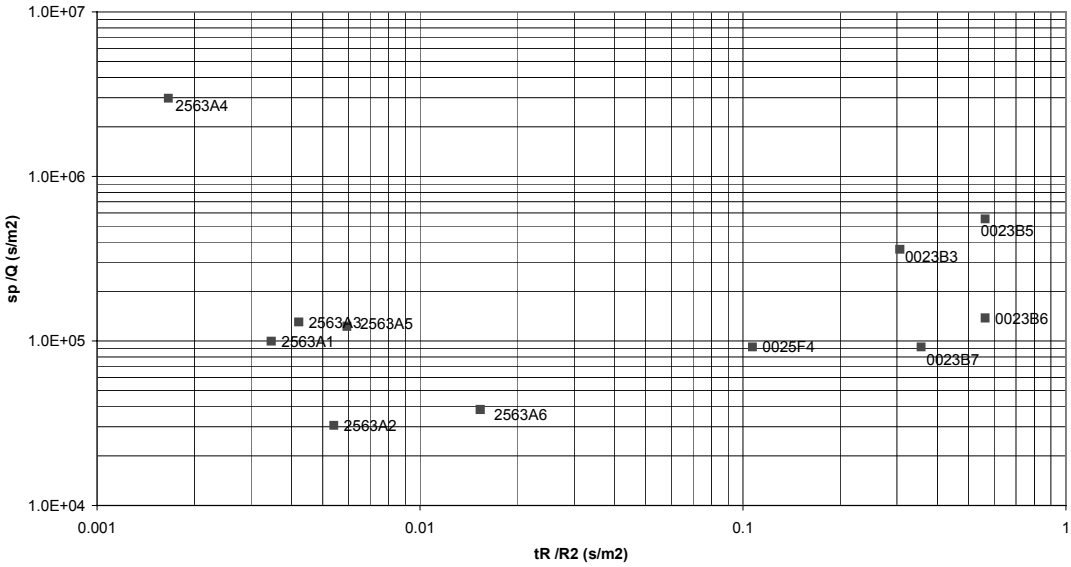

TRUE Block Scale Interference test #2 - Source KA2512A. Structure #5

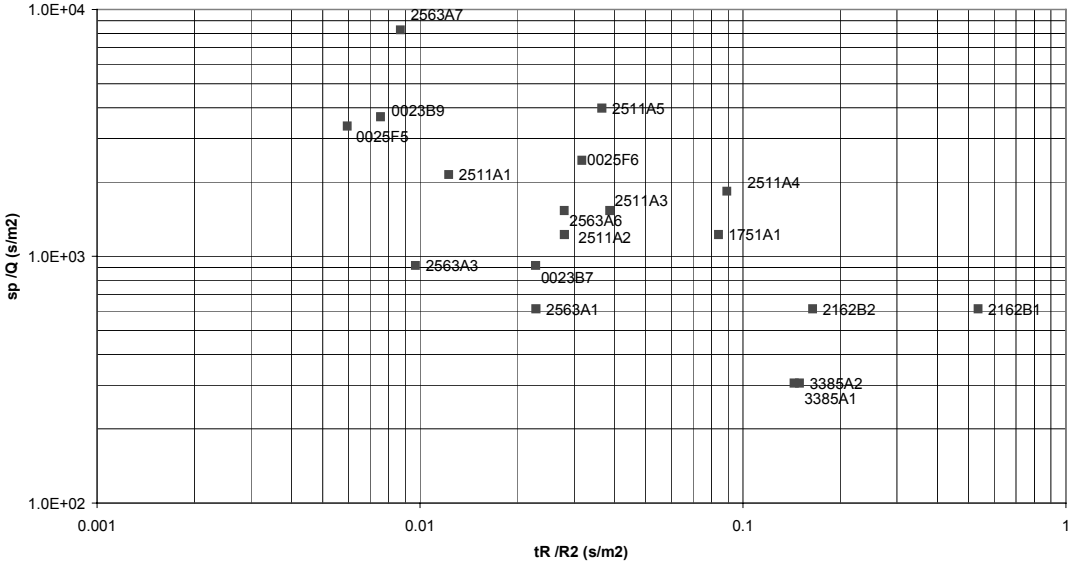

TRUE Block Scale Interference test #3 - Source KA2598A. Structure #1, #8

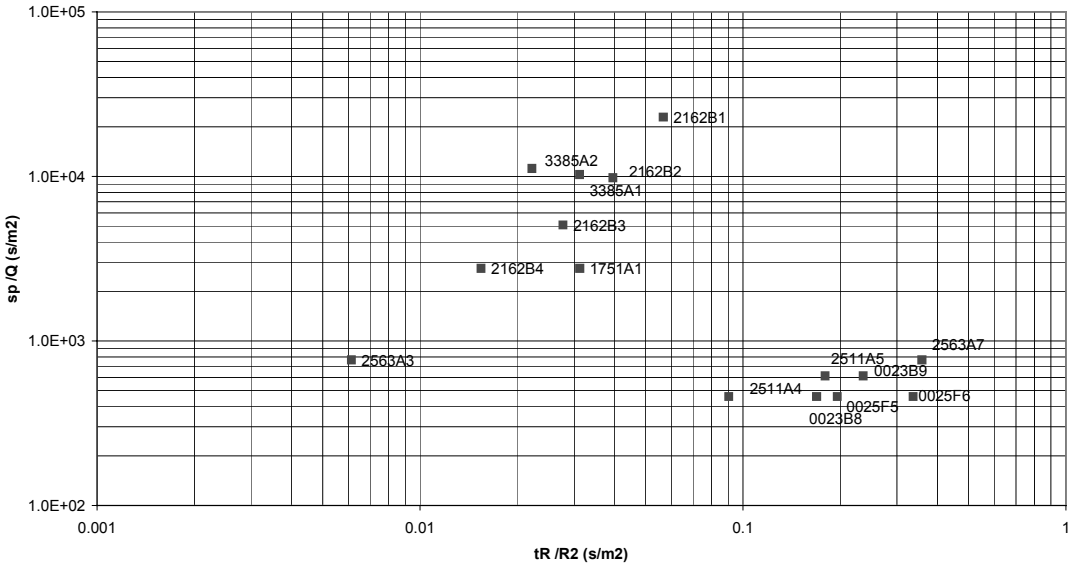

TRUE Block Scale Short-time Interference test #4 - Source KA2563A:R1 : 262-363 m. Structure #9, #10

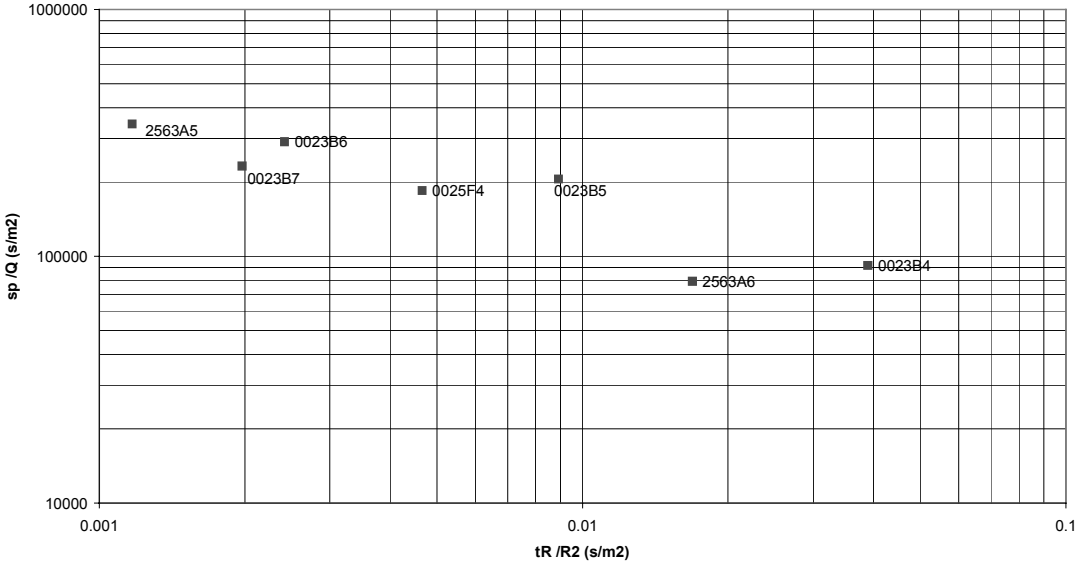

TRUE Block Scale Short-time Interference test #5- Source KA2563A:R4 : 191-219 m. Structure #13, #18

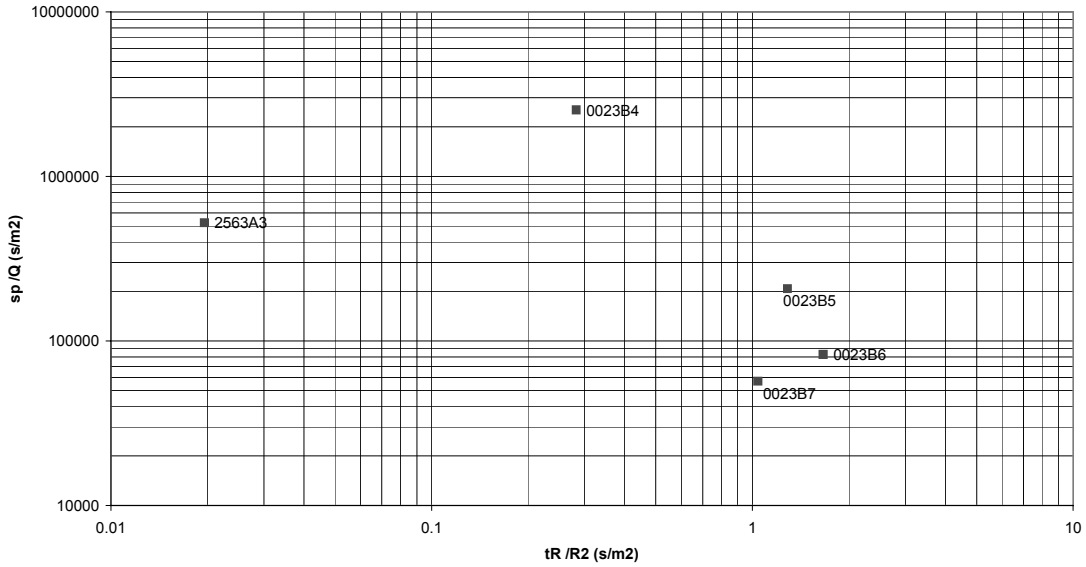

TRUE Block Scale Short-time Interference test #6 - Source KA2511A:S4 : 92-109 m. Structure #6, #16

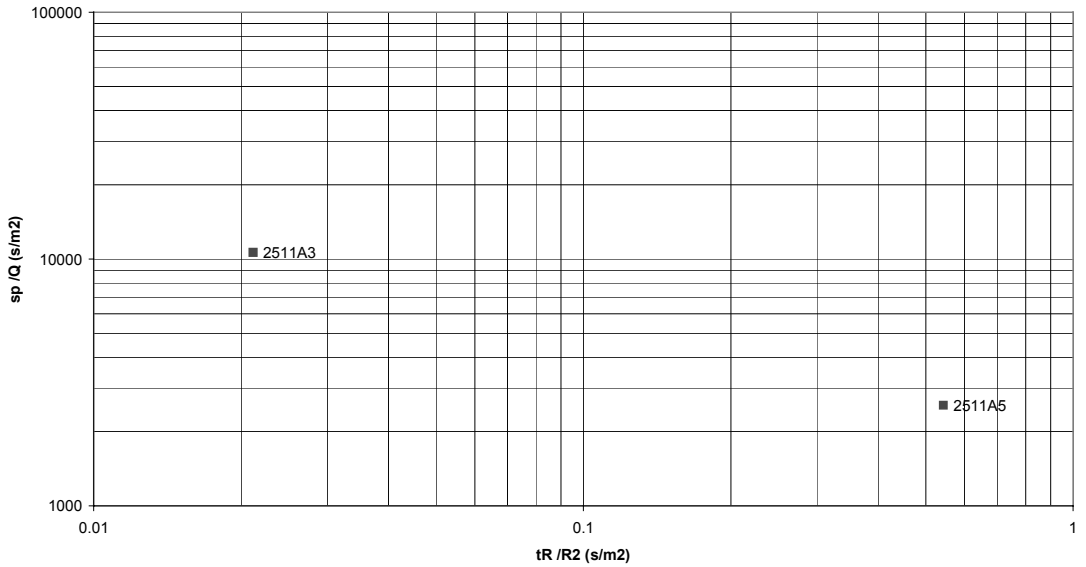

TRUE Block Scale Short-time Interference test #7 - Source KI0025F:R3 : 89-163 m. Structure #?

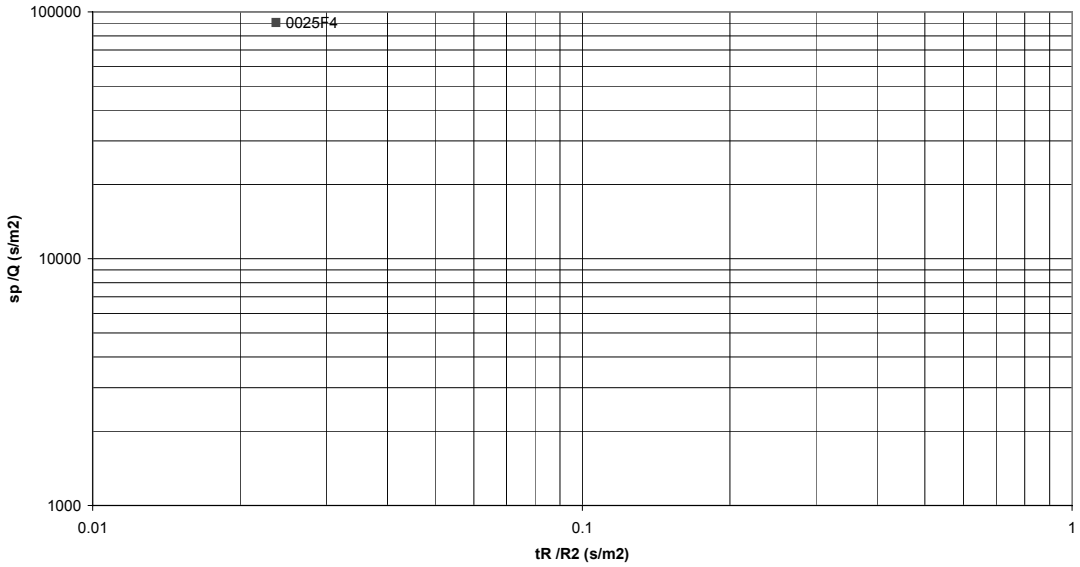

TRUE Block Scale Short-time Interference test #8 - Source KI0025F:R5 : 41-85 m. Structure #6, #7

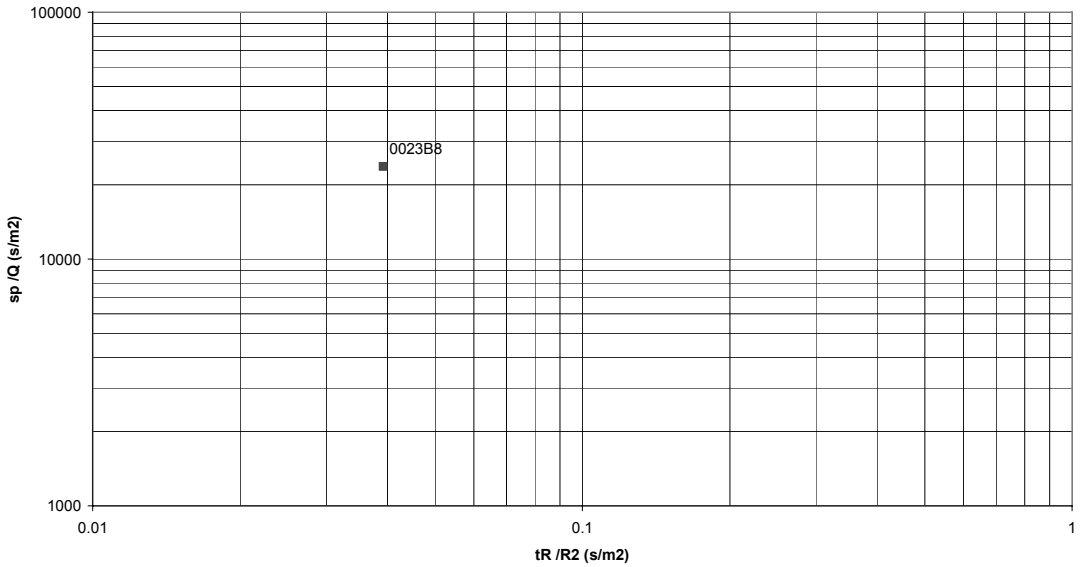

TRUE Block Scale Short-time Interference test #9 - Source KI0025F:R2 : 164-168 m. Structure #19

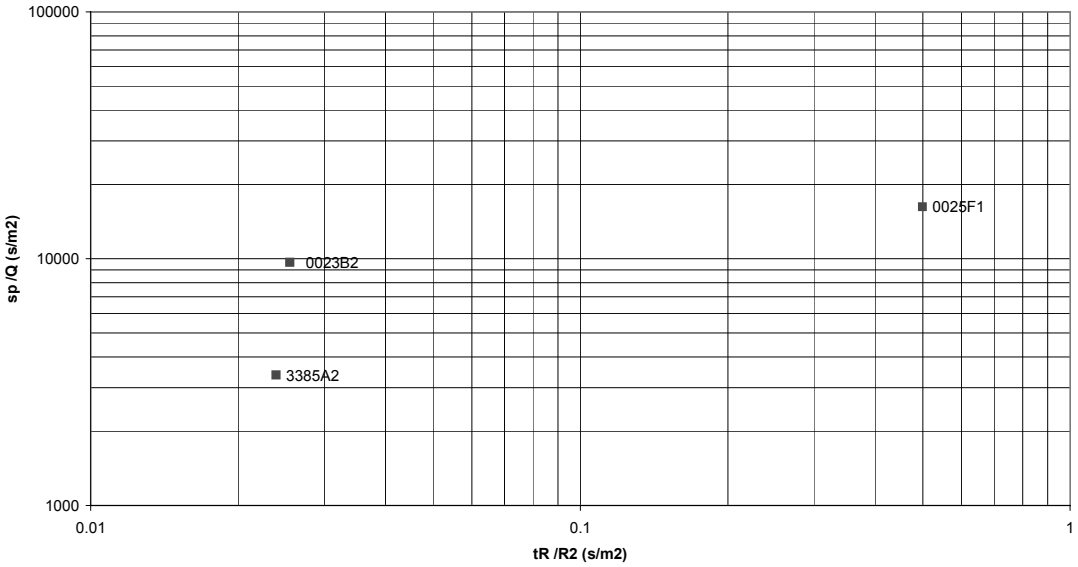

TRUE Block Scale Short-time Interference test#10-Source KI0023B:P7: 43.45-69.95m. Structure #6,#20

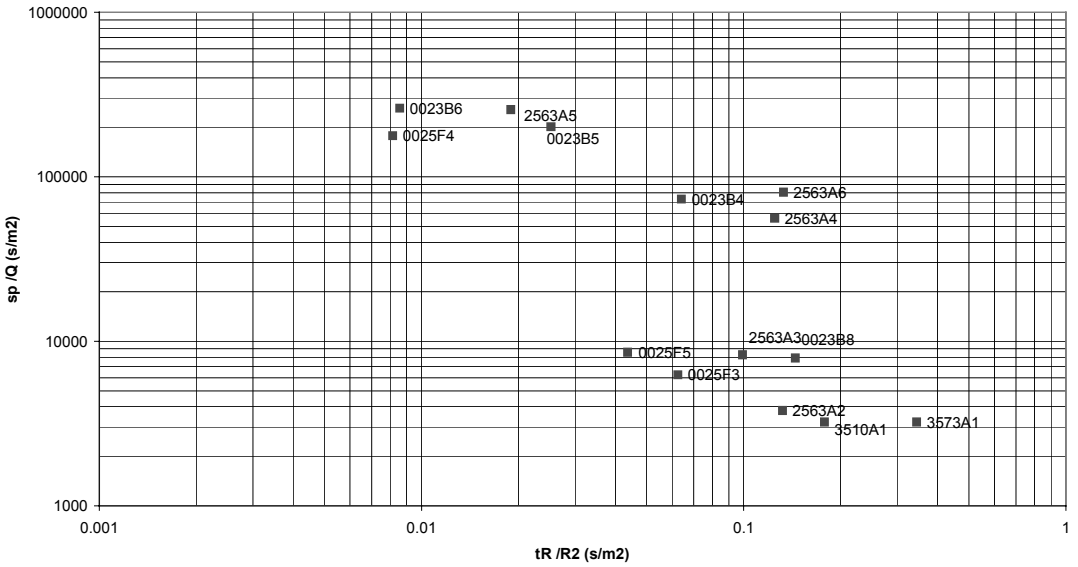

TRUE Block Scale Short-time Interference test #11 - Source KI0023B:P5 : 72.95-83.75 m. Structure #18

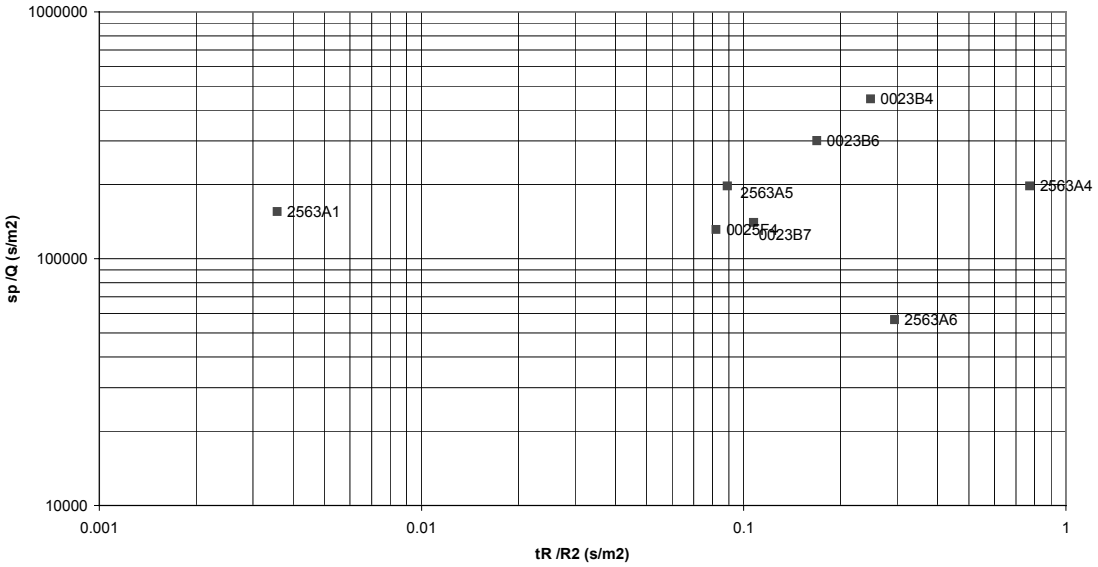

TRUE Block Scale Short-time Interference test #12 -Source KI0023B:P2: 111.25-112.7 m. Structure #19

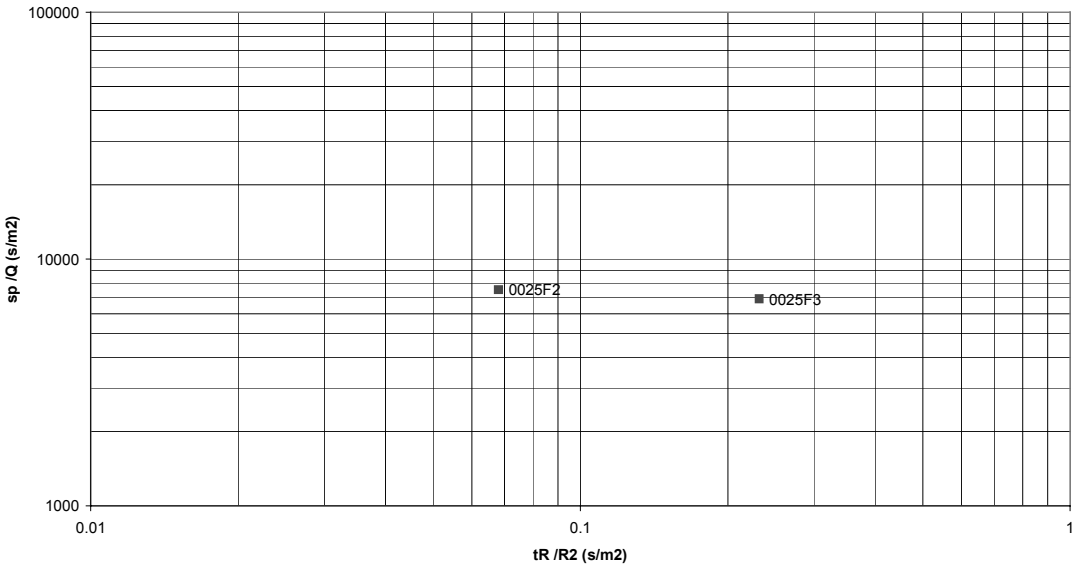

TRUE Block Scale Short-time Interference test #13 - Source KA3573A:P1 : 18-40 m. Structure #15

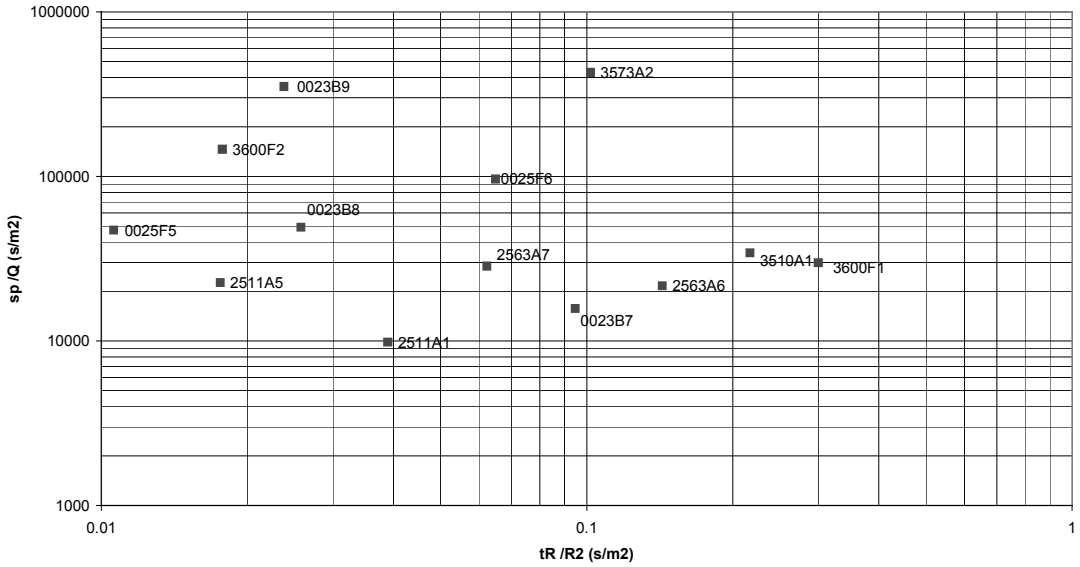

APPENDIX 2: Distances between source sections and observation sections

Borehole	ENW-2	ENW-1	ESV-2	ESV-1a	ESV-1b	ESV-1c	1	2	3	4	5	6	7	8	9	10	11	12	13
KA2511A:S1	190	170	136	114	110	109	243	221	277	99	105	143	92	125	89	123	103	73	152
KA2511A:S2	176	161	125	105	99	99	229	207	263	105	96	129	83	114	85	112	93	65	143
KA2511A:S3	110	129	86	76	67	71	163	142	199	149	79	63	72	74	95	78	68	67	112
KA2511A:S4	48	126	87	94	86	92	101	82	141	201	106		108	80	138	89	95	113	115
KA2511A:S5		144	114	129	122	128	53	41	100	245	143	47	147	111	178	120	132	156	137
KA2563A:R1	245	163	147	124	140	122	294	271	310		108	201	133	148	139	135	116	92	150
KA2563A:R2	163	90	62	38	70	39	211	188	225	86	22	124	87	70	115	50	34	32	74
KA2563A:R3	159	87	58	34	68	35	207	184	221	90	18	120	86	67	116	46	31	32	71
KA2563A:R4	143	75	41	17	60	21	190	167	203	108		106	85	54	119	29	19	39	59
KA2563A:R5	129	67	27		57	16	174	152	187	124	17	94	88	45	124	16	20	50	51
KA2563A:R6	109	61	14	23	61	30	153	131	165	146	39	80	96	42	135	18	36	69	48
KA2563A:R7	71	79	58	79	96	83	103	83	112	202	95	69	132	74	171	70	90	121	76
KI0025F:R1	191	206	148	139	95	125	114	230	264	144	133	151	55	118	15	136	119	97	190
KI0025F:R2	178	192	133	124	79	110	100	217	250	139	119	138	40	103		121	105	84	175
KI0025F:R3	147	155	93	88	39	73	65	185	216	133	85	108		63	40	82	69	58	139
KI0025F:R4	122	120	65	57		42	41	157	184	139	60	86	39	24	79	47	41	52	106
KI0025F:R5	111	101	35	45	24	33	41	142	166	148	54	80	63		103	31	37	62	89
KI0025F:R6	101	74	25	51	65	52	66	123	140	171	66	84	104	41	144	38	59	92	68
KI0023B:P1	195	158	120	99	91	91	77	227	271	71	86	149	74	108	75	106	84	50	141
KI0023B:P2	156	114	70	50	52	41	27	186	225	92	39	113	58	62	84	56	34		97
KI0023B:P3	146	103	57	38	45	28	14	176	213	100	28	105	60	51	91	43	21	13	87
KI0023B:P4	137	92	44	26	41	15		165	201	111	21	98	65	41	100	29	7	27	76
KI0023B:P5	133	87	36	20	41	7.3	7	160	194	116	19	95	69	37	105	22		34	71
KI0023B:P6	128	82	29	16	42		15	155	188	122	21	92	73	33	110	14	7	41	67
KI0023B:P7	120	73	15	16	47	15	29	145	175	135	29	89	82	31	121		22	56	59
KI0023B:P8	114	66		27	56	29	44	137	163	147	41	87	93	35	133	14	36	70	55
KI0023B:P9	107	61	20	44	71	48	63	126	147	165	59	89	109	47	149	34	56	90	55
KA3510A:P1	164	43	58	53	104	65	72	178	201	130	54	139	134	88	170	58	68	91	39
KA3573A:P1	137	18	55	51	106	67	76	147	183	150	59	115	139	89	175	59	71	97	
KA3573A:P2	144		66	67	120	82	90	150	180	163	75	126	154	101	191	73	87	114	18
KA3600F:P1	188	59	112	100	157	115	119	192	235	150	99	164	183	143	215	113	117	131	60
KA3600F:P2	175	39	99	92	149	108	114	178	215	159	94	155	179	133	213	130	111	130	45
KA1751A:P1	245	245	285	297	332	309	321	207	219	402	310	274	367	310	404	297	315	343	256
KA2162B:P1	95	194	174	197	190	197	209	82	23	319	213	140	219	174	251	185	203	231	195
KA2162B:P2	158	265	240	263	247	261	273	148	87	382	279	201	271	234	299	250	267	293	267
KA2162B:P3	215	325	297	321	301	318	329	207	147	438	336	258	322	290	346	308	323	350	326
KA2162B:P4	265	376	347	371	348	367	377	257	197	486	386	306	367	338	389	357	372	397	377
KA3385A:P1	144	209	167	192	167	186	196	158	98	298	205	166	190	156	218	176	191	216	208
KA3385A:P2	144	202	164	190	168	185	196	155	90	297	203	166	194	156	224	174	190	217	203
KA2512A	41	150	150	152	157	155	165		88	283	178	90	190	148	222	145	160	186	147
KA2598A	100	180	163	187	184	188	201	88		310	203	141	216	166	250	175	194	225	183
Source =																			

APPENDIX 3: Tracer dilution graphs (Ln C versus time) including best regression estimate (straight line).

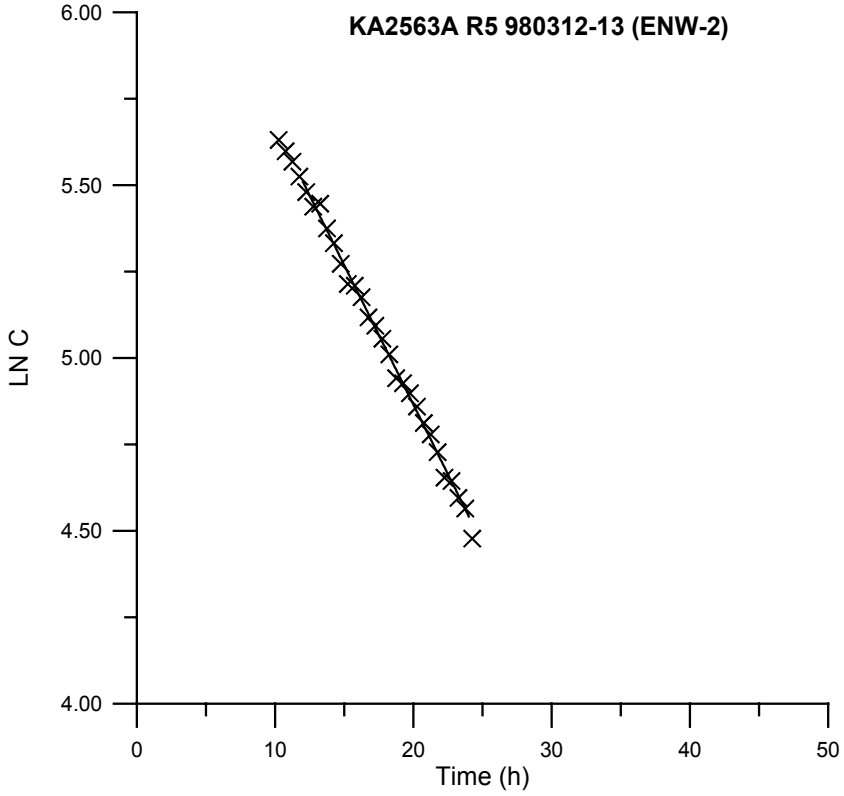

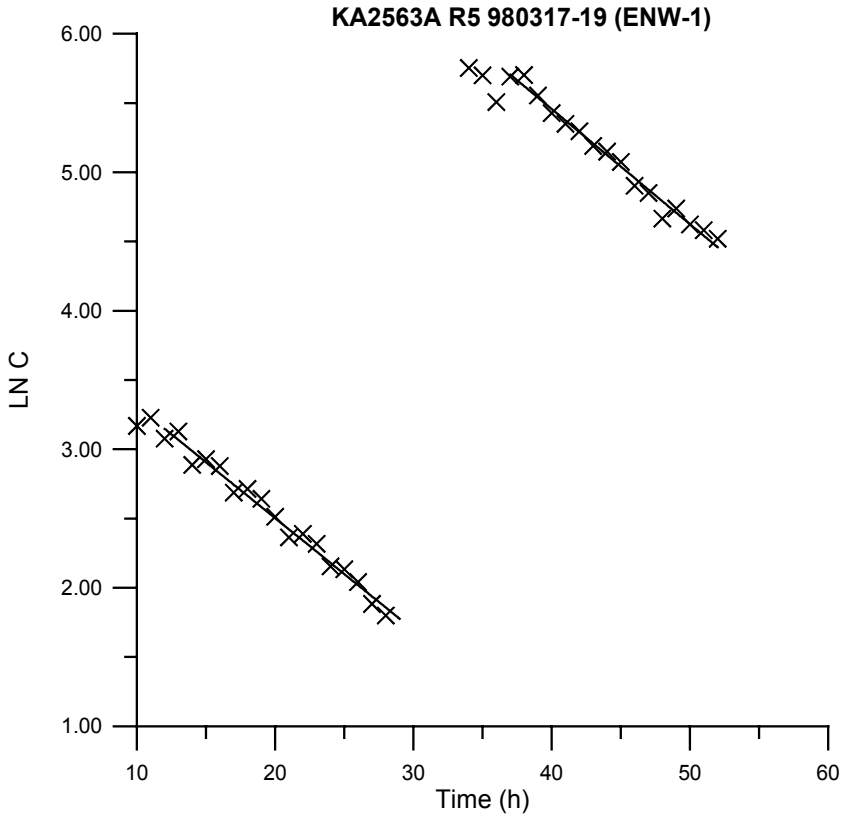
KA2563A R5 980317-19 (ENW-1)
6.00
5.00
4.00
3.00
2.00
1.00
LN C
10
20
30
40
50
60
Time (h)

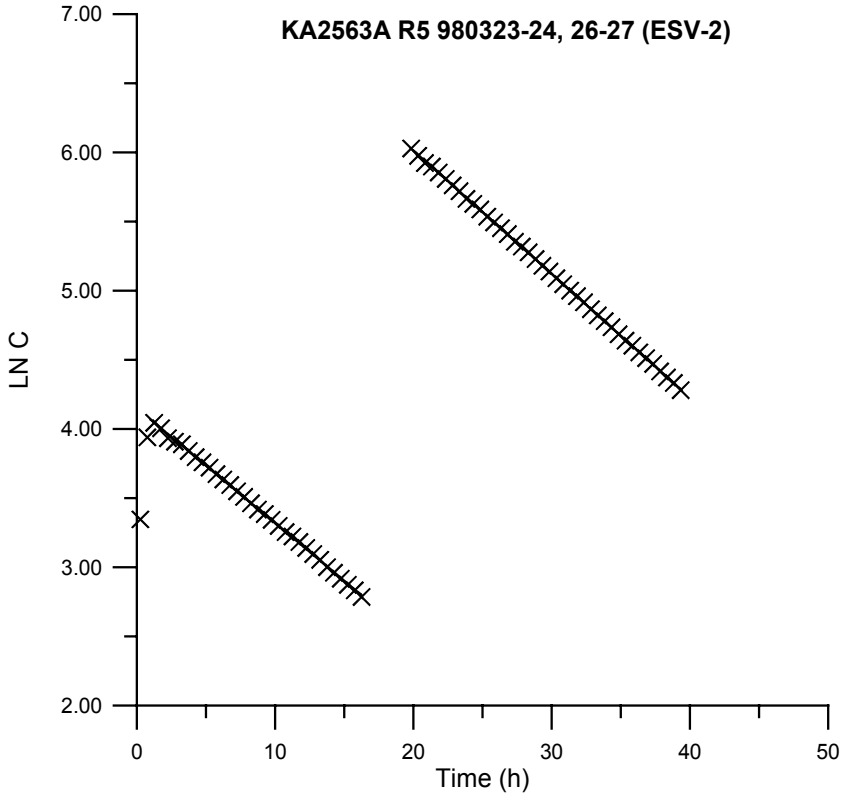
KA2563A R5 980323-24, 26-27 (ESV-2)
7.00
6.00
5.00
4.00
3.00
2.00
LN C
0
10
20
30
40
50
Time (h)

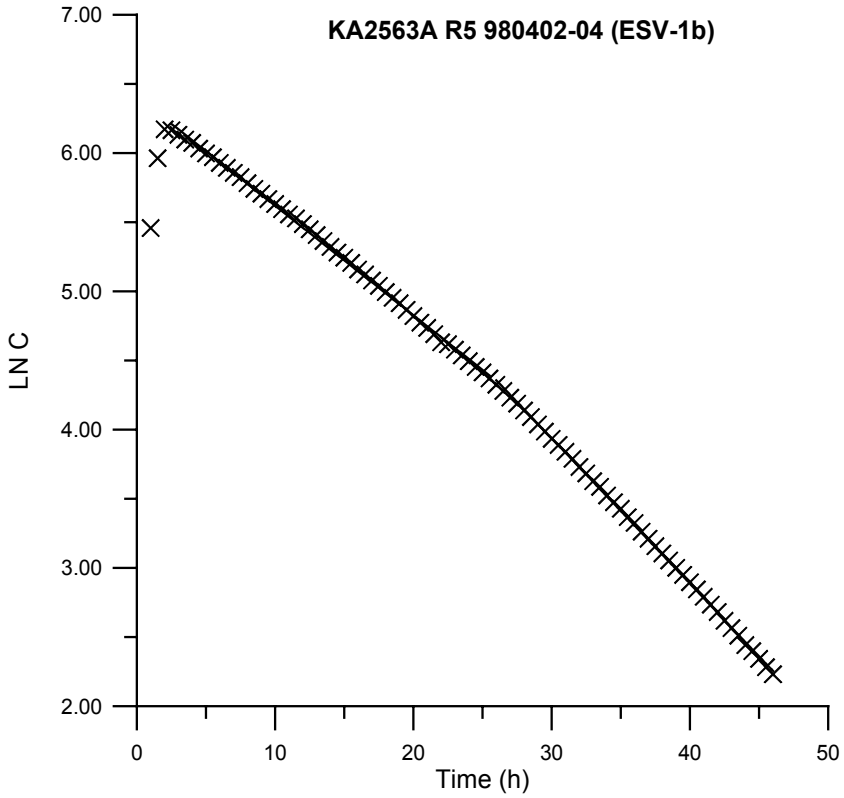
KA2563A R5 980402-04 (ESV-1b)
7.00
6.00
5.00
4.00
3.00
2.00
LN C
0
10
20
30
40
50
Time (h)

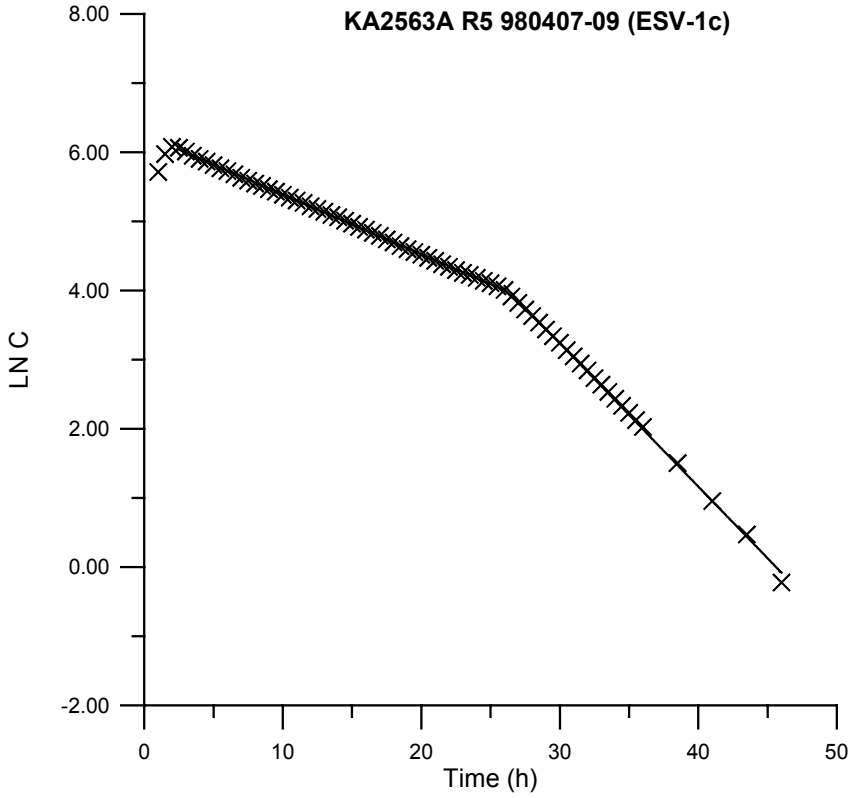
KA2563A R5 980407-09 (ESV-1c)
8.00
6.00
4.00
2.00
0.00
-2.00
LN C
0
10
20
30
40
50
Time (h)

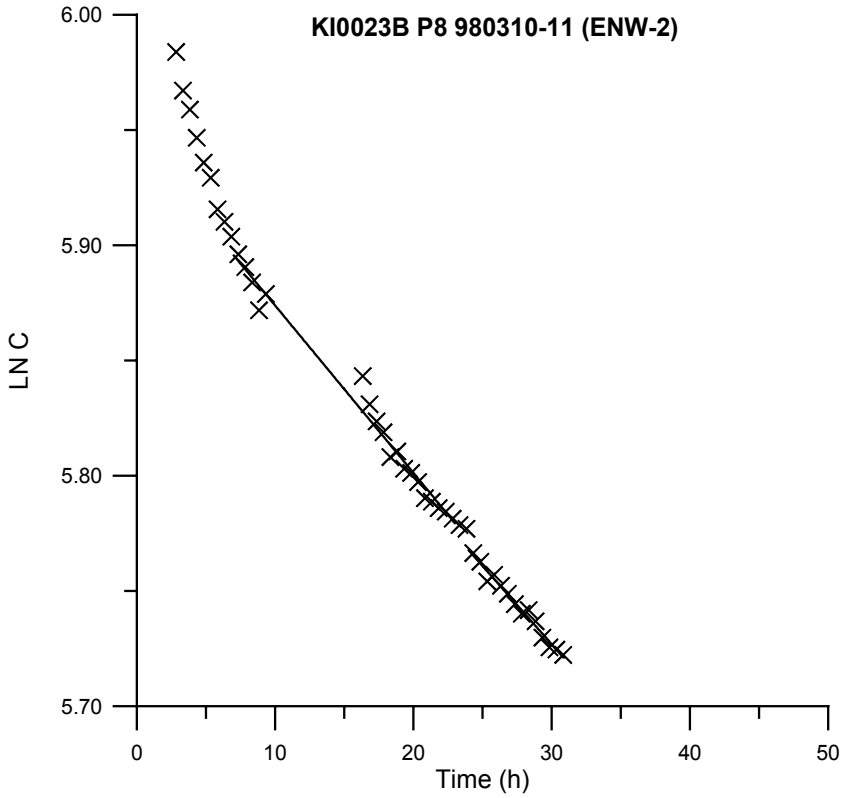
KI0023B P8 980310-11 (ENW-2)
6.00
5.90
5.80
5.70
LN C
0
10
20
30
40
50
Time (h)

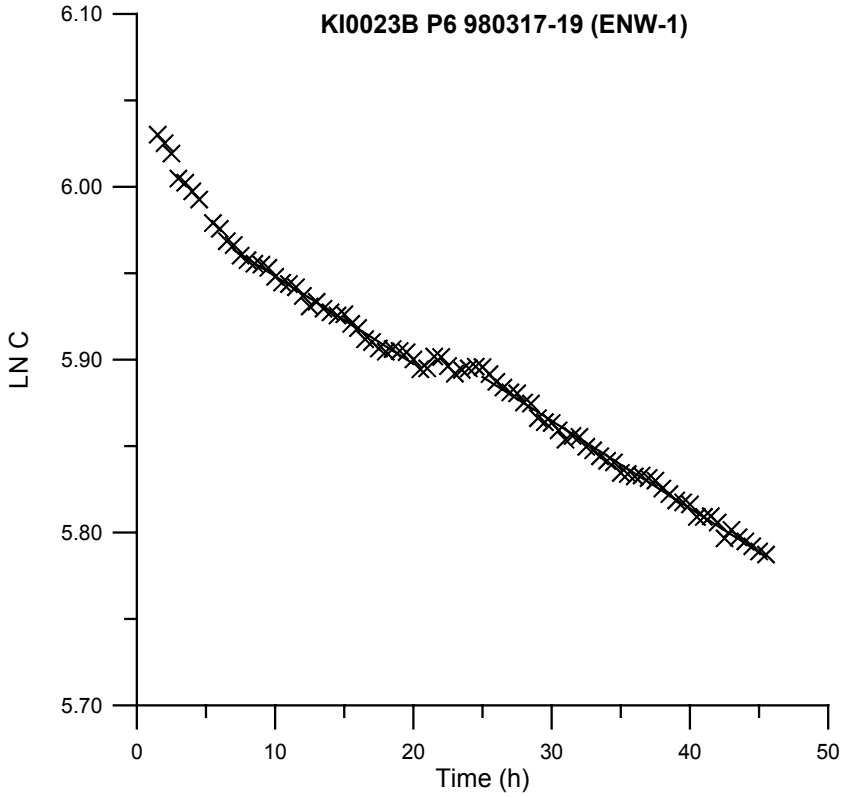
KI0023B P6 980317-19 (ENW-1)
6.10
6.00
5.90
5.80
5.70
LN C
0
10
20
30
40
50
Time (h)

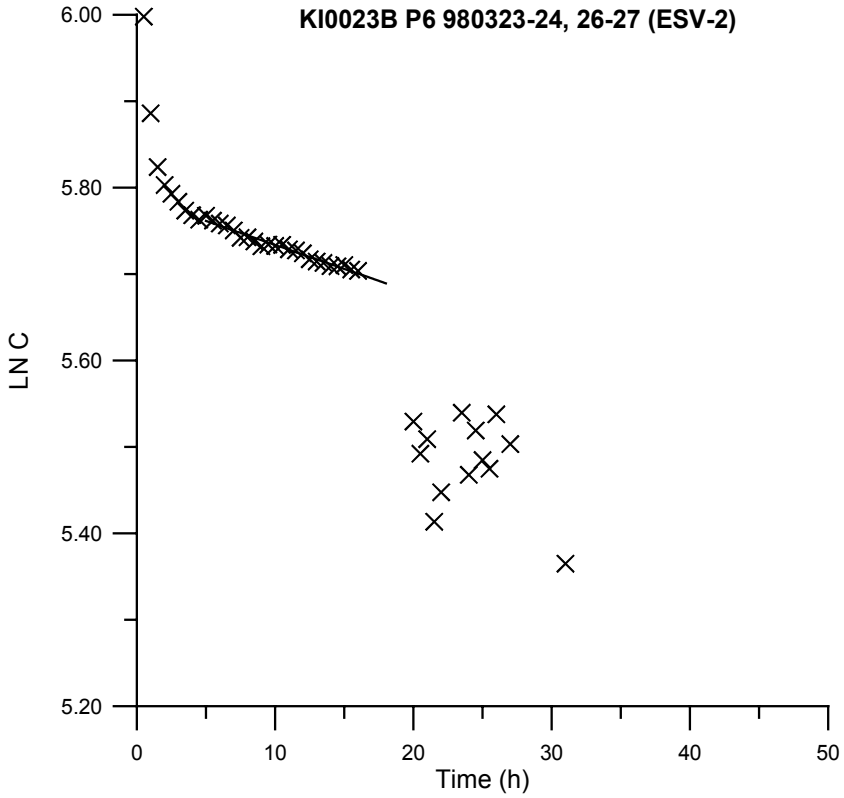
KI0023B P6 980323-24, 26-27 (ESV-2)
LN C
Time (h)
6.00
5.80
5.60
5.40
5.20
0
10
20
30
40
50

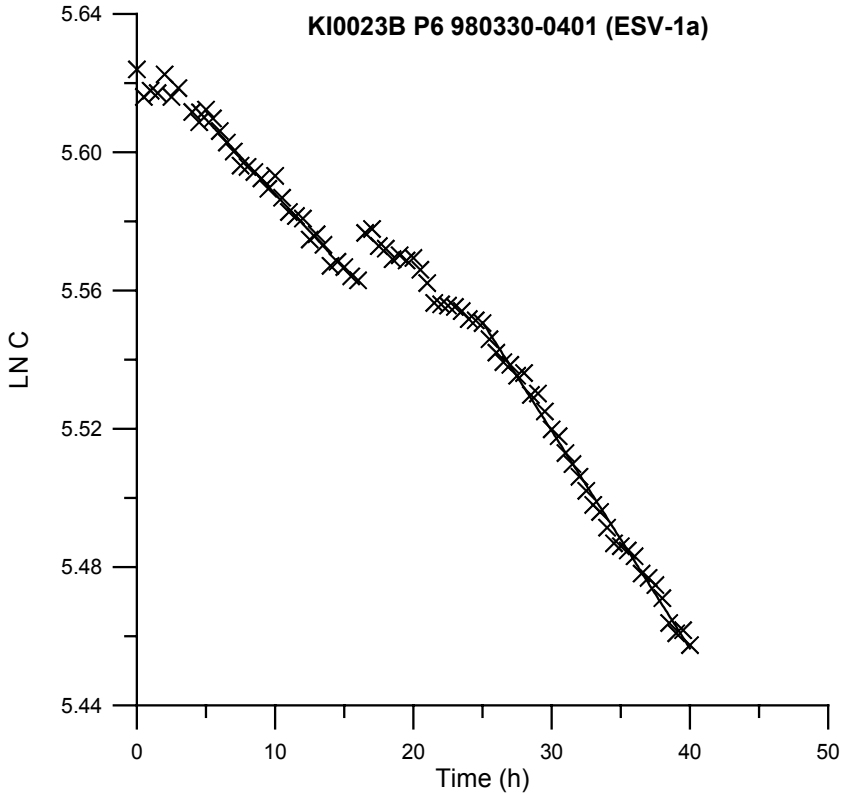
KI0023B P6 980330-0401 (ESV-1a)
LN C
Time (h)
5.64
5.60
5.56
5.52
5.48
5.44
0
10
20
30
40
50

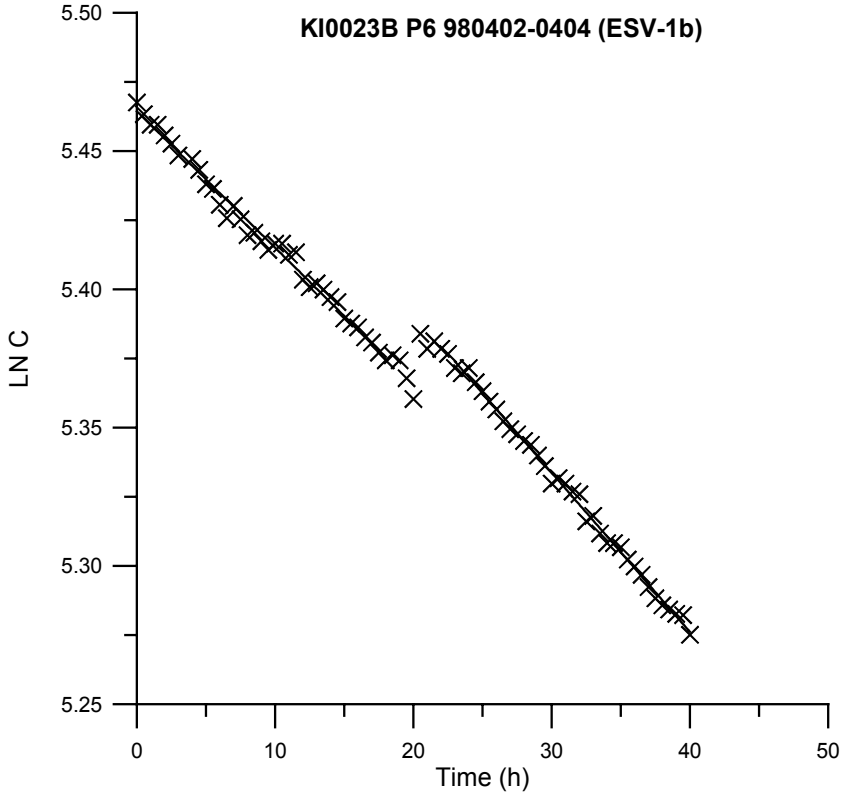
KI0023B P6 980402-0404 (ESV-1b)
LN C
5.50
5.45
5.40
5.35
5.30
5.25
0
10
20
30
40
50
Time (h)

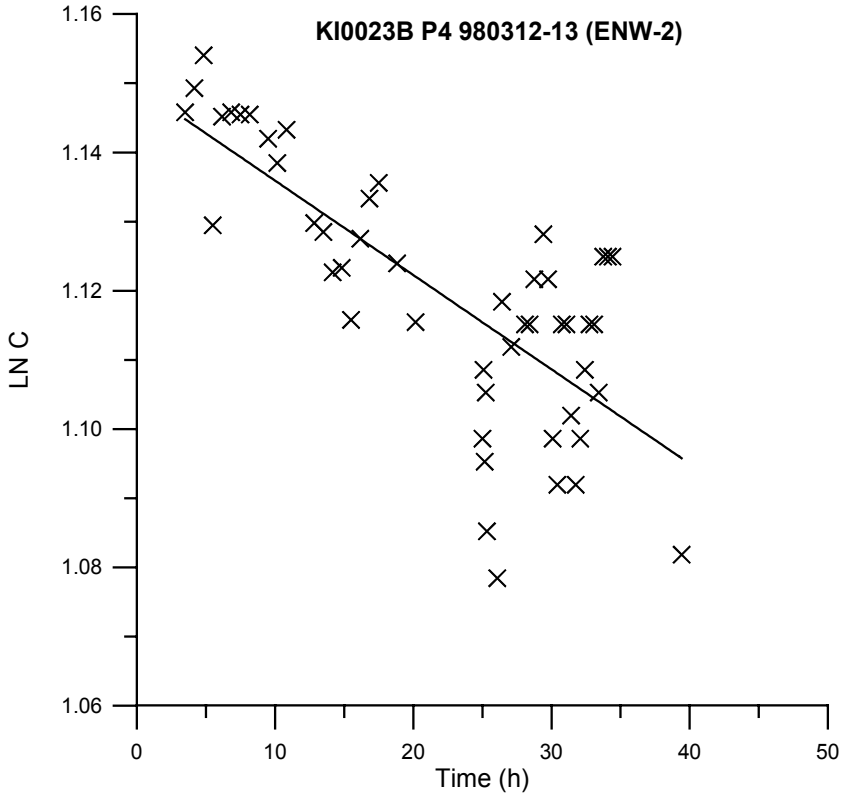
KI0023B P4 980312-13 (ENW-2)
LN C
1.16
1.14
1.12
1.10
1.08
1.06
0
10
20
30
40
50
Time (h)

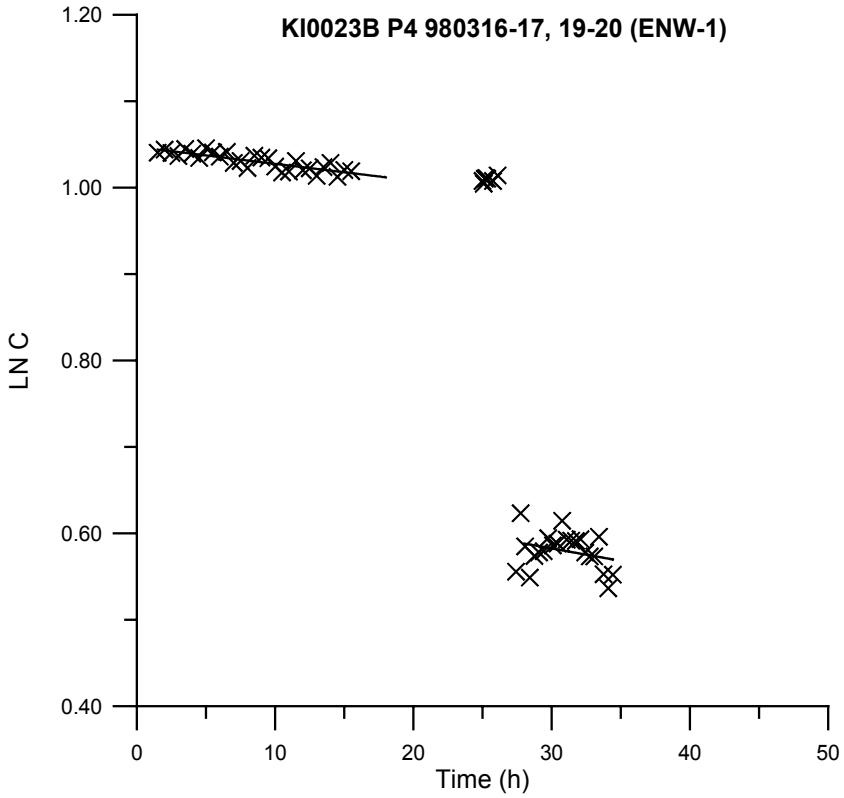
KI0023B P4 980316-17, 19-20 (ENW-1)
LN C
1.20
1.00
0.80
0.60
0.40
0
10
20
30
40
50
Time (h)

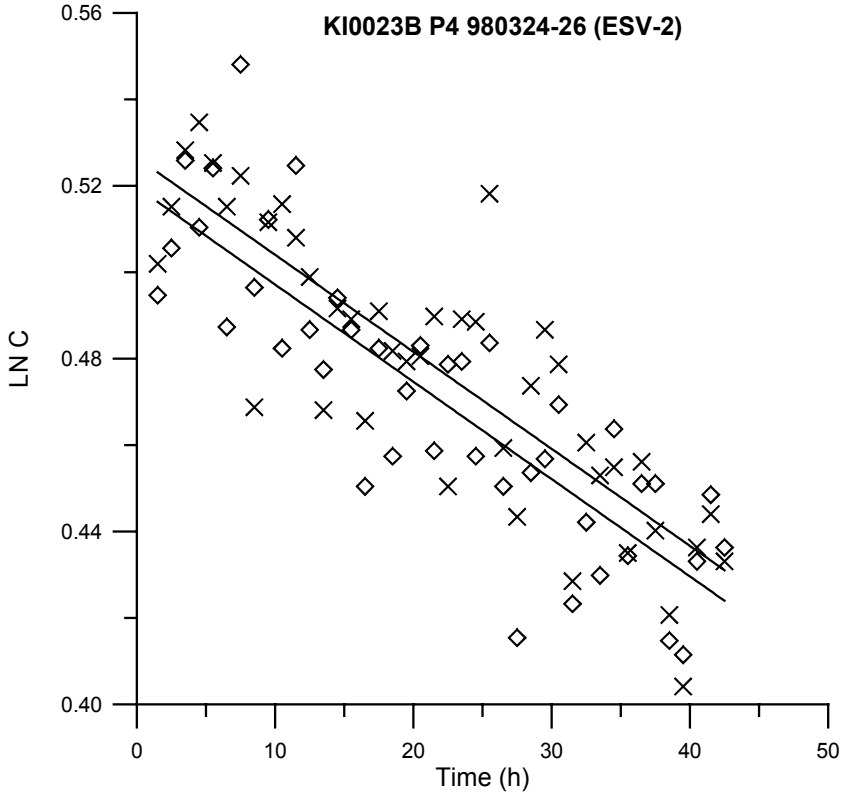
KI0023B P4 980324-26 (ESV-2)
LN C
0.56
0.52
0.48
0.44
0.40
0
10
20
30
40
50
Time (h)

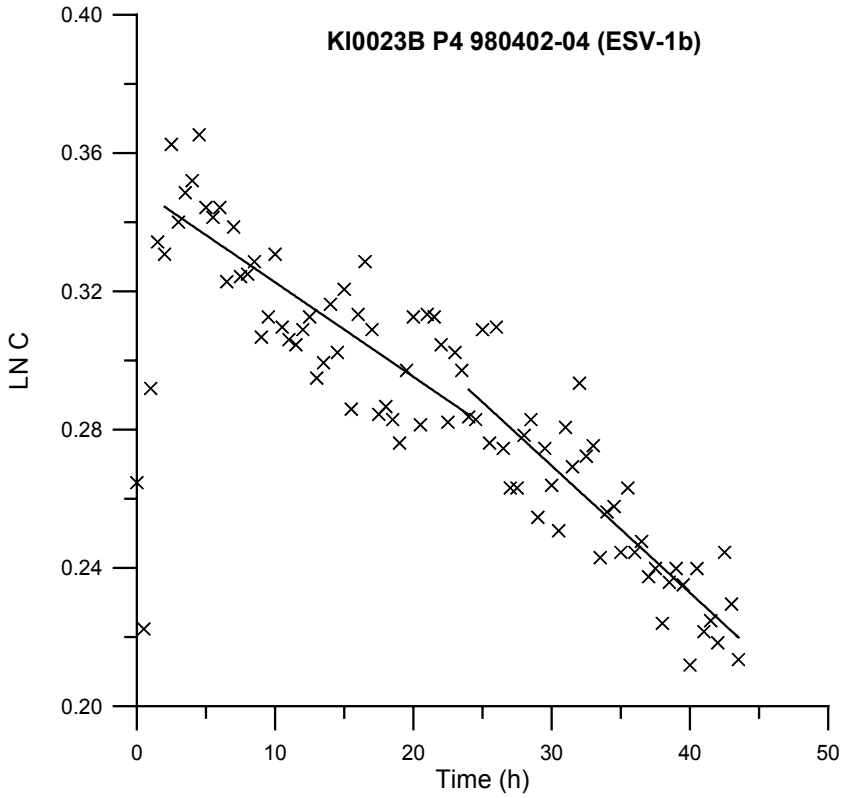
KI0023B P4 980402-04 (ESV-1b)
LN C
Time (h)
0.40
0.36
0.32
0.28
0.24
0.20
0
10
20
30
40
50

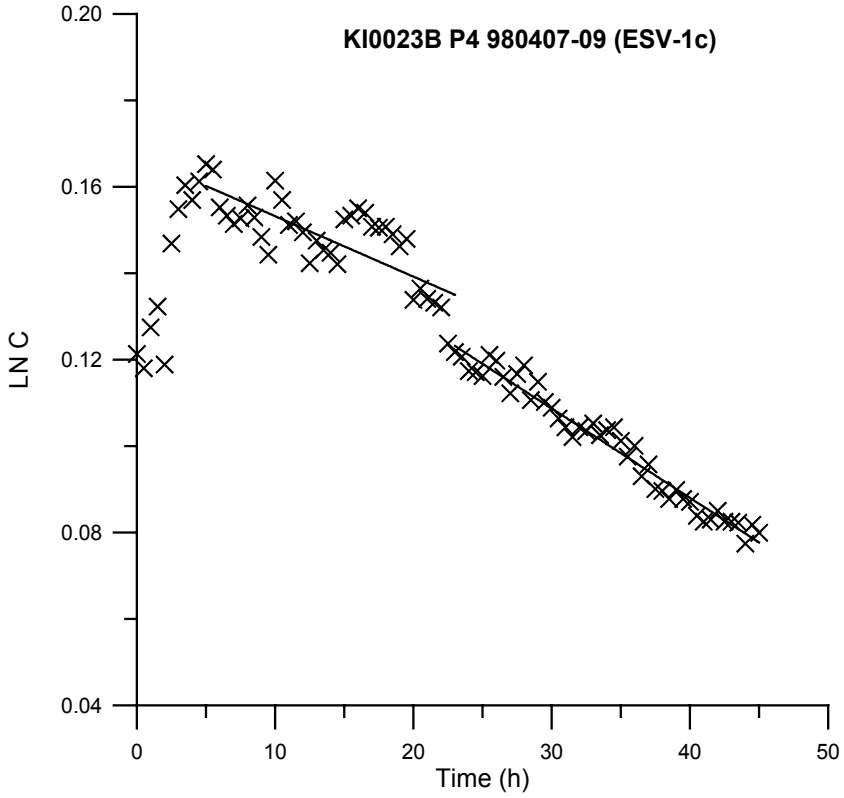
KI0023B P4 980407-09 (ESV-1c)
LN C
Time (h)
0.20
0.16
0.12
0.08
0.04
0
10
20
30
40
50

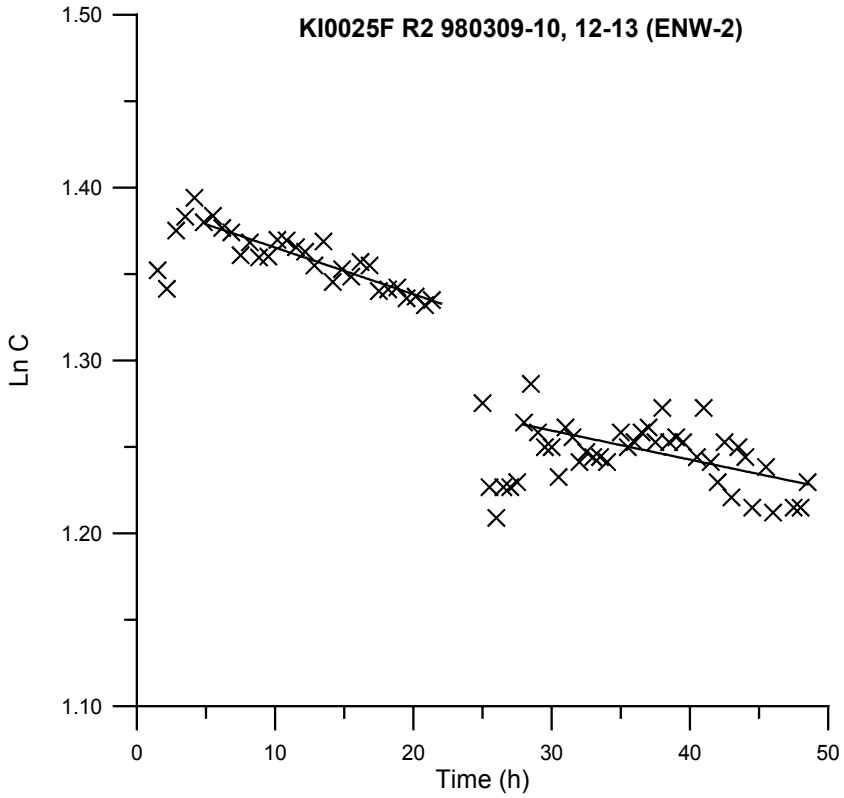
KI0025F R2 980309-10, 12-13 (ENW-2)
Ln C
1.50
1.40
1.30
1.20
1.10
0
10
20
30
40
50
Time (h)

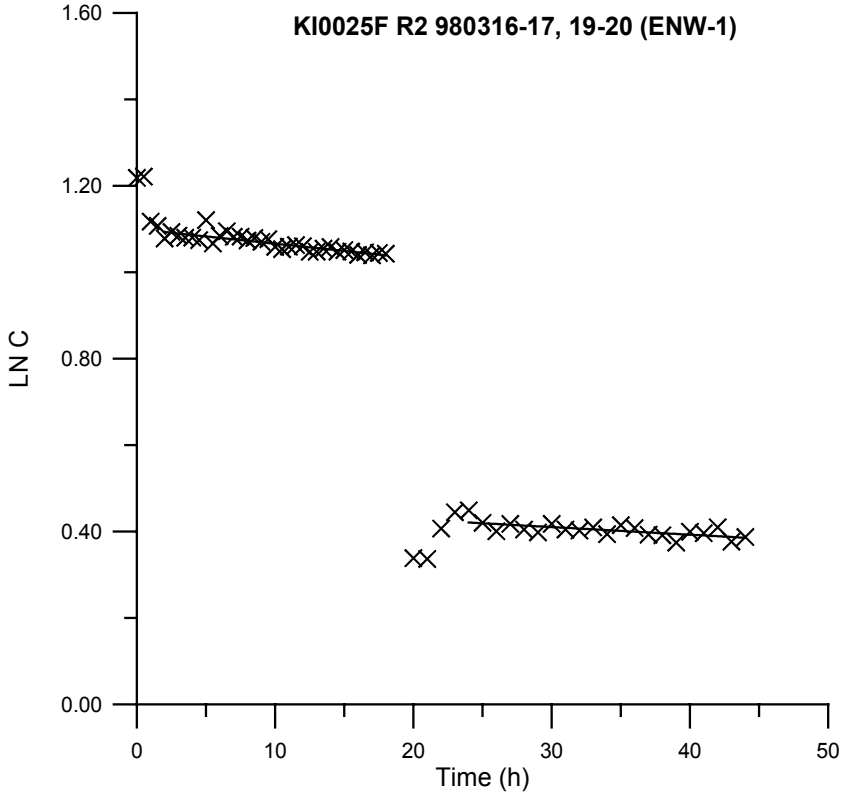
KI0025F R2 980316-17, 19-20 (ENW-1)
LN C
1.60
1.20
0.80
0.40
0.00
0
10
20
30
40
50
Time (h)

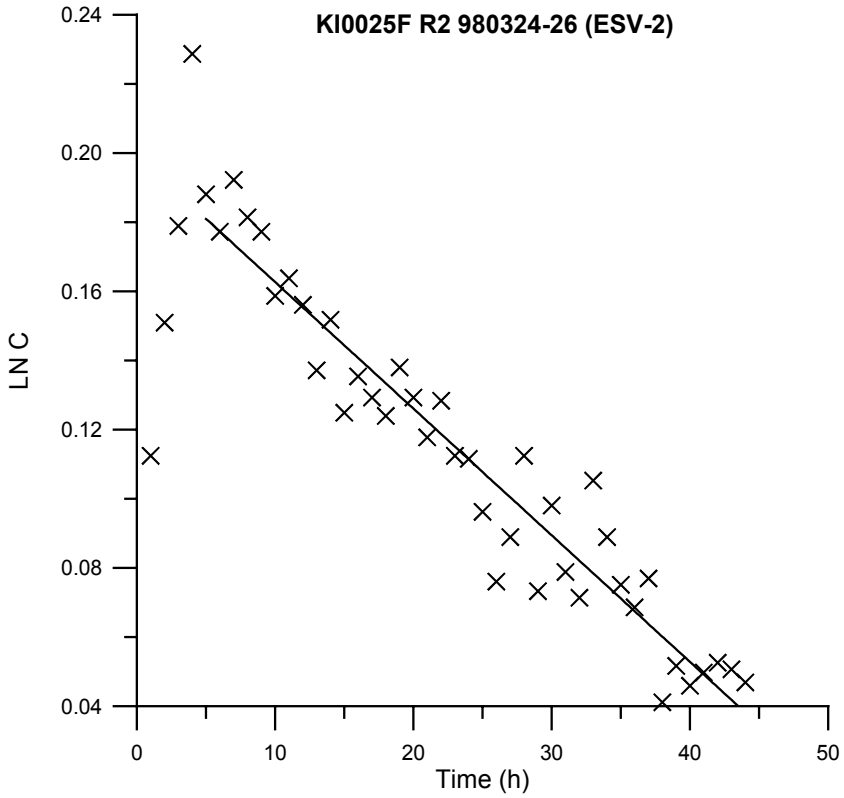
KI0025F R2 980324-26 (ESV-2)
LN C
0.24
0.20
0.16
0.12
0.08
0.04
0
10
20
30
40
50
Time (h)

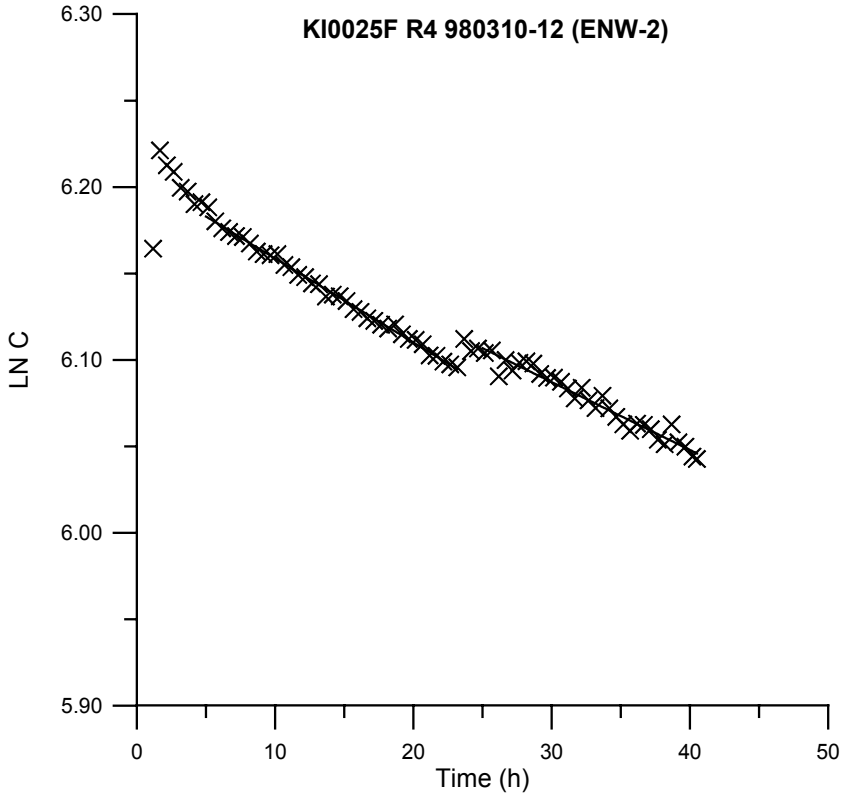
KI0025F R4 980310-12 (ENW-2)
LN C
6.30
6.20
6.10
6.00
5.90
0
10
20
30
40
50
Time (h)

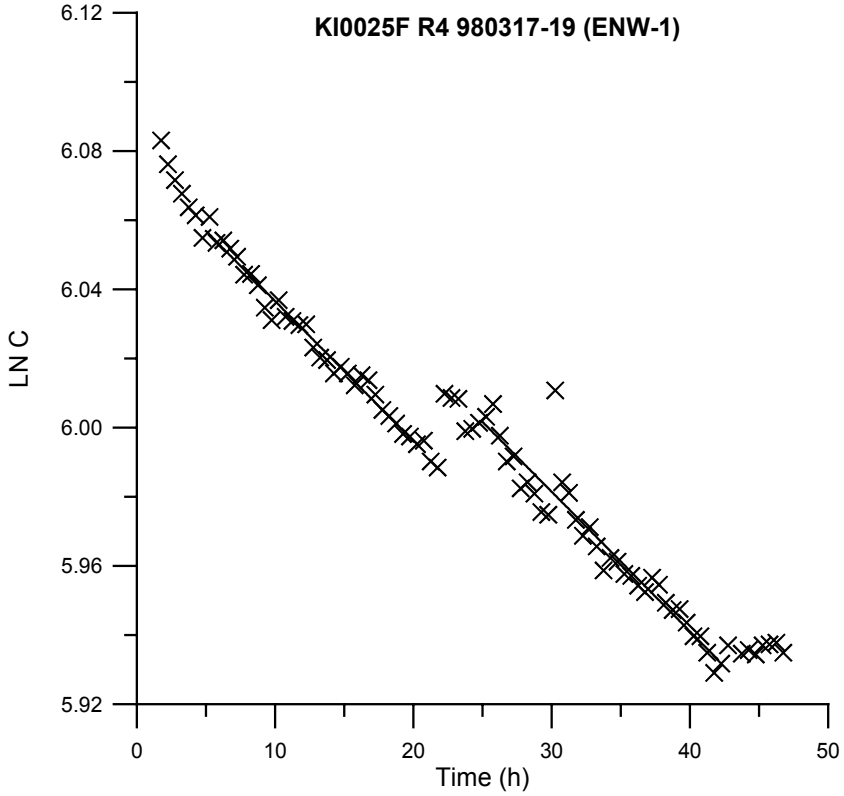
KI0025F R4 980317-19 (ENW-1)
LN C
6.12
6.08
6.04
6.00
5.96
5.92
0
10
20
30
40
50
Time (h)

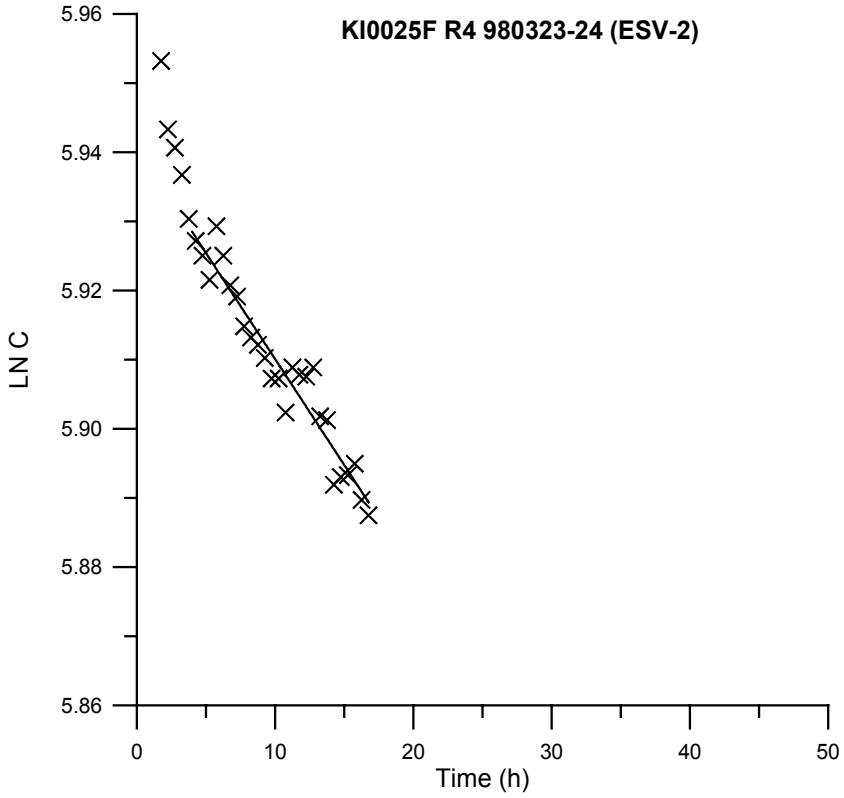
KI0025F R4 980323-24 (ESV-2)
LN C
5.96
5.94
5.92
5.90
5.88
5.86
0
10
20
30
40
50
Time (h)

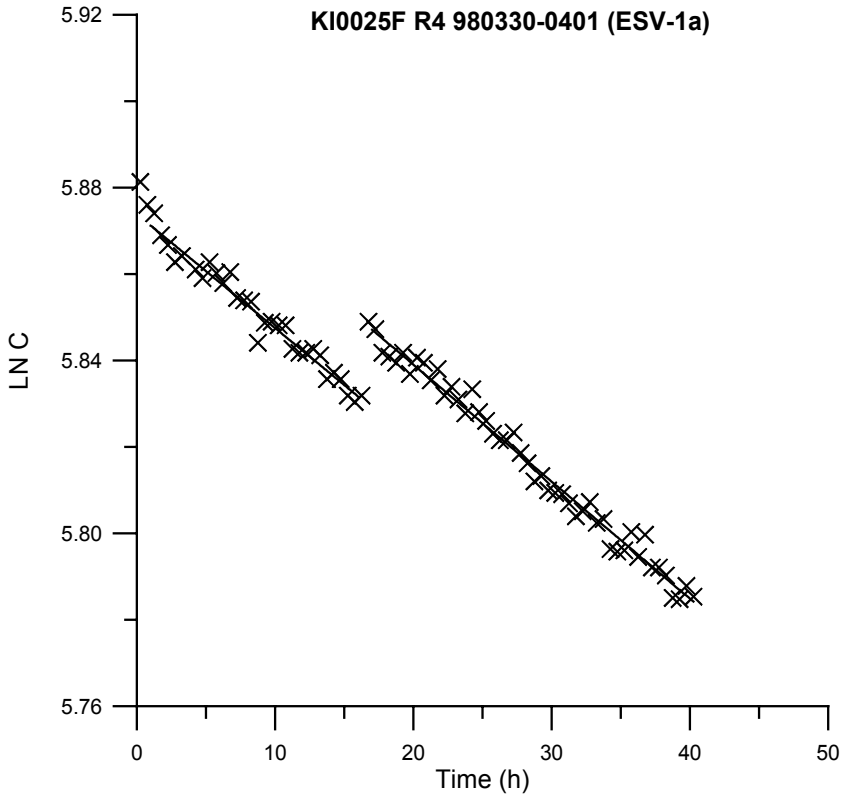
KI0025F R4 980330-0401 (ESV-1a)
5.92
5.88
5.84
5.80
5.76
LN C
0
10
20
30
40
50
Time (h)

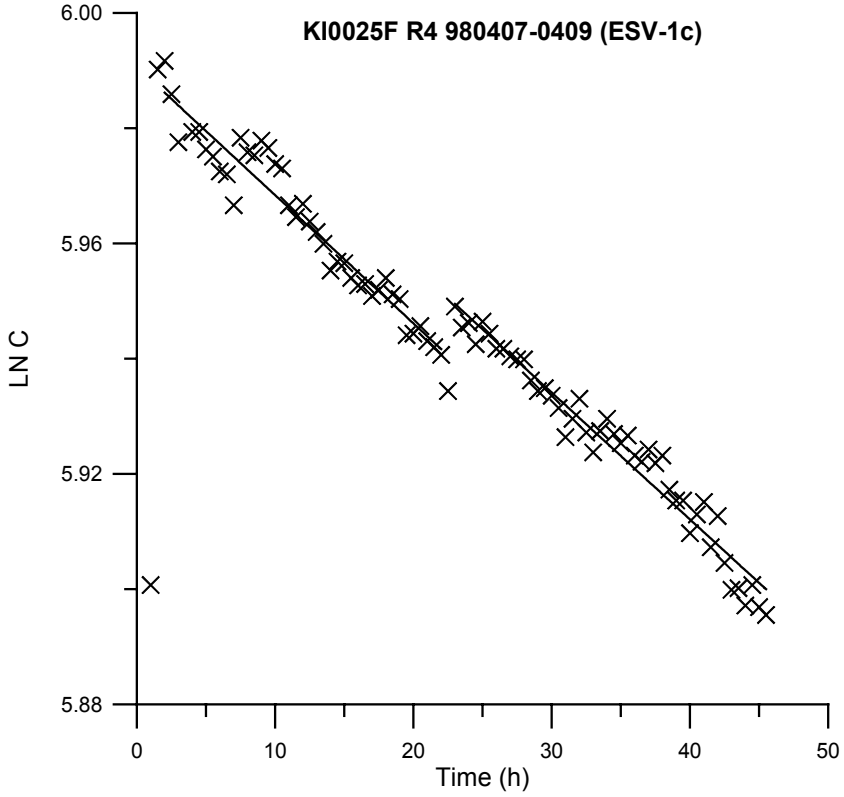
KI0025F R4 980407-0409 (ESV-1c)
6.00
5.96
5.92
5.88
LN C
0
10
20
30
40
50
Time (h)

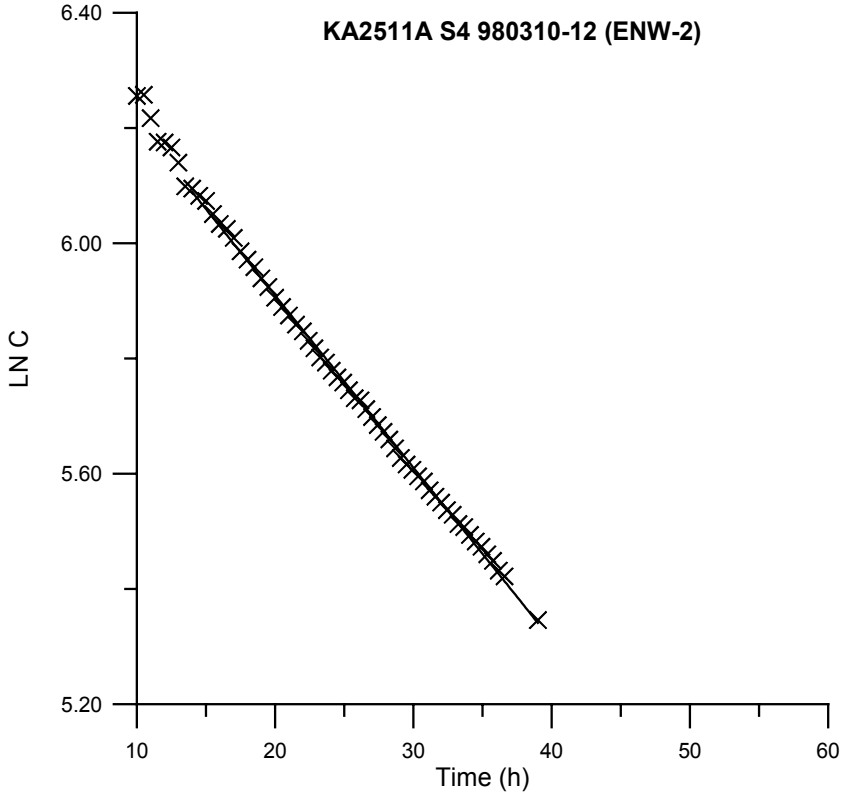
KA2511A S4 980310-12 (ENW-2)
6.40
6.00
5.60
5.20
LN C
10
20
30
40
50
60
Time (h)

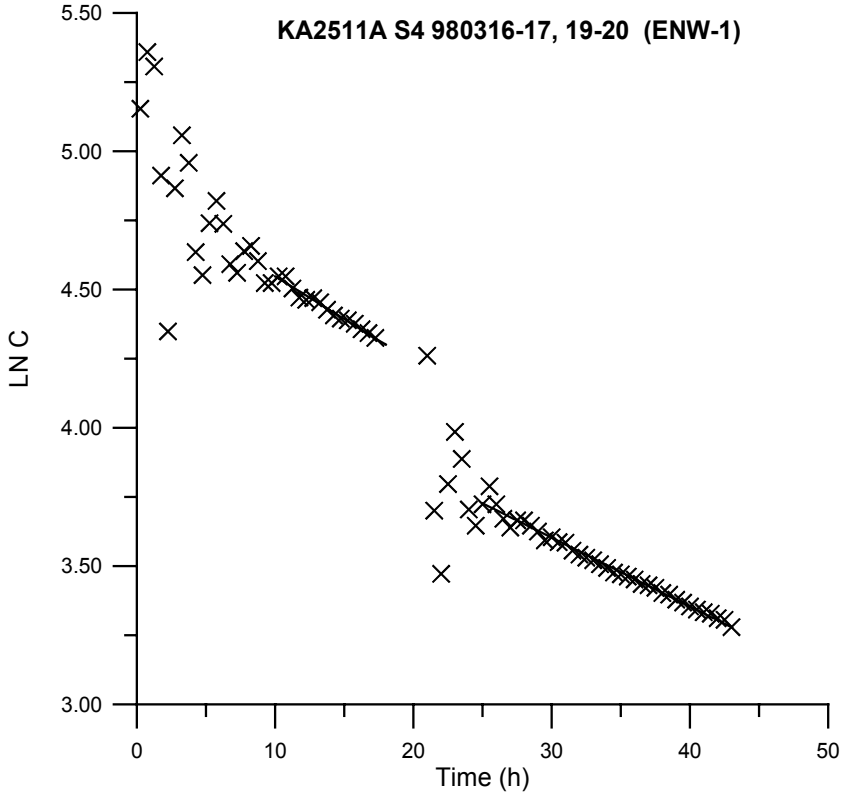
KA2511A S4 980316-17, 19-20 (ENW-1)
5.50
5.00
4.50
4.00
3.50
3.00
LN C
0
10
20
30
40
50
Time (h)

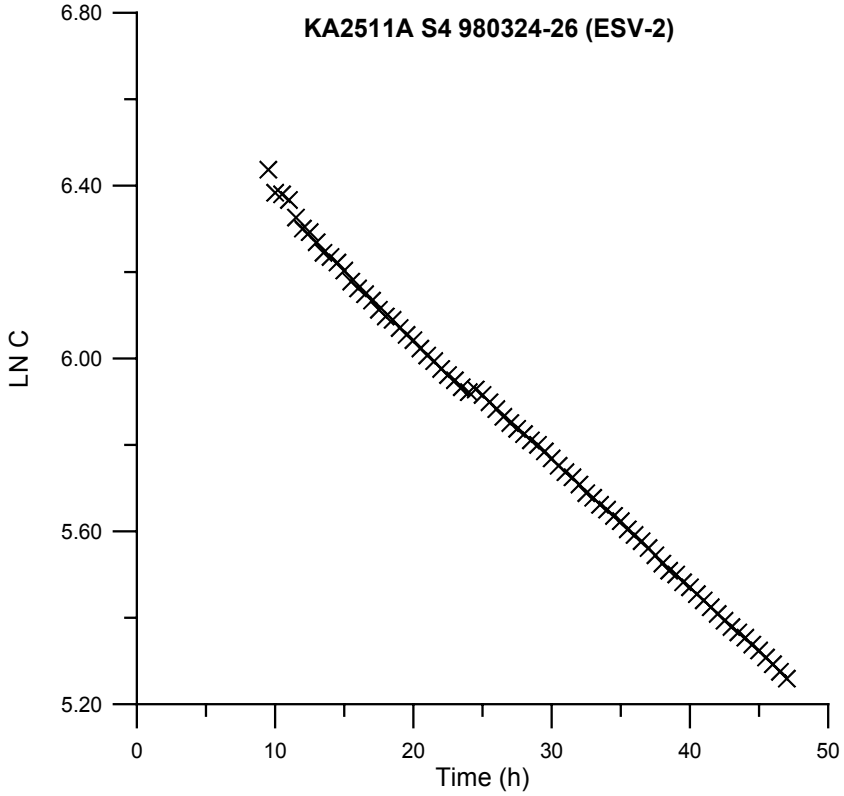
KA2511A S4 980324-26 (ESV-2)
LN C
6.80
6.40
6.00
5.60
5.20
0
10
20
30
40
50
Time (h)

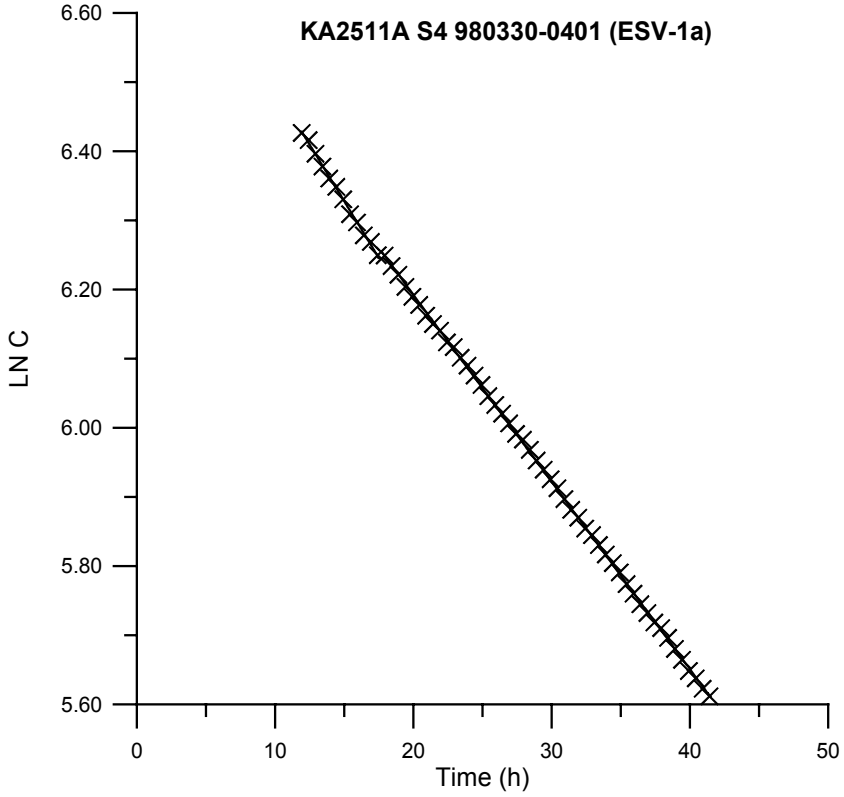
KA2511A S4 980330-0401 (ESV-1a)
LN C
6.60
6.40
6.20
6.00
5.80
5.60
0
10
20
30
40
50
Time (h)